

## **Supporting Information**

### **Structural and Reactivity Comparison of Analogous Organometallic Pd(III) and Pd(IV) Complexes**

Fengzhi Tang,<sup>a</sup> Fengrui Qu,<sup>a</sup> Julia R. Khusnutdinova,<sup>a</sup> Nigam P. Rath,<sup>b</sup> and Liviu M.  
Mirica<sup>a\*</sup>

<sup>a</sup> *Department of Chemistry, Washington University, One Brookings Drive, St. Louis, Missouri 63130-4899*  
and <sup>b</sup> *Department of chemistry and Biochemistry, University of Missouri-St. Louis, One University  
Boulevard, St. Louis, Missouri 63121-4400.*

## Table of Contents

<b>I. General specifications</b>	S3
<b>II. Synthesis of <sup>iPr</sup>N4 and (<sup>R</sup>N4)Pd complexes (R = Me, iPr)</b>	
Synthesis of <sup>iPr</sup> N4	S5
Preparation of ( <sup>R</sup> N4)Pd <sup>II</sup> MeCl	S7
Preparation of ( <sup>R</sup> N4)Pd <sup>II</sup> Me <sub>2</sub>	S9
Preparation of ( <sup>R</sup> N4)Pd <sup>II</sup> (CD <sub>3</sub> ) <sub>2</sub>	S12
Preparation of ( <sup>Me</sup> N4)Pd <sup>II</sup> Cl <sub>2</sub>	S14
Preparation of [( <sup>R</sup> N4)Pd <sup>III</sup> MeCl]ClO <sub>4</sub>	S15
Preparation of [( <sup>R</sup> N4)Pd <sup>III</sup> Me <sub>2</sub> ]ClO <sub>4</sub> and [( <sup>R</sup> N4)Pd <sup>III</sup> (CD <sub>3</sub> ) <sub>2</sub> ]ClO <sub>4</sub>	S17
Preparation of [( <sup>R</sup> N4)Pd <sup>IV</sup> MeCl](ClO <sub>4</sub> ) <sub>2</sub>	S20
Preparation of [( <sup>R</sup> N4)Pd <sup>IV</sup> Me <sub>2</sub> ](PF <sub>6</sub> ) <sub>2</sub> and [( <sup>R</sup> N4)Pd <sup>IV</sup> (CD <sub>3</sub> ) <sub>2</sub> ](PF <sub>6</sub> ) <sub>2</sub>	S23
<b>III. Cyclic voltammograms of 1-4</b>	S27
<b>IV. UV-vis spectra of 1<sup>+</sup>-4<sup>+</sup>, 1<sup>2+</sup>, 3<sup>2+</sup>, and 4<sup>2+</sup></b>	S31
<b>V. EPR spectra of 1<sup>+</sup>-4<sup>+</sup> and [(<sup>tBu</sup>N4)Pd<sup>III</sup>MeCl]<sup>+</sup></b>	S34
<b>VI. ORTEP and space filling models of 1<sup>+</sup>-4<sup>+</sup>, 1<sup>2+</sup>, 3<sup>2+</sup>, and 4<sup>2+</sup></b>	S37
<b>VII. Photolysis and thermolysis (<sup>R</sup>N4)Pd<sup>III</sup> and (<sup>R</sup>N4)Pd<sup>IV</sup> complexes</b>	S42
Photolysis of ( <sup>R</sup> N4)Pd <sup>III</sup> complexes	S46
Thermolysis of ( <sup>R</sup> N4)Pd <sup>IV</sup> complexes	S54
Photolysis of [( <sup>R</sup> N4)Pd <sup>IV</sup> Me <sub>2</sub> ] <sup>2+</sup> complexes	S59
Synthesis of [( <sup>R</sup> N4)Pd <sup>II</sup> Me(MeCN)] <sup>+</sup> and [( <sup>iPr</sup> N4)Pd <sup>II</sup> (MeCN) <sub>2</sub> ] <sup>2+</sup> complexes	S61
<b>VIII. Crossover reactivity studies</b>	S65
<b>IX. X-ray structure characterization of [1<sup>+</sup>]ClO<sub>4</sub>, [2<sup>+</sup>]ClO<sub>4</sub>, [3<sup>+</sup>]ClO<sub>4</sub>, [4<sup>+</sup>]ClO<sub>4</sub>, [1<sup>2+</sup>](ClO<sub>4</sub>)<sub>2</sub>, [3<sup>2+</sup>](PF<sub>6</sub>)<sub>2</sub>, and [4<sup>2+</sup>](PF<sub>6</sub>)<sub>2</sub></b>	S69
<b>X. References</b>	S92

## I. General specifications

All operations were performed under a nitrogen atmosphere using standard Schlenk and glove box techniques if not indicated otherwise. All reagents for which the syntheses are not given were purchased from Sigma-Aldrich, Acros, STREM, or Pressure Chemical and were used as received without further purification. Solvents were purified prior to use by passing through a column of activated alumina using an MBRAUN SPS. 2,11-diaza[3,3](2,6)pyridinophane ( $^{\text{H}}\text{N}_4$ ),<sup>1</sup> N,N'-methyl-2,11-diaza[3,3](2,6)pyridinophane ( $^{\text{Me}}\text{N}_4$ ),<sup>1</sup> (PhCN)Pd<sup>II</sup>Cl<sub>2</sub>,<sup>2</sup> (COD)Pd<sup>II</sup>Cl<sub>2</sub>,<sup>3</sup> (COD)Pd<sup>II</sup>MeCl,<sup>4</sup> and (Me<sub>2</sub>S)<sub>2</sub>Pd<sup>II</sup>Cl<sub>2</sub><sup>5</sup> were prepared according to literature procedures. The synthesis and characterization of complexes ( $^{\text{tBu}}\text{N}_4$ )PdMeCl, ( $^{\text{tBu}}\text{N}_4$ )PdMe<sub>2</sub>, [ $^{\text{tBu}}\text{N}_4$ ]Pd<sup>III</sup>MeCl<sup>+</sup>, and [ $^{\text{tBu}}\text{N}_4$ ]Pd<sup>III</sup>Me<sub>2</sub><sup>+</sup> were reported previously.<sup>6</sup> NMR spectra were obtained on a Varian Mercury-300 spectrometer (300.121 MHz) or a Varian Unity Inova-600 spectrometer (599.746 MHz). Chemical shifts are reported in parts per million (ppm) with residual solvent resonance peaks as internal references.<sup>7</sup> Abbreviations for the multiplicity of NMR signals are singlet (s), doublet (d), triplet (t), quartet (q), septet (sep), multiplet (m), broad resonance (br). Solution magnetic susceptibility measurements for Pd<sup>III</sup> complexes were obtained at 293 K by the Evans method<sup>8</sup> using coaxial NMR tubes and CD<sub>3</sub>CN as solvents, and the corresponding diamagnetic corrections were included.<sup>9</sup> UV-visible spectra were recorded on a Varian Cary 50 Bio spectrophotometer and are reported as  $\lambda_{\text{max}}$ , nm ( $\epsilon$ , M<sup>-1</sup>\*cm<sup>-1</sup>). EPR spectra were recorded on a JEOL JES-FA X-band (9.2 GHz) EPR spectrometer in PrCN-MeCN (3:1) at 77 K. ESI-MS experiments were performed using a linear quadrupole ion trap Fourier transform ion cyclotron resonance mass spectrometer (LTQ-FTMS, Thermo, San Jose, CA) or a Bruker Maxis Q-TOF mass spectrometer with an electrospray ionization source. ESI mass-spectrometry was provided by the Washington University Mass Spectrometry Resource. Elemental analyses were carried out by the Columbia Analytical Services Tucson Laboratory.

## Electrochemical measurements

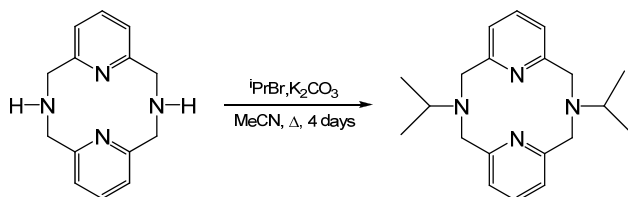
Cyclic voltammetry (CV) studies were performed with a BASi EC Epsilon electrochemical workstation or CHI Electrochemical Analyzer 660D. Electrochemical grade Bu<sub>4</sub>NClO<sub>4</sub>, Bu<sub>4</sub>NPF<sub>6</sub>, or Bu<sub>4</sub>NBF<sub>4</sub> from Fluka were used as the supporting electrolytes. The electrochemical measurements were performed under a blanket of nitrogen, and the analyzed solutions were deaerated by purging with nitrogen. A glassy carbon disk electrode (GCE) was used as the working electrode, and a Pt wire as the auxiliary electrode. The non-aqueous Ag-wire reference electrode assembly was filled with 0.01 M AgNO<sub>3</sub>/0.1 M Bu<sub>4</sub>NClO<sub>4</sub>/MeCN solution. The reference electrodes were calibrated against ferrocene at the end of each CV measurement.

### **Controlled potential electrolysis**

Electrochemical oxidations were performed in a two-compartment bulk electrolysis cell (BASi) separated by a fine-frit glass junction at room temperature. A reticulated vitreous carbon working electrode was used in the anodic compartment equipped with a magnetic stirring bar. A platinum gauze (25 mm x 10 mm) was used as the auxiliary electrode in the cathodic compartment. A non-aqueous Ag/0.01 M AgNO<sub>3</sub> electrode was used as a reference electrode. Prior to electrolysis, a CV of the Pd<sup>II</sup> precursor was performed in the same setup. The potential of electrolysis was set to be 100 mV-200 mV more positive than the corresponding oxidation peak potential observed in the CV scan. All solvents (CH<sub>2</sub>Cl<sub>2</sub> or MeCN) were dried by passing through a column of activated alumina. Electrochemical grade Bu<sub>4</sub>NClO<sub>4</sub> from Fluka was used as supporting electrolyte (0.03-0.1 M).

## II. Synthesis of ${}^{\text{iPr}}\text{N4}$ and $({}^{\text{R}}\text{N4})\text{Pd}$ complexes ( $\text{R} = \text{Me}, \text{iPr}$ )

### Synthesis of ${}^{\text{iPr}}\text{N4}$



${}^{\text{H}}\text{N4}$  (0.62 g, 2.58 mmol), isopropylbromide (12.1 mL, 129 mmol, 50 equiv), anhydrous  $\text{K}_2\text{CO}_3$  (4.3 g, 31 mmol, 12 equiv), and dry MeCN (150 mL) were charged into a 250 mL RB flask with a magnetic stir bar. The reaction mixture was refluxed under  $\text{N}_2$  for 4 days. The solution was then cooled to RT and the solvent removed under reduced pressure. The residue was suspended in 100 mL of  $\text{CH}_2\text{Cl}_2$  and then washed with 1 M NaOH and water. The  $\text{CH}_2\text{Cl}_2$  layer was isolated, dried over anhydrous  $\text{MgSO}_4$ , evaporated, and further dried under vacuum to give a pale yellow powder. Yield: 0.59 g, 71.3%.

${}^1\text{H}$  NMR (300MHz,  $\text{CDCl}_3$ ),  $\delta$ : 7.08 (t,  $J = 7.5$  Hz, 2H, py-H), 6.74 (d,  $J = 7.5$  Hz, 4H, py-H), 3.88 (s, 8H,  $-\text{CH}_2-$ ), 3.26 (sep,  $J = 6.6$  Hz, 2H, iPr-CH), 1.24 (d,  $J = 6.3$  Hz, 12H, iPr- $\text{CH}_3$ ).  ${}^{13}\text{C}$  NMR (300MHz,  $\text{CDCl}_3$ ),  $\delta$ : 158.9, 135.5, 122.5, 60.1, 58.3, and 19.2.

The protonated ligands  $[{}^{\text{iPr}}\text{N4}\cdot\text{H}]^+$  and  $[{}^{\text{iPr}}\text{N4}\cdot 2\text{H}]^{2+}$  were generated by mixing  ${}^{\text{iPr}}\text{N4}$  with 1 or 2 equiv of  $\text{H}^+$ :

$[{}^{\text{iPr}}\text{N4}\cdot\text{H}]^+$ :  ${}^1\text{H}$  NMR (300MHz,  $\text{CD}_3\text{CN}$ ),  $\delta$ : 7.97, (t,  $J = 7.5$  Hz, 2 H, py-H), 7.41 (d,  $J = 7.8$  Hz, 4H, py-H), 4.17 (br, 8H,  $-\text{CH}_2-$ ), 3.03 (m,  $J = 6.6$  Hz, 2H, iPr-CH), 1.03 (d,  $J = 6.3$  Hz, 12H, iPr- $\text{CH}_3$ ).

$[{}^{\text{iPr}}\text{N4}\cdot 2\text{H}]^{2+}$ :  ${}^1\text{H}$  NMR (300MHz,  $\text{CD}_3\text{CN}$ ),  $\delta$ : 10.74, (br, 2H, amine- $\text{NH}^+$ ), 7.51 (t,  $J = 7.8$  Hz, 2H, py-H), 7.07 (d,  $J = 7.8$  Hz, 4H, py-H), 4.71 (d,  $J = 14.7$  Hz, 4H,  $-\text{CH}_2-$ ), 4.29 (dd,  $J^1 = 15$  Hz,  $J^2 = 3.6$  Hz, 4H,  $-\text{CH}_2-$ ), 4.20 (m,  $J = 6.6$  Hz, iPr-CH), 1.57 (d,  $J = 6.6$  Hz, 12H, iPr- $\text{CH}_3$ ).

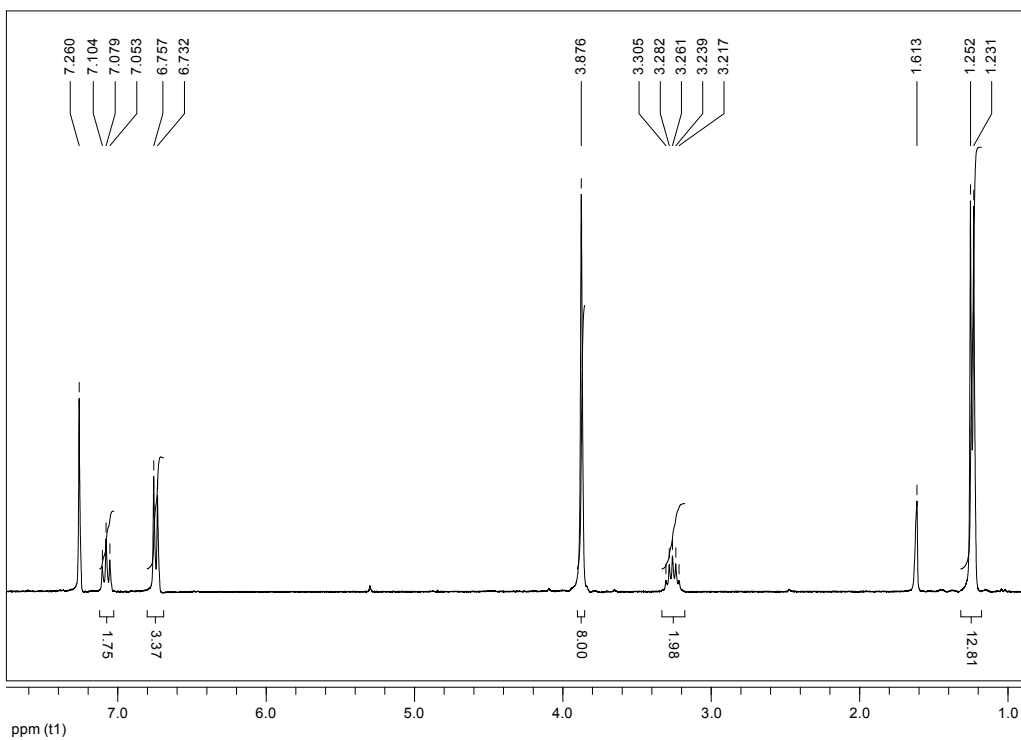


**Figure S1.**  $^1\text{H}$  NMR spectrum of  $i\text{PrN}_4$  in  $\text{CDCl}_3$ .

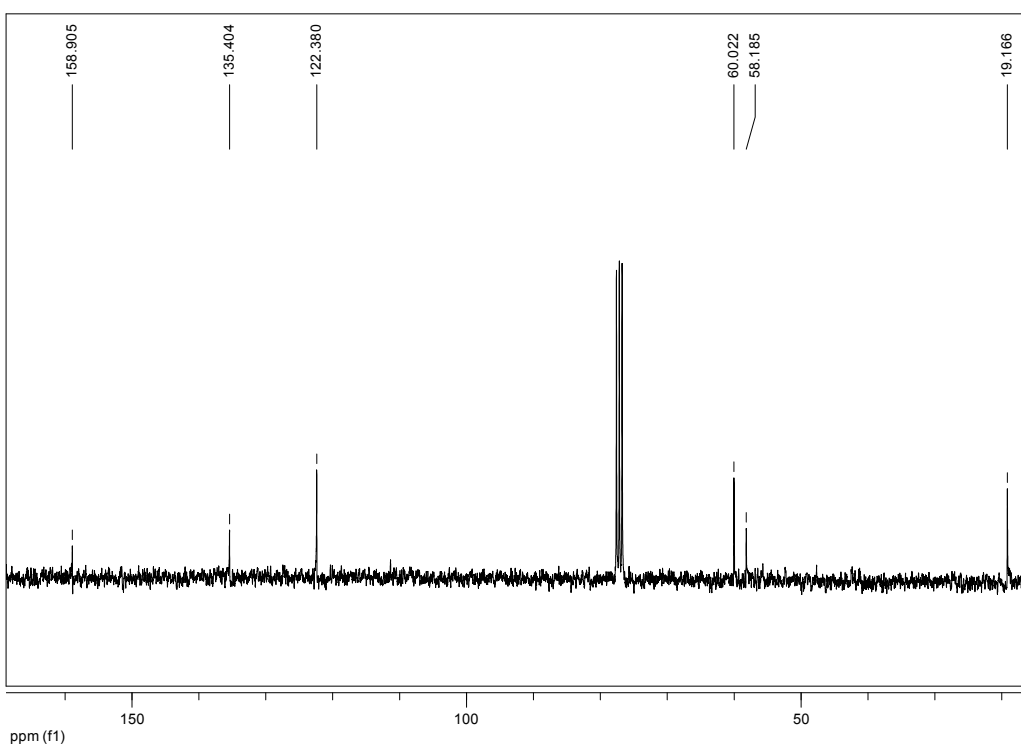
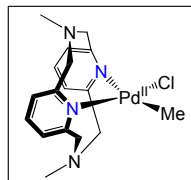


**Figure S2.**  $^{13}\text{C}$  NMR spectrum of  $i\text{PrN}_4$  in  $\text{CDCl}_3$ .

## Preparation of (<sup>R</sup>N<sub>4</sub>)Pd<sup>II</sup>MeCl



R = Me, iPr

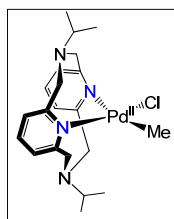


Under N<sub>2</sub>, <sup>Me</sup>N<sub>4</sub> (106 mg, 0.395 mmol) and (COD)Pd<sup>II</sup>MeCl (104 mg, 0.395 mmol) were loaded in a 100 mL RB flask and 40 mL anhydrous diethyl ether was added to form a yellowish suspension. This suspension was stirred for two days in the dark. The generated pale yellow precipitate was filtered off, washed with ether and pentane and dried *in vacuo*. The product (<sup>Me</sup>N<sub>4</sub>)Pd<sup>II</sup>MeCl was isolated as a pale yellow solid. Yield: 154.8 mg, 93.2%.

ESI-MS (<sup>Me</sup>N<sub>4</sub>)Pd<sup>II</sup>MeCl in MeCN, m/z 409.0405; calcd. for [(<sup>Me</sup>N<sub>4</sub>)Pd<sup>II</sup>Cl]<sup>+</sup>, C<sub>16</sub>H<sub>20</sub>ClN<sub>4</sub>Pd, 409.0411.

Anal. Found: C, 47.72; H, 6.09; N, 12.74; calcd. for C<sub>17</sub>H<sub>23</sub>ClN<sub>4</sub>Pd: C, 48.01; H, 5.45; N, 13.17.

<sup>1</sup>H NMR (300MHz, CDCl<sub>3</sub>), δ: 7.47 (br, 2H, py-H), 7.03 (d, *J* = 26.7 Hz, 4H, py-H), 6.21 (dd, *J* = 55.8 Hz, 9.9 Hz, 4H, -CH<sub>2</sub>-), 4.18 (br, 4H, -CH<sub>2</sub>-), 2.37 (s, 6H, N-CH<sub>3</sub>), 0.74 (s, 3H, Pd-CH<sub>3</sub>).



The (<sup>iPr</sup>N<sub>4</sub>)Pd<sup>II</sup>MeCl was synthesized following a similar procedure. Yield: 79.2%.

ESI-MS of (<sup>iPr</sup>N<sub>4</sub>)Pd<sup>II</sup>MeCl in MeCN, m/z 445.1579; calcd. for [(<sup>iPr</sup>N<sub>4</sub>)Pd<sup>II</sup>Me]<sup>+</sup>, C<sub>21</sub>H<sub>31</sub>N<sub>4</sub>Pd, 445.1583.

Anal. Found: C, 51.80; H, 6.47; N, 11.03; calcd. for C<sub>21</sub>H<sub>31</sub>ClN<sub>4</sub>Pd: C, 52.40; H, 6.49; N, 11.64.

<sup>1</sup>H NMR (300MHz, CD<sub>3</sub>CN), δ: 7.50 (br, 2H, py-H), 7.09 (br, 4H, py-H), 5.64 (br, 4H, -CH<sub>2</sub>-), 4.23 (br, 4H, -CH<sub>2</sub>-), 3.37 (sep, *J* = 6.6 Hz, 2H, iPr-CH), 1.28 (d, *J* = 6.6 Hz, 12H, iPr-CH<sub>3</sub>), 0.56 (s, 3H, Pd-CH<sub>3</sub>).

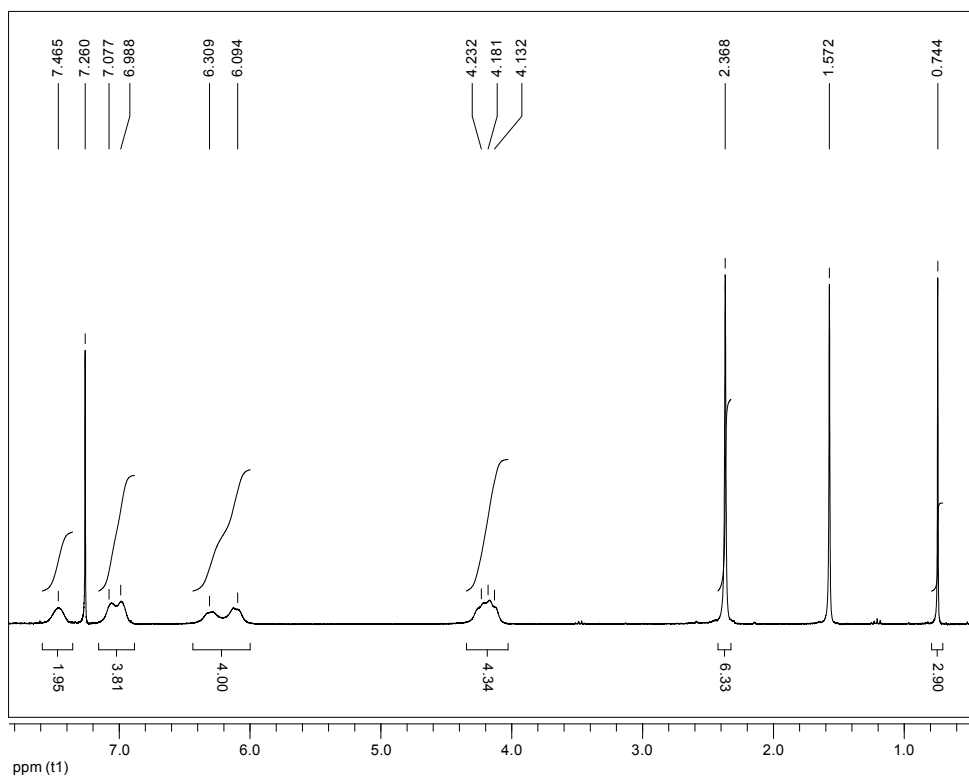


**Figure S3.**  $^1\text{H}$  NMR spectrum of  $(\text{Me}_4\text{N})\text{Pd}^{\text{II}}\text{MeCl}$  (**1**) in  $\text{CDCl}_3$ .

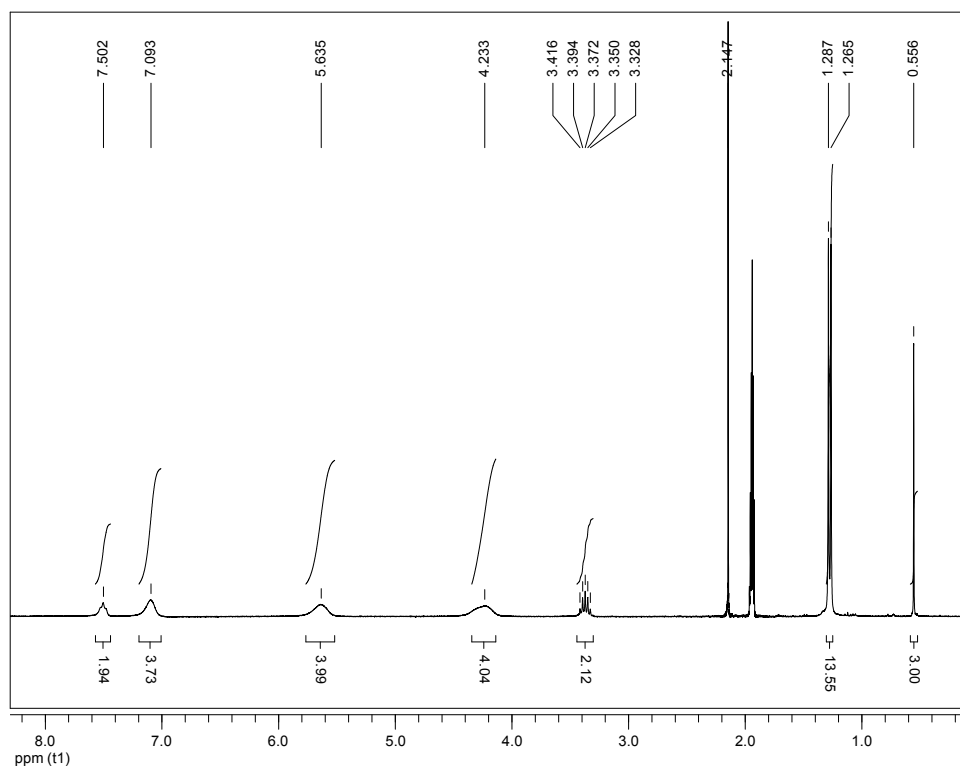
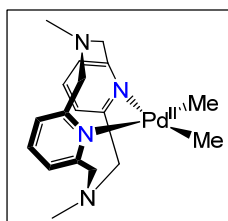
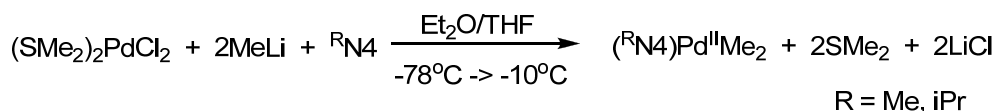


**Figure S4.**  $^1\text{H}$  NMR spectrum of  $(\text{iPr}_4\text{N})\text{Pd}^{\text{II}}\text{MeCl}$  (**2**) in  $\text{CD}_3\text{CN}$ .

### Preparation of $(^R\text{N}_4)\text{Pd}^{\text{II}}\text{Me}_2$



Under  $\text{N}_2$ ,  $(\text{Me}_2\text{S})_2\text{PdCl}_2$  (50 mg, 0.17 mmol) was suspended in 20 mL diethyl ether at  $-75^\circ\text{C}$  in a dry ice/acetone cold bath. MeLi in diethyl ether (0.48 mL 1.6 M, 4.5 equiv) was then added to the solution dropwise. This mixture was allowed to slowly warm up to  $-65^\circ\text{C}$  until the solution turned colorless in a course of a few hours. To this solution,  $^{\text{Me}}\text{N}_4$  (44 mg, 0.17 mmol) in diethyl ether/THF (3 mL/20 mL) mixture was added to the reaction mixture dropwise to give a pale yellow/brown suspension. The mixture was slowly warmed up to  $-25^\circ\text{C}$  during a course of 5-7 hours to give a clear light yellow/brown solution. To this solution, 1.5 mL water was added dropwise, and stirred for 30 min at a temperature between  $-25^\circ\text{C}$  and  $-10^\circ\text{C}$ . Then the clear solution was removed from the reaction vessel with a syringe, filtered through a syringe filter and transferred to a round bottom flask under  $\text{N}_2$ . The solvent was removed under vacuum at  $0^\circ\text{C}$ . White crystals were formed during evaporation of the solvents. The product was transferred to a nitrogen filled glove box immediately and stored at  $-35^\circ\text{C}$ . Yield: 65 mg, 90%.

ESI-MS ( $^{\text{Me}}\text{N}_4$ ) $\text{Pd}^{\text{II}}\text{Me}_2$  in MeCN,  $m/z$  373.0638; calcd. for [ $(^{\text{Me}}\text{N}_4)\text{Pd}^{\text{II}}\text{Me}_2\text{-Me-CH}_4$ ] $^+$ , 373.0644.

Anal. Found: C, 53.45; H, 6.49; N, 12.07; calcd. for ( $^{\text{Me}}\text{N}_4$ ) $\text{Pd}^{\text{II}}\text{Me}_2$ : C, 53.40; H, 6.47; N, 13.87. The experimental elemental analysis results are slightly off, likely due to the slow decomposition of the ( $^{\text{Me}}\text{N}_4$ ) $\text{Pd}^{\text{II}}\text{Me}_2$  complex at RT (see below).

$^1\text{H}$  NMR (300MHz, acetone- $d_6$ ),  $\delta$ : 7.57 (t,  $J = 7.8$  Hz, 2H, py-H), 7.13 (d,  $J = 7.5$  Hz, 4H, py-H), 6.11 (d,  $J = 14.4$  Hz, 4H,  $-\text{CH}_2-$ ), 4.10 (d,  $J = 13.5$  Hz, 4H,  $-\text{CH}_2-$ ), 2.34 (s, 6H,  $-\text{N-CH}_3$ ), -0.02 (s, 6H, Pd- $\text{CH}_3$ ).

Note: ( $^{\text{Me}}\text{N}_4$ ) $\text{Pd}^{\text{II}}\text{Me}_2$  slowly decomposes in solution with loss of a methyl group and methane, likely through ligand decomposition. The mechanism of ligand decomposition is currently under investigation.

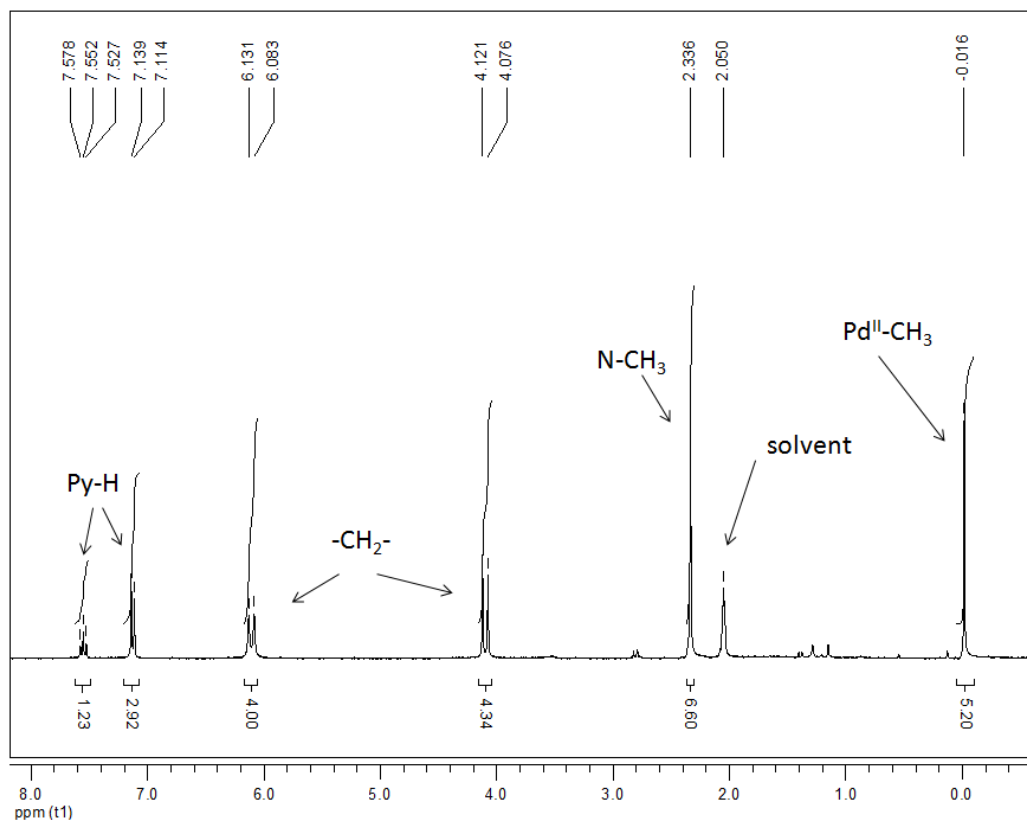
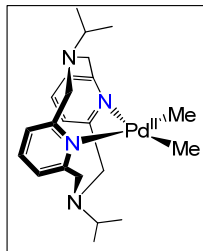


**Figure S5.**  $^1\text{H}$  NMR spectrum of  $(^{\text{Me}}\text{N}_4)\text{Pd}^{\text{II}}\text{Me}_2$  (**3**) in acetone- $d_6$ .



(<sup>iPr</sup>N<sub>4</sub>)Pd<sup>II</sup>Me<sub>2</sub> (**4**) was synthesized following a similar procedure. Yield: 52.8%.

ESI-MS of (<sup>iPr</sup>N<sub>4</sub>)Pd<sup>II</sup>Me<sub>2</sub> in MeCN, *m/z* 445.1579; calcd. for [(<sup>iPr</sup>N<sub>4</sub>)Pd<sup>II</sup>Me]<sup>+</sup>, 445.1583.

Anal. Found: C, 56.39; H, 7.41; N, 10.73; calcd. for (<sup>iPr</sup>N<sub>4</sub>)Pd<sup>II</sup>Me<sub>2</sub>: C, 57.32; H, 7.43; N, 12.15. The experimental elemental analysis results are slightly off, likely due to the slow decomposition of the (<sup>iPr</sup>N<sub>4</sub>)Pd<sup>II</sup>Me<sub>2</sub> complex at RT.

<sup>1</sup>H NMR (300MHz, acetone-*d*<sub>6</sub>), δ: 7.42, (t, *J* = 7.8 Hz, 2H, py-H), 7.02 (d, *J* = 7.7 Hz, 4H, py-H), 5.81 (d, *J* = 12.2 Hz, 4H, -CH<sub>2</sub>-), 4.06 (d, *J* = 12.1 Hz, 4H, -CH<sub>2</sub>-), 3.37 (sep, *J* = 6.6 Hz, 2H, iPr-CH), 1.28 (d, *J* = 6.6 Hz, 12H, iPr-CH<sub>3</sub>), 0.07 (s, 3H, Pd-CH<sub>3</sub>).

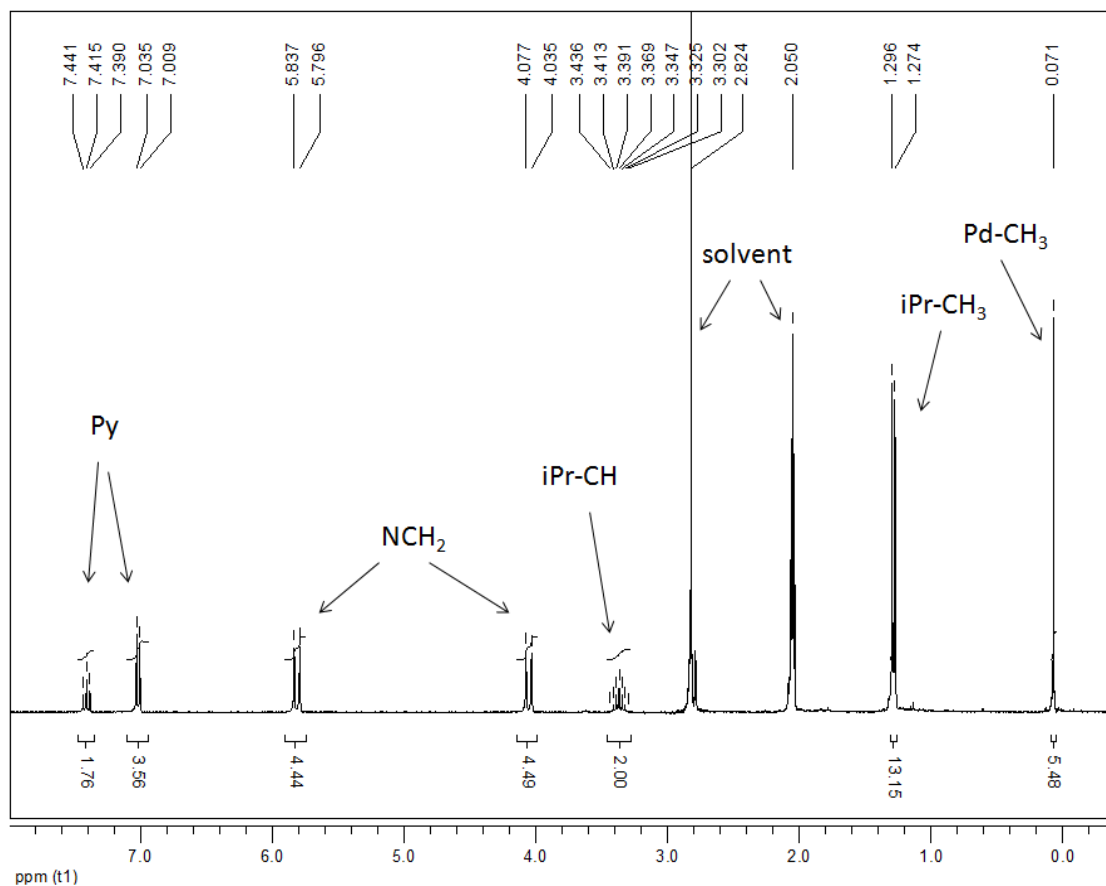


**Figure S6.** <sup>1</sup>H NMR spectrum of (<sup>iPr</sup>N<sub>4</sub>)Pd<sup>II</sup>Me<sub>2</sub> (**4**) in acetone-*d*<sub>6</sub>.

### Preparation of $(^R\text{N4})\text{Pd}^{\text{II}}(\text{CD}_3)_2$

The deuterated complex  $(^R\text{N4})\text{Pd}^{\text{II}}(\text{CD}_3)_2$  (**3-d<sub>6</sub>**) was prepared by reacting  $^{\text{Me}}\text{N4}$  with freshly prepared  $(\text{COD})\text{Pd}^{\text{II}}(\text{CD}_3)_2$  following a reported procedure.<sup>10</sup>  $(^{\text{Me}}\text{N4})\text{Pd}^{\text{II}}(\text{CD}_3)_2$  was obtained as a white solid in 31% yield. The  $^1\text{H}$  NMR spectrum of the product is identical to that of  $(^{\text{Me}}\text{N4})\text{Pd}^{\text{II}}\text{Me}_2$  except for the missing singlet of Pd-Me group.

$^1\text{H}$  NMR (300MHz, acetone-*d*<sub>6</sub>),  $\delta$ : 7.58 (t,  $J = 7.8$  Hz, 2H, py-H), 7.12 (d,  $J = 7.5$  Hz, 4H, py-H), 6.10 (d,  $J = 13.8$  Hz, 4H, -CH<sub>2</sub>-), 4.10 (d,  $J = 13.8$  Hz, 4H, -CH<sub>2</sub>-), 2.34 (s, 6H, -N-CH<sub>3</sub>).

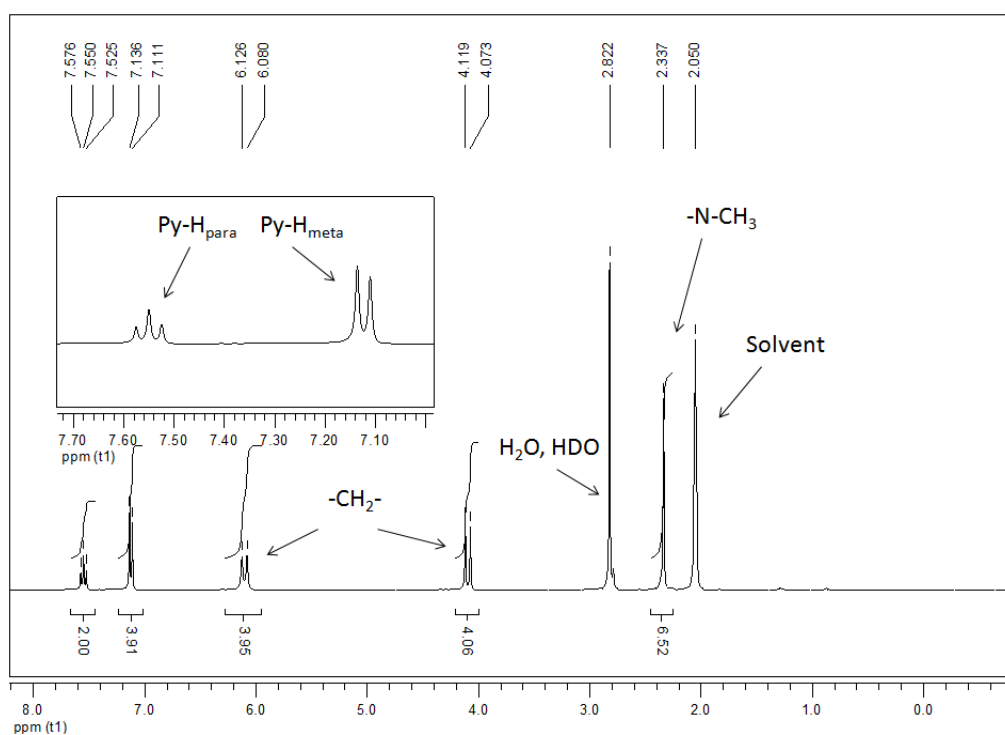


**Figure S7.**  $^1\text{H}$  NMR spectrum of  $(^{\text{Me}}\text{N4})\text{Pd}^{\text{II}}(\text{CD}_3)_2$  in acetone-*d*<sub>6</sub>.

$(i\text{Pr}_4\text{N})\text{Pd}^{\text{II}}(\text{CD}_3)_2$  (**4-d<sub>6</sub>**) was synthesized following a similar procedure in 46% yield. The  $^1\text{H}$  NMR spectrum of the product is identical to that of  $(i\text{Pr}_4\text{N})\text{Pd}^{\text{II}}\text{Me}_2$  except for the missing singlet of Pd-Me group.

$^1\text{H}$  NMR (300 MHz, acetone- $d_6$ ),  $\delta$ : 7.41 (t,  $J = 7.7$  Hz, 2H, Py-H), 7.02 (d,  $J = 7.7$  Hz, 4H, py-H), 5.81 (d,  $J = 12.4$  Hz, 4H, -CH<sub>2</sub>-), 4.05 (d,  $J = 12.4$  Hz, 4H, -CH<sub>2</sub>-), 3.37 (m,  $J = 6.6$  Hz, 2H, iPr-CH), 1.28 (d,  $J = 6.6$  Hz, 12H, iPr-CH<sub>3</sub>).

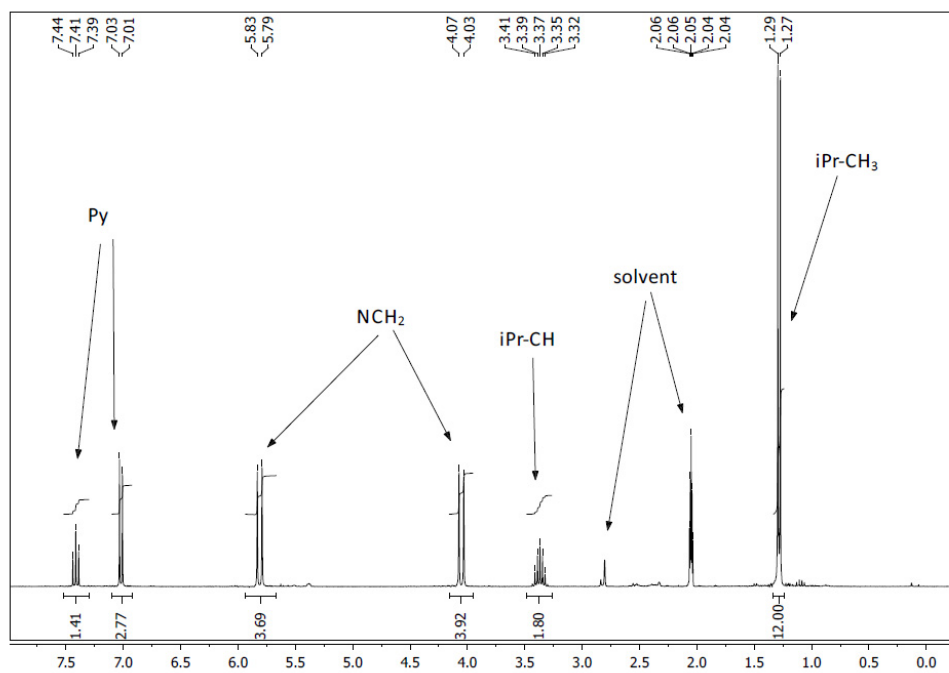
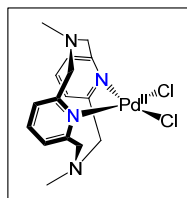


**Figure S8.**  $^1\text{H}$  NMR spectrum of  $(i\text{Pr}_4\text{N})\text{Pd}^{\text{II}}(\text{CD}_3)_2$  in acetone- $d_6$ .

### Preparation of (<sup>Me</sup>N<sub>4</sub>)Pd<sup>II</sup>Cl<sub>2</sub>



(PhCN)<sub>2</sub>Pd<sup>II</sup>Cl<sub>2</sub> (96.9 mg, 0.253 mmol) and <sup>Me</sup>N<sub>4</sub> (67.8 mg, 0.253 mmol) were each dissolved in 2 mL CH<sub>2</sub>Cl<sub>2</sub>. With stirring, the ligand solution was added dropwise to the (PhCN)<sub>2</sub>Pd<sup>II</sup>Cl<sub>2</sub> solution as the solution turned brownish and cloudy. The stirring was continued for 24 h. The yellow precipitate was filtered off, washed with diethyl ether and pentane and dried *in vacuo*. The product (<sup>Me</sup>N<sub>4</sub>)Pd<sup>II</sup>Cl<sub>2</sub> was isolated as a yellow solid. Yield: 65.8 mg, 58.4%.

ESI-MS of solution of (<sup>Me</sup>N<sub>4</sub>)Pd<sup>II</sup>Cl<sub>2</sub> in MeCN, m/z 409.0406; calcd. for [(<sup>Me</sup>N<sub>4</sub>)Pd<sup>II</sup>Cl]<sup>+</sup>, 409.0411.

<sup>1</sup>H NMR (300MHz, DMSO-*d*<sub>6</sub>), δ: 7.82 (t, *J* = 7.2Hz, 2H, py-H), 7.43 (d, *J* = 7.8Hz, 4H, py-H), 6.29 (d, *J* = 14.4Hz, 4H, -CH<sub>2</sub>-), 4.48 (d, *J* = 14.1Hz, 4H, -CH<sub>2</sub>-), 2.21 (s, 6H, N-CH<sub>3</sub>).

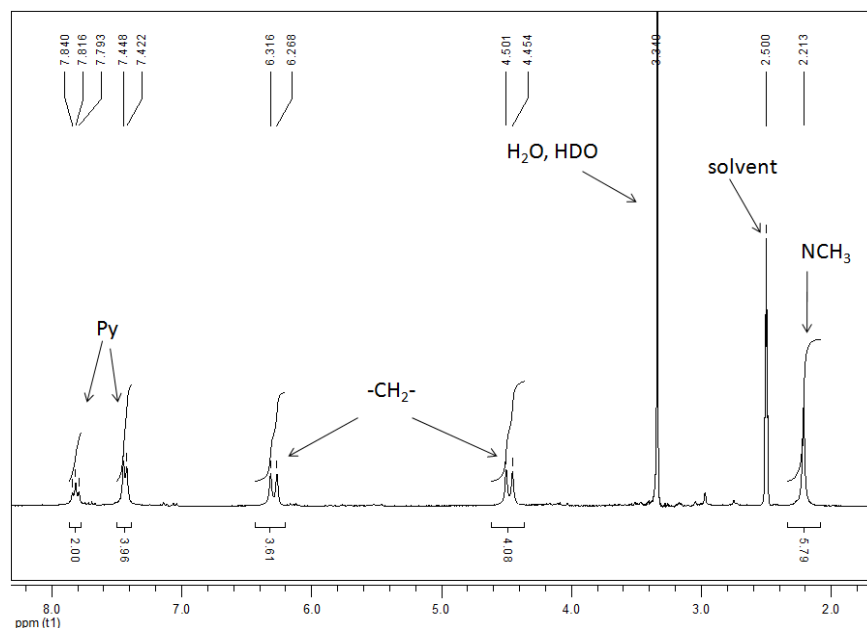
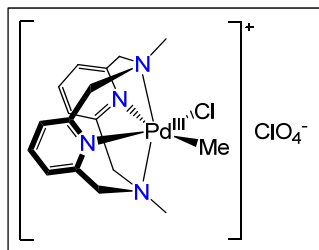


**Figure S9.** <sup>1</sup>H NMR spectrum of (<sup>Me</sup>N<sub>4</sub>)Pd<sup>II</sup>Cl<sub>2</sub> in DMSO-*d*<sub>6</sub>.

### Preparation of $[(^{\text{Me}}\text{N}_4)\text{Pd}^{\text{III}}\text{MeCl}]\text{ClO}_4$



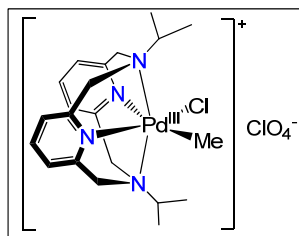
The controlled potential electrolysis was performed in a stirred suspension of  $(^{\text{Me}}\text{N}_4)\text{Pd}^{\text{II}}\text{MeCl}$  (107.2 mg, 0.2 mmol) in 12.0 mL 0.03 M  $\text{Bu}_4\text{NClO}_4$  solution in MeCN inside the anodic compartment of the electrolysis cell, while 12.0 mL 0.03 M  $\text{Bu}_4\text{NClO}_4$  solution in MeCN was in the cathodic compartment. The electrolysis potential was set as 260 mV vs. Ag/0.01 M  $\text{AgNO}_3$  based on the CV measured in the same electrolysis cell. The color of the solution turned dark purple quickly during the electrochemical oxidation. The electrolysis was stopped after the charge corresponding to a one-electron oxidation has passed through the cell. The remaining dark purple solution was filtered and then diethylether was diffused at  $-20\text{ }^\circ\text{C}$  for a few days to afford dark purple crystals suitable for X-ray crystallography. The crystals were filtered, washed with ether and pentane and dried *in vacuo*. Yield: 95.7 mg, 72.3%.

UV-vis,  $\lambda$ , nm ( $\epsilon$ ,  $\text{M}^{-1}\cdot\text{cm}^{-1}$ ), MeCN: 606 (615), 475 (480), 316 (3550).

$\mu_{\text{eff}} = 1.86\ \mu_{\text{B}}$  (298 K, Evans method,  $\text{DMSO}-d_6$ ).

ESI-MS  $[(^{\text{Me}}\text{N}_4)\text{Pd}^{\text{III}}\text{MeCl}]^+$  in MeCN,  $m/z$  424.0657; calcd. for  $[(^{\text{Me}}\text{N}_4)\text{Pd}^{\text{III}}\text{MeCl}]^+$ , 424.0646.

Anal. Found: C, 39.09; H, 4.46; N, 11.46; calcd. for  $[(^{\text{Me}}\text{N}_4)\text{Pd}^{\text{III}}\text{MeCl}]\text{ClO}_4$ : C, 38.91; H, 4.42; N, 10.68. The experimental elemental analysis results are slightly off, likely due to the slow decomposition of  $[(^{\text{Me}}\text{N}_4)\text{Pd}^{\text{III}}\text{MeCl}]^+$  at RT.



$[(iPr_4N)Pd^{III}MeCl]^+ (2^+)$  was synthesized following a similar procedure. Yield: 44.1%.

UV-vis,  $\lambda$ , nm ( $\epsilon$ ,  $M^{-1} \cdot cm^{-1}$ ), MeCN: 658 (810), 517 (580), 312 (4020).

$\mu_{eff} = 1.92 \mu_B$  (298 K, Evans method,  $dms\text{-}d_6$ ).

ESI-MS  $[(iPr_4N)Pd^{III}MeCl]ClO_4$  in MeCN,  $m/z$  480.1269; calculated for  $[(iPr_4N)Pd^{III}MeCl]^+$ , 480.1272.

Anal. Found: C, 43.91; H, 5.67; N, 9.62; calcd. for  $[(iPr_4N)Pd^{III}MeCl]ClO_4$ : C, 43.43; H, 5.38; N, 9.65.

Note: The diamagnetic impurities in the freshly synthesized  $[(iPr_4N)Pd^{III}MeCl](ClO_4)$  are present in less than 5%, as observed by NMR.

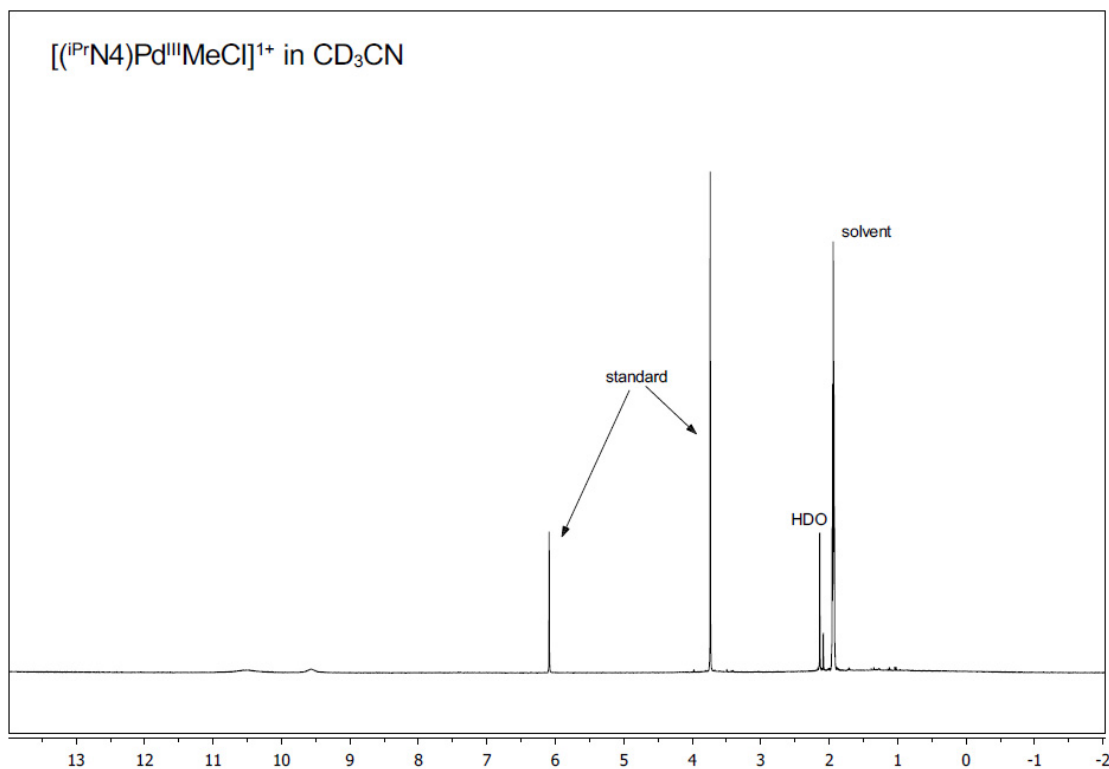
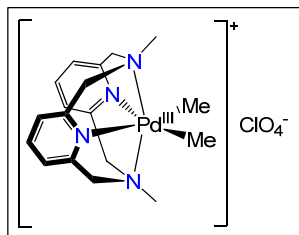


**Figure S10.**  $^1H$  NMR spectrum of  $[(iPr_4N)Pd^{III}MeCl]^+, 2^+$ , in  $CD_3CN$ .

### Preparation of $[(^R\text{N}4)\text{Pd}^{\text{III}}\text{Me}_2]\text{ClO}_4$ and $[(^R\text{N}4)\text{Pd}^{\text{III}}(\text{CD}_3)_2]\text{ClO}_4$



A solution of  $\text{FcPF}_6$  (41.3 mg, 0.125 mmol) in 2.1 mL MeCN was added dropwise to a stirred suspension of  $(^{\text{Me}}\text{N}4)\text{Pd}^{\text{II}}\text{Me}_2$  (50.6 mg, 0.125 mmol) in 5 mL MeCN at room temperature under  $\text{N}_2$ . The stirring was continued for 30 minutes after the addition and the resulting dark green solution was filtered through a syringe filter and then concentrated to about 2 mL. Solid  $\text{LiClO}_4$  (5 equiv, 66.1 mg, 0.624 mmol) was added to the filtrate to precipitate a dark green crystalline solid. Upon storing at the solution at  $-35^\circ\text{C}$ , big dark green crystals formed that were isolated by filtration, washed with small amounts of diethyl ether and pentane, and dried under vacuum. Yield: 13.4 mg, 21.3%.

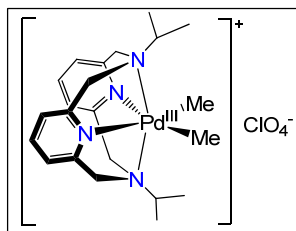
UV-vis,  $\lambda$ , nm ( $\epsilon$ ,  $\text{M}^{-1}\cdot\text{cm}^{-1}$ ), MeCN: 620 (405), 490 (430), 365 (1500).

$\mu_{\text{eff}} = 1.56 \mu_{\text{B}}$  (298 K, Evans method,  $\text{CD}_3\text{CN}$ ).

ESI-MS  $[(^{\text{Me}}\text{N}4)\text{Pd}^{\text{III}}\text{Me}_2]^+$  in MeCN,  $m/z$  404.1212; calcd. for  $[(^{\text{Me}}\text{N}4)\text{Pd}^{\text{III}}\text{Me}_2]^+$ , 404.1192.

Anal. Found: C, 44.43; H, 5.78; N, 12.86; calcd. for  $[(^{\text{Me}}\text{N}4)\text{Pd}^{\text{III}}\text{Me}_2]\text{ClO}_4\cdot\text{MeCN}$ : C, 44.05; H, 5.36; N, 12.84.

$[(^{\text{Me}}\text{N}4)\text{Pd}^{\text{III}}(\text{CD}_3)_2]\text{ClO}_4$ , ( $3^+-d_6$ ) $\text{ClO}_4$ , was synthesized using a similar procedure by treating  $(^{\text{Me}}\text{N}4)\text{Pd}^{\text{II}}(\text{CD}_3)_2$  with 1eq of  $\text{FcPF}_6$  to give dark green crystals. Yield 25.3%.



$[(iPr_4N)Pd^{III}Me_2]ClO_4$  ( $4^+$ ) was synthesized following a similar procedure. Yield: 26.7%.

UV-vis,  $\lambda$ , nm ( $\epsilon$ ,  $M^{-1} \cdot cm^{-1}$ ), MeCN: 666 (623), 500 (500), 339 (4545).

$\mu_{eff} = 1.97 \mu_B$  (298 K, Evans method,  $CD_3CN$ ).

ESI-MS of  $[(iPr_4N)Pd^{III}Me_2]ClO_4$ , MeCN:  $m/z$  460.1814, calcd. for  $[(iPr_4N)Pd^{III}Me_2]^+$  460.1818.

Anal. Found: C, 45.63; H, 5.92; N, 10.12; calcd. for  $[(iPr_4N)Pd^{III}Me_2]ClO_4 \cdot MeCN$ : C, 47.93; H, 6.20; N, 11.64. The experimental elemental analysis results are slightly off, likely due to the slow decomposition of  $[(iPr_4N)Pd^{III}Me_2]^+$  at RT.

Note: The diamagnetic impurities in the freshly synthesized  $[(iPr_4N)Pd^{III}Me_2](ClO_4)$  are present in less than 7%, as observed by NMR.

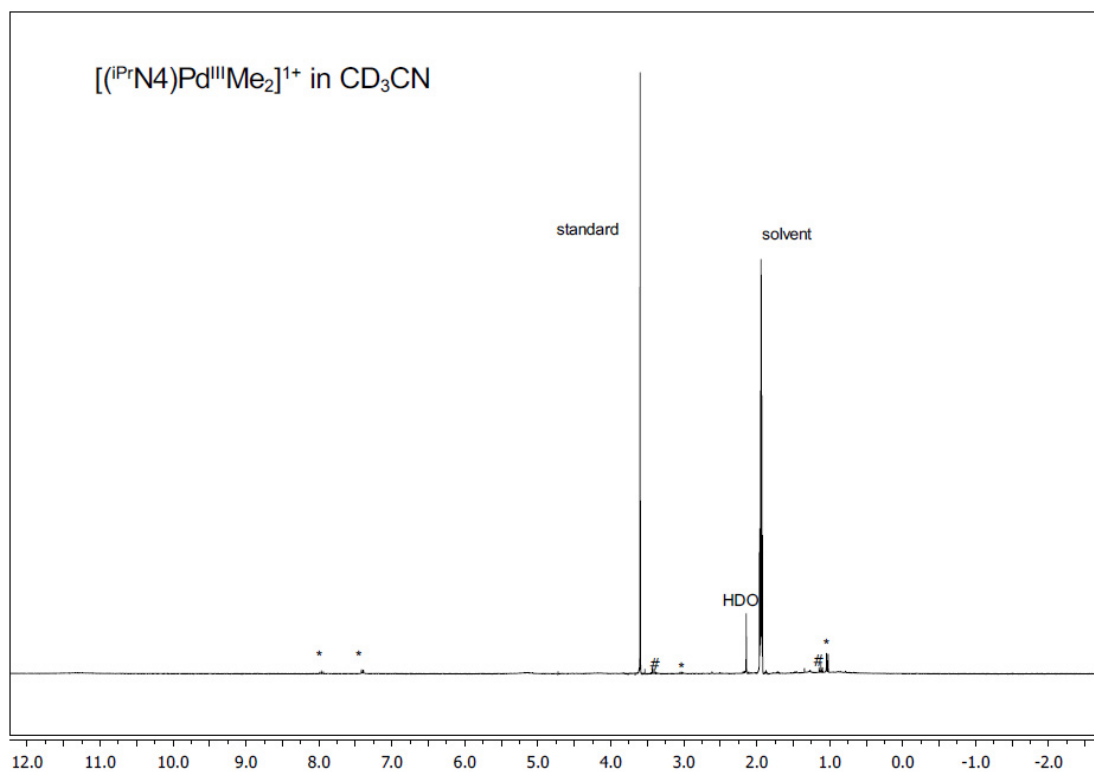
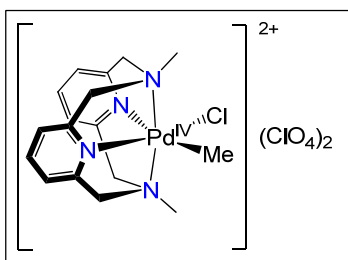


**Figure S11.**  $^1\text{H}$  NMR spectrum of  $[(^i\text{PrN4})\text{Pd}^{\text{III}}\text{Me}_2]^+$ ,  $\mathbf{4}^+$ , in  $\text{CD}_3\text{CN}$ . The peaks marked with an asterisk correspond to the protonated ligand,  $[(^i\text{PrN4}\cdot\text{H})]^+$ , which amounts to  $<5\%$ , based on integration vs. an internal standard. The peaks marked with # correspond to diethyl ether, which amounts to  $<2\%$ .

$[(^i\text{PrN4})\text{Pd}^{\text{III}}(\text{CD}_3)_2]\text{ClO}_4$ ,  $(\mathbf{4}^+-d_6)\text{ClO}_4$ , was synthesized using a similar procedure as for  $(\mathbf{3}^+-d_6)\text{ClO}_4$  and obtained in 28% yield.

## Preparation of [(<sup>R</sup>N<sub>4</sub>)Pd<sup>IV</sup>MeCl](ClO<sub>4</sub>)<sub>2</sub>

### 1) Preparation of [(<sup>Me</sup>N<sub>4</sub>)Pd<sup>IV</sup>MeCl](ClO<sub>4</sub>)<sub>2</sub>



A solution of NOBF<sub>4</sub> (16.0 mg, 0.137 mmol) in 2 mL MeCN was added dropwise to a stirred solution of [(<sup>Me</sup>N<sub>4</sub>)Pd<sup>III</sup>MeCl]ClO<sub>4</sub> (47.8 mg, 0.091 mmol) in 3 mL MeCN at room temperature under N<sub>2</sub>. The stirring was continued for 30 minutes and then solid LiClO<sub>4</sub> (14.5 mg, 0.548 mmol) was added. The solution was concentrated to about 1 mL and set up for ether diffusion at -35 °C to give yellow crystals overnight. The crystals were filtered off and dried under vacuum. Yield: 34.5 mg, 53.8%.

UV-vis, λ, nm (ε, M<sup>-1</sup>\*cm<sup>-1</sup>), MeCN: 590 (55), 410 (810), 330 (2630).

ESI-MS of [(<sup>Me</sup>N<sub>4</sub>)Pd<sup>IV</sup>MeCl](ClO<sub>4</sub>)<sub>2</sub> in MeCN, m/z 523.0134; calculated for [[(<sup>Me</sup>N<sub>4</sub>)Pd<sup>IV</sup>MeCl](ClO<sub>4</sub>)]<sup>+</sup>, 523.0131; m/z 212.0318; calculated for [(<sup>Me</sup>N<sub>4</sub>)Pd<sup>IV</sup>MeCl]<sup>2+</sup>, 212.0323.

Anal. Found: C, 33.33; H, 3.62; N, 9.65; calcd. for [(<sup>Me</sup>N<sub>4</sub>)Pd<sup>IV</sup>MeCl](ClO<sub>4</sub>)<sub>2</sub>•½(CH<sub>3</sub>CN): C, 33.53; H, 3.83; N, 9.78.

Note: The freshly synthesized product [(<sup>Me</sup>N<sub>4</sub>)Pd<sup>IV</sup>MeCl](ClO<sub>4</sub>)<sub>2</sub> is more than 95% pure, as observed by NMR.

<sup>1</sup>H NMR (300MHz, CD<sub>3</sub>CN), δ: 8.07 (t, *J* = 7.8 Hz, 1H, py-H), 8.03 (t, *J* = 7.8 Hz, 1H, py-H), 7.57 (d, *J* = 9.0 Hz, 2H, py-H), 7.54 (d, *J* = 8.4 Hz, 2H, py-H), 5.48(d, *J* = 16.5 Hz, 2H, -CH<sub>2</sub>-), 5.40 (d, *J* = 18.0 Hz, 2H, -CH<sub>2</sub>-), 4.85 (d, *J* = 16.0 Hz, 4H, -CH<sub>2</sub>-), 3.37 (s, 3H, Pd-CH<sub>3</sub>), 3.30 (s, 6H, N-CH<sub>3</sub>).

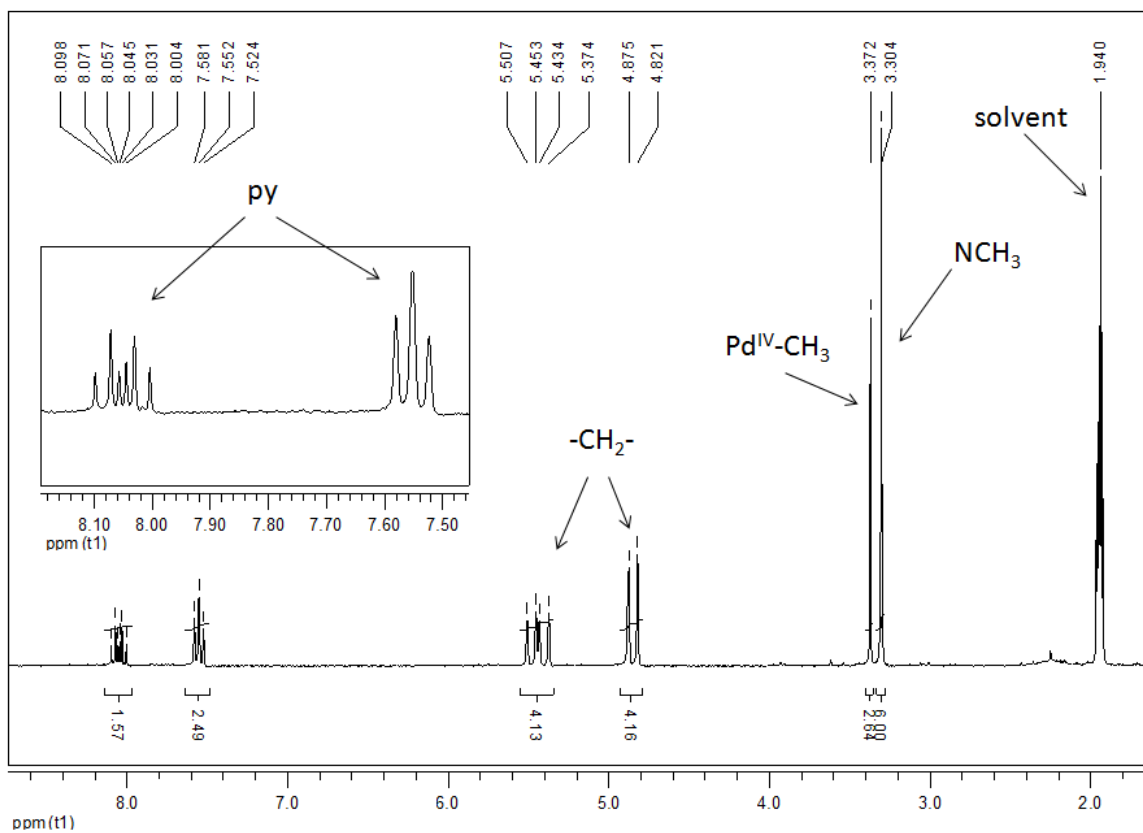
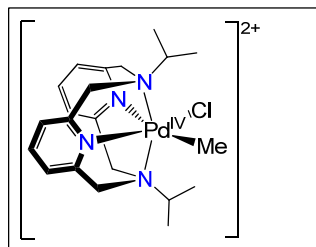


**Figure S12.**  $^1\text{H}$  NMR spectrum of  $[(^{\text{Mc}}\text{N}_4)\text{Pd}^{\text{IV}}\text{MeCl}]^{2+}$ ,  $\mathbf{1}^{2+}$  in  $\text{CD}_3\text{CN}$ .

## 2) Preparation of $[(iPr_4N)Pd^{IV}MeCl]^{2+}$



$[(iPr_4N)Pd^{III}MeCl]ClO_4$  (3.0 mg, 0.005 mmol) was dissolved in 1.0 mL of  $CD_3CN$  and transferred into an NMR tube. 1 equiv of  $NOBF_4$  (21.1 mM in  $CD_3CN$ ) was added to the NMR tube, mixed, and the  $^1H$  NMR was recorded immediately. The product could not be isolated due to its instability.

**Note:** The freshly synthesized product  $[(iPr_4N)Pd^{IV}MeCl](ClO_4)_2$  is more than 95% pure, as observed by NMR.

$^1H$  NMR of  $[(iPr_4N)Pd^{IV}MeCl]^{2+}$  in  $CD_3CN$ :  $\delta$ : 8.14 (d,  $J = 8.1$  Hz, 1H, py-H), 8.10 (t,  $J = 8.1$  Hz, 1H, py-H), 7.60 (t,  $J = 8.1$  Hz, 4H, py-H), 5.44 (d,  $J = 16.2$  Hz, 2H,  $-CH_2-$ ), 5.34 (d,  $J = 17.4$  Hz, 2H,  $-CH_2-$ ), 4.65 (d,  $J = 16.8$  Hz, 2H,  $-CH_2-$ ), 4.63 (d,  $J = 17.4$  Hz, 2H,  $-CH_2-$ ), 4.09 (m,  $J = 6.6$  Hz, 2H,  $iPr-CH$ ), 3.39 (s, 3H, Pd-Me), 1.59 (d,  $J = 6.3$  Hz, 6H,  $iPr-CH_3$ ), 1.53 (d,  $J = 6.6$  Hz, 6H,  $iPr-CH_3$ ).

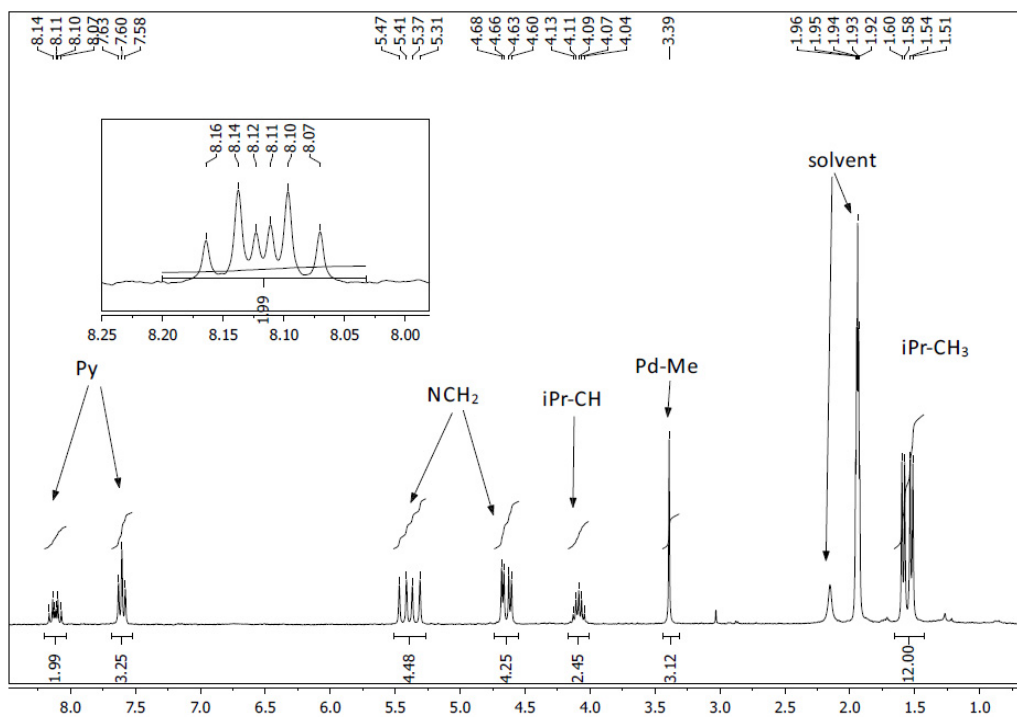
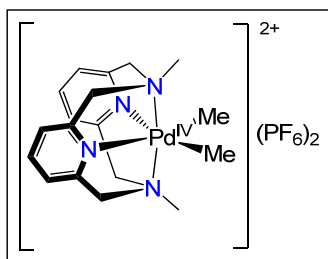


**Figure S13.**  $^1H$  NMR spectrum of  $[(iPr_4N)Pd^{IV}MeCl]^{2+}$ ,  $2^{2+}$  in  $CD_3CN$ .

## Preparation of $[(^R\text{N}4)\text{Pd}^{\text{IV}}\text{Me}_2](\text{PF}_6)_2$ and $[(^R\text{N}4)\text{Pd}^{\text{IV}}(\text{CD}_3)_2](\text{PF}_6)_2$

### 1) Preparation of $[(^{\text{Me}}\text{N}4)\text{Pd}^{\text{IV}}\text{Me}_2](\text{PF}_6)_2$



A solution of  $\text{FcPF}_6$  (61.9 mg, 0.187 mmol) in 3 mL MeCN was added dropwise to a stirred suspension of  $(^{\text{Me}}\text{N}4)\text{Pd}^{\text{II}}\text{Me}_2$  (37.9 mg, 0.0935 mmol) in 4 mL MeCN at room temperature under  $\text{N}_2$ . The stirring was continued for 30 minutes and the resulting red solution was filtered through a cotton plug, concentrated to about 2 mL and set up for ether diffusion at  $-35\text{ }^\circ\text{C}$ . Red needle-like crystals formed within 2-3 days. Yield: 39.5 mg, 61%.

UV-vis,  $\lambda$ , nm ( $\epsilon$ ,  $\text{M}^{-1}\cdot\text{cm}^{-1}$ ), MeCN: 527 (170), 328 (3060), 264 (5090).

ESI-MS of  $[(^{\text{Me}}\text{N}4)\text{Pd}^{\text{IV}}\text{Me}_2](\text{PF}_6)_2$  in MeCN,  $m/z$  549.0828; calcd. for  $[(^{\text{Me}}\text{N}4)\text{Pd}^{\text{IV}}\text{Me}_2](\text{PF}_6)^+$ , 549.0834;  $m/z$  202.0591; calculated for  $[(^{\text{Me}}\text{N}4)\text{Pd}^{\text{IV}}\text{Me}_2]^{2+}$ , 202.0596.

Anal. Found: C, 32.28; H, 3.43; N, 8.25; calcd. for  $[(^{\text{Me}}\text{N}4)\text{Pd}^{\text{IV}}\text{Me}_2](\text{PF}_6)_2 \cdot \frac{1}{2}(\text{CH}_3\text{CN})$ : C, 31.90; H, 3.88; N, 8.81. The experimental elemental analysis results are slightly off, likely due to the slow decomposition of  $[(^{\text{Me}}\text{N}4)\text{Pd}^{\text{IV}}\text{Me}_2]^{2+}$  at RT.

Note: The freshly synthesized product  $[(^{\text{Me}}\text{N}4)\text{Pd}^{\text{IV}}\text{Me}_2](\text{PF}_6)_2$  is more than 95% pure, as observed by NMR.

$^1\text{H}$  NMR (300MHz,  $\text{CD}_3\text{CN}$ ):  $\delta$ : 7.90 (t,  $J = 8.1$  Hz, 2H, py-H), 7.39 (d,  $J = 7.8$  Hz, 4H, py-H), 5.11 (d,  $J = 16.2$  Hz, 4H,  $-\text{CH}_2-$ ), 4.60 (d,  $J = 16.2$  Hz, 4H,  $-\text{CH}_2-$ ), 3.11 (s, 6H, N- $\text{CH}_3$ ), 2.40 (s, 6H, Pd- $\text{CH}_3$ ).

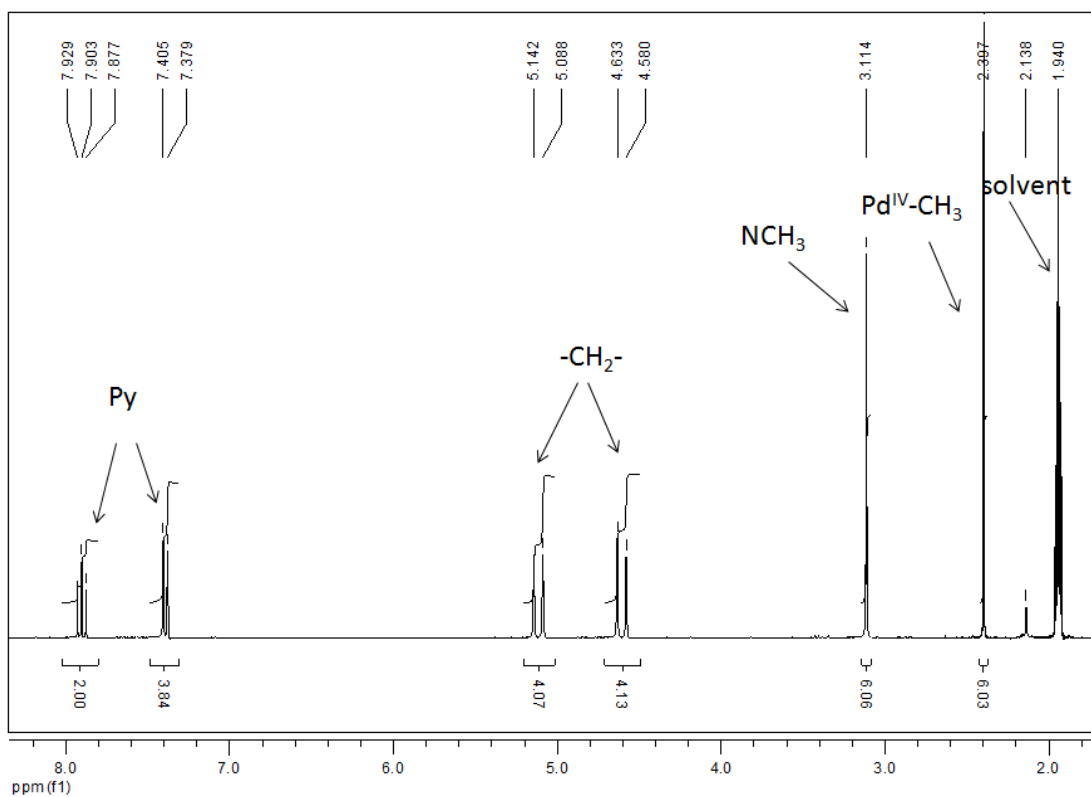
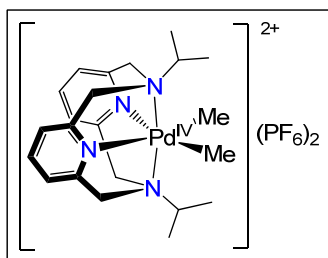


**Figure S14.** <sup>1</sup>H NMR spectrum of [<sup>14</sup>C]Pd<sup>IV</sup>Me<sub>2</sub>(PF<sub>6</sub>)<sub>2</sub>, [**3**<sup>2+</sup>](PF<sub>6</sub>)<sub>2</sub> in CD<sub>3</sub>CN.

A similar procedure was used to make [<sup>14</sup>C]Pd<sup>IV</sup>(CD<sub>3</sub>)<sub>2</sub>(PF<sub>6</sub>)<sub>2</sub>, [**3**<sup>2+</sup>-d<sub>6</sub>](PF<sub>6</sub>)<sub>2</sub> by treating <sup>14</sup>CN<sub>4</sub>Pd<sup>II</sup>(CD<sub>3</sub>)<sub>2</sub> (17.0 mg, 0.0414 mmol) with 2eq FcPF<sub>6</sub>. Yield 17.4mg, 60%. The <sup>1</sup>H NMR spectrum of the product is identical to that of [<sup>14</sup>C]Pd<sup>IV</sup>Me<sub>2</sub>(PF<sub>6</sub>)<sub>2</sub> except for the missing singlet corresponding to the Pd-Me group.

## 2) Preparation of [(<sup>i</sup>PrN<sub>4</sub>)Pd<sup>IV</sup>Me<sub>2</sub>](PF<sub>6</sub>)<sub>2</sub>



A solution of FcPF<sub>6</sub> (41.2 mg, 0.1245 mmol) in 2 mL MeCN was added dropwise into a stirred suspension of (<sup>i</sup>PrN<sub>4</sub>)Pd<sup>II</sup>Me<sub>2</sub> (28.0 mg, 0.0607 mmol) in 5 mL MeCN under N<sub>2</sub>. The solution was stirred in the dark for 30 min and then filtered through a cotton plug. The solvent was evaporated and the residue dissolved in a small amount of MeCN, followed by addition of large amount of ether. The dark blue-green solution was decanted and the brown yellow precipitate was washed with diethyl ether until the ether wash became colorless; the brown yellow powder was dried under vacuum. X-ray quality crystals were obtained by ether diffusion into a MeCN solution. Yield: 25.8 mg, 56.7%.

UV-vis, λ, nm (ε, M<sup>-1</sup>\*cm<sup>-1</sup>), MeCN: 580 (164), 349 (3648), 251 (12875).

ESI-MS of [(<sup>i</sup>PrN<sub>4</sub>)Pd<sup>IV</sup>Me<sub>2</sub>](PF<sub>6</sub>)<sub>2</sub> in MeCN, m/z 230.0907; calcd. for [(<sup>Me</sup>cN<sub>4</sub>)Pd<sup>IV</sup>Me<sub>2</sub>]<sup>2+</sup>, 230.0908.

Anal. Found: C, 35.48; H, 4.12; N, 7.34; calcd. for [(<sup>i</sup>PrN<sub>4</sub>)Pd<sup>IV</sup>Me<sub>2</sub>](PF<sub>6</sub>)<sub>2</sub>: C, 35.19; H, 4.56; N, 7.46. The experimental elemental analysis results are slightly off, likely due to the slow decomposition of [(<sup>i</sup>PrN<sub>4</sub>)Pd<sup>IV</sup>Me<sub>2</sub>]<sup>2+</sup> at RT.

Note: The freshly synthesized product [(<sup>i</sup>PrN<sub>4</sub>)Pd<sup>IV</sup>Me<sub>2</sub>](PF<sub>6</sub>)<sub>2</sub> is more than 95% pure, as observed by NMR.

<sup>1</sup>H NMR in CD<sub>3</sub>CN: δ: 7.91 (t, *J* = 7.8 Hz, 2H, py-H), 7.39 (d, *J* = 7.8 Hz, 4H, py-H), 5.11 (d, *J* = 16.2 Hz, 4H, -CH<sub>2</sub>-), 4.49 (d, *J* = 16.2 Hz, 4H, -CH<sub>2</sub>-), 3.87 (m, *J* = 6.6 Hz, 2H, *i*Pr-CH), 2.61 (s, 6H, Pd-Me), 1.46 (d, *J* = 6.6 Hz, 12H, *i*Pr-CH<sub>3</sub>).

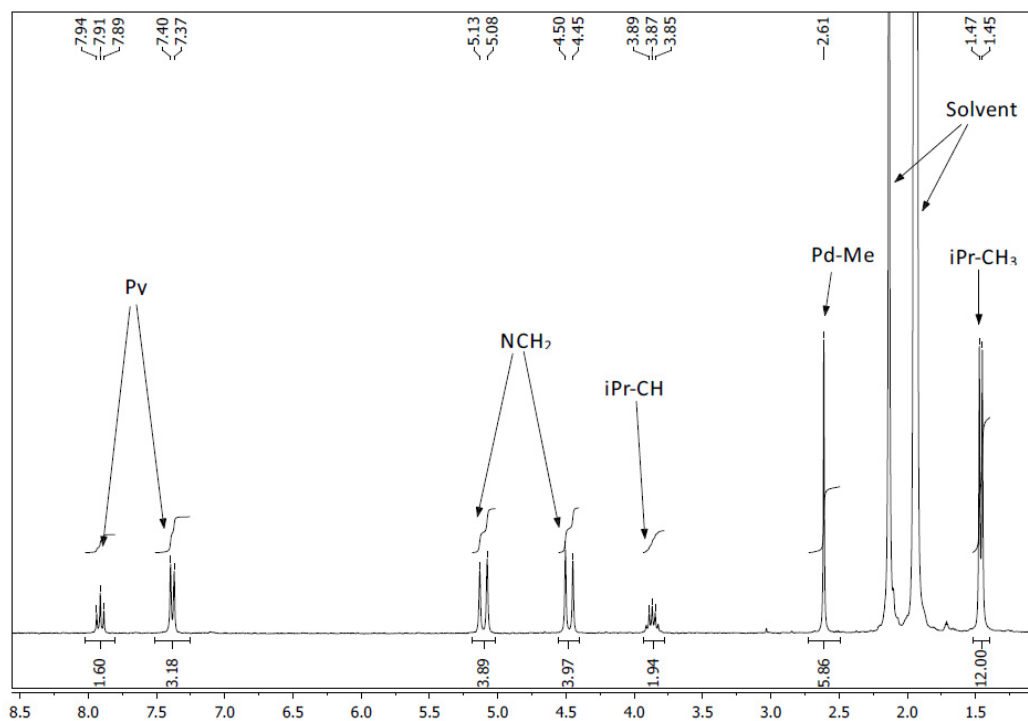


**Figure S15.** <sup>1</sup>H NMR spectrum of [(<sup>i</sup>PrN<sub>4</sub>)Pd<sup>IV</sup>Me<sub>2</sub>](PF<sub>6</sub>)<sub>2</sub>, **4**<sup>2+</sup>(PF<sub>6</sub>)<sub>2</sub> in CD<sub>3</sub>CN.

[(<sup>i</sup>PrN<sub>4</sub>)Pd<sup>IV</sup>(CD<sub>3</sub>)<sub>2</sub>](PF<sub>6</sub>)<sub>2</sub>, [**4**<sup>2+</sup>-d<sub>6</sub>](PF<sub>6</sub>)<sub>2</sub>, was synthesized following a similar procedure to give the product in 43% yield. The <sup>1</sup>H NMR spectrum of the product is identical to that of [(<sup>i</sup>PrN<sub>4</sub>)Pd<sup>IV</sup>Me<sub>2</sub>](PF<sub>6</sub>)<sub>2</sub> except for the missing singlet of the Pd-Me group.

### III. Cyclic voltammograms of 1-4

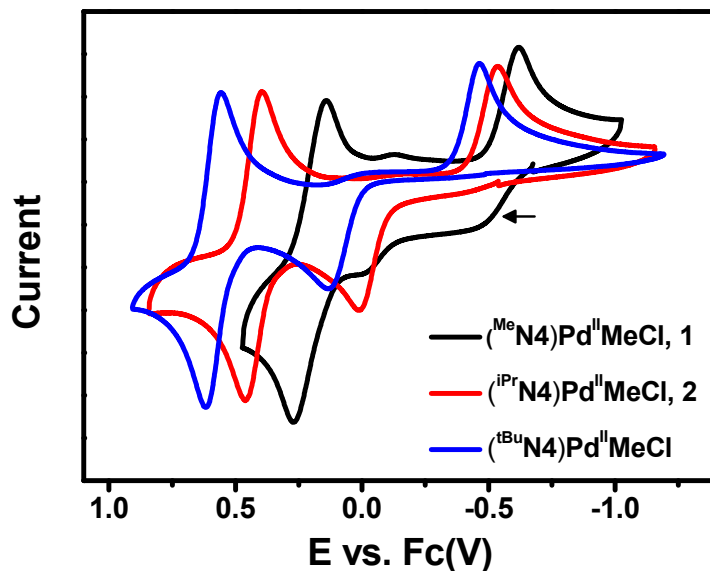


**Figure S16.** Overlay of the CV's of (R<sub>4</sub>N)<sup>+</sup>Pd<sup>II</sup>MeCl complexes 1, 2, and (tBu<sub>4</sub>N)<sup>+</sup>Pd<sup>II</sup>MeCl. Conditions: GCE, 0.1 M Bu<sub>4</sub>NClO<sub>4</sub>/CH<sub>2</sub>Cl<sub>2</sub>, 100 mV/s.

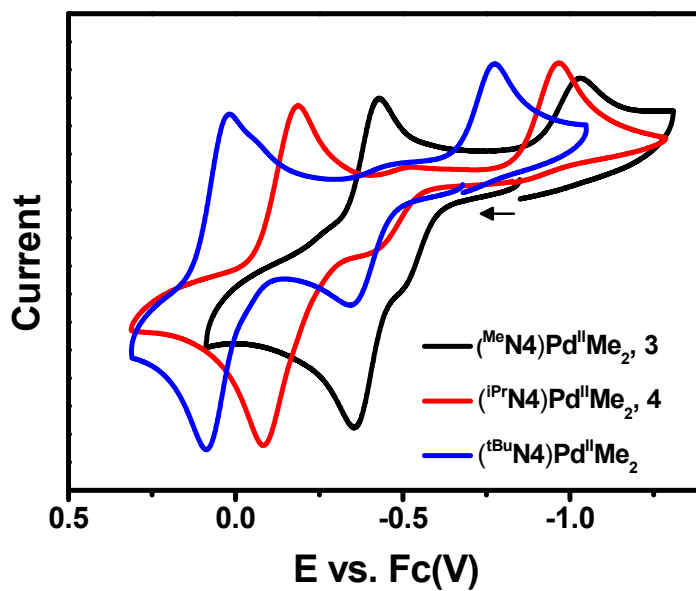


**Figure S17.** Overlay of the CV's of (R<sub>4</sub>N)<sup>+</sup>Pd<sup>II</sup>Me<sub>2</sub> complexes 3, 4, and (tBu<sub>4</sub>N)<sup>+</sup>Pd<sup>II</sup>Me<sub>2</sub>. Conditions: GCE, 0.1 M Bu<sub>4</sub>NClO<sub>4</sub>/MeCN, 100 mV/s.

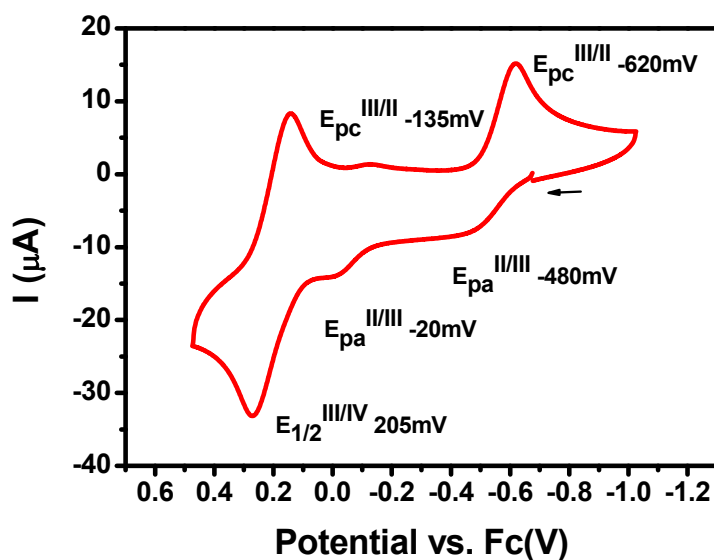


**Figure S18.** Cyclic voltammogram ( $\text{Me}_4\text{N}$ ) $\text{Pd}^{\text{II}}$ MeCl (**1**) in 0.1 M  $\text{Bu}_4\text{NClO}_4/\text{CH}_2\text{Cl}_2$ . Conditions: GCE, 100 mV/s.

Note: The presence of two oxidation and two reduction waves for the  $\text{Pd}^{\text{II/III}}$  redox couple is likely due to presence of two conformations of **1** in solution. More detailed electrochemical studies of these systems will be reported elsewhere.

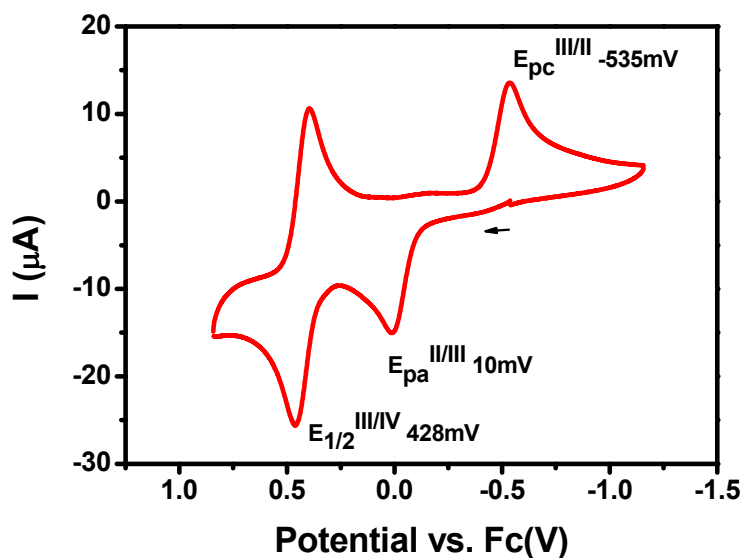


**Figure S19.** Cyclic voltammogram ( $\text{iPr}_4\text{N}$ ) $\text{Pd}^{\text{II}}$ MeCl (**2**) in 0.1 M  $\text{Bu}_4\text{NClO}_4/\text{CH}_2\text{Cl}_2$ . Conditions: GCE, 100 mV/s.

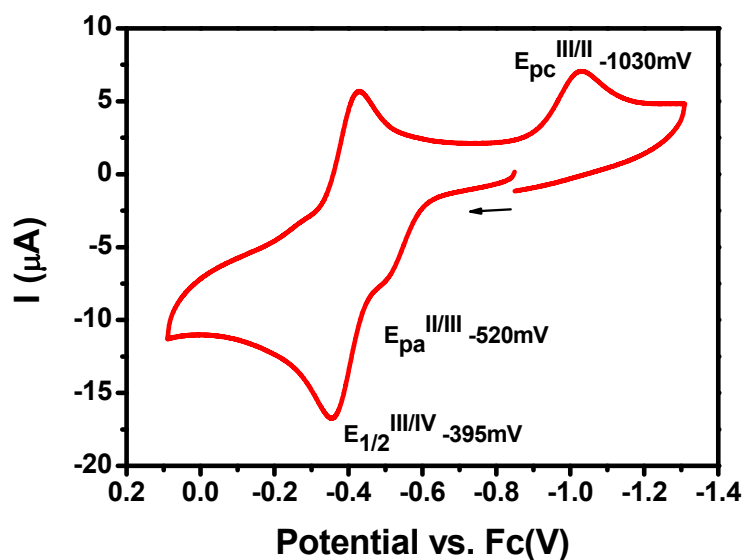


**Figure S20.** Cyclic voltammogram ( $^{\text{Me}}\text{N4}$ )Pd<sup>II</sup>Me<sub>2</sub> (3) in 0.1 M Bu<sub>4</sub>NClO<sub>4</sub>/MeCN. Conditions: GCE, 100 mV/s.

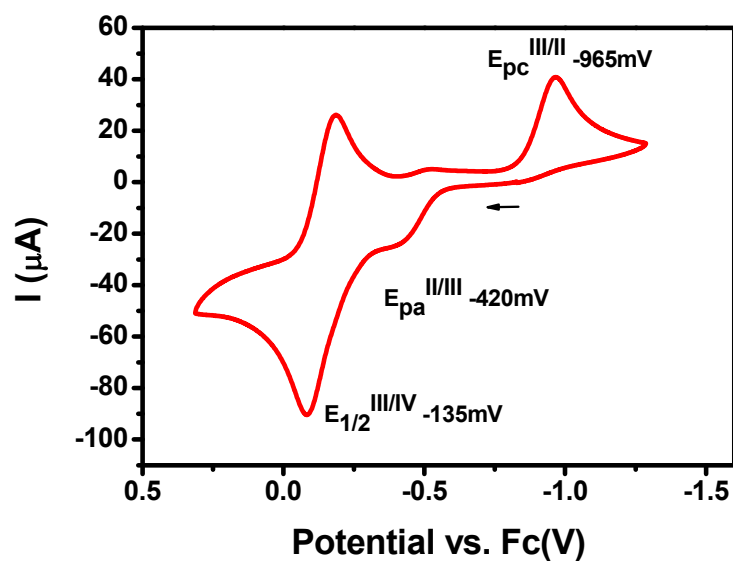


**Figure S21.** Cyclic voltammogram ( $^{\text{iPr}}\text{N4}$ )Pd<sup>II</sup>Me<sub>2</sub> (4) in 0.1 M Bu<sub>4</sub>NClO<sub>4</sub>/MeCN. Conditions: GCE, 100 mV/s.

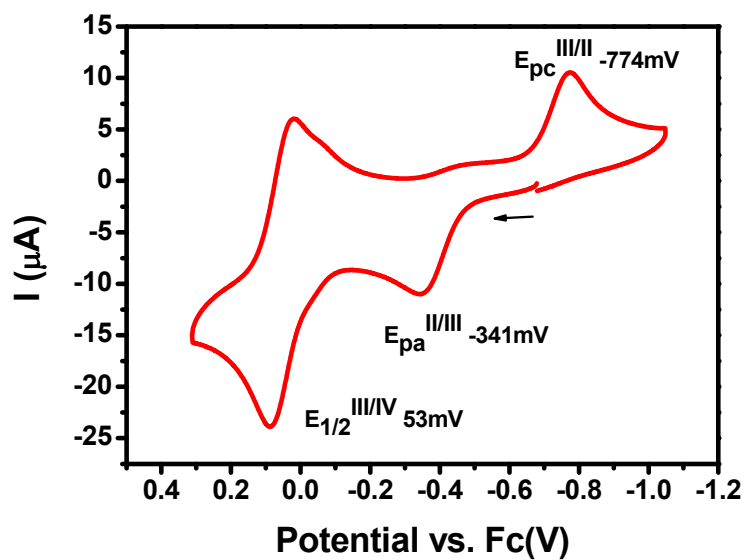


**Figure S22.** Cyclic voltammogram ( $^t\text{Bu}_4\text{N}$ ) $\text{Pd}^{\text{II}}\text{Me}_2$  in 0.1 M TBAP/MeCN. Conditions: GCE, 100 mV/s.

#### IV. UV-vis spectra of $1^{+}$ - $4^{+}$ , $1^{2+}$ , $3^{2+}$ , and $4^{2+}$

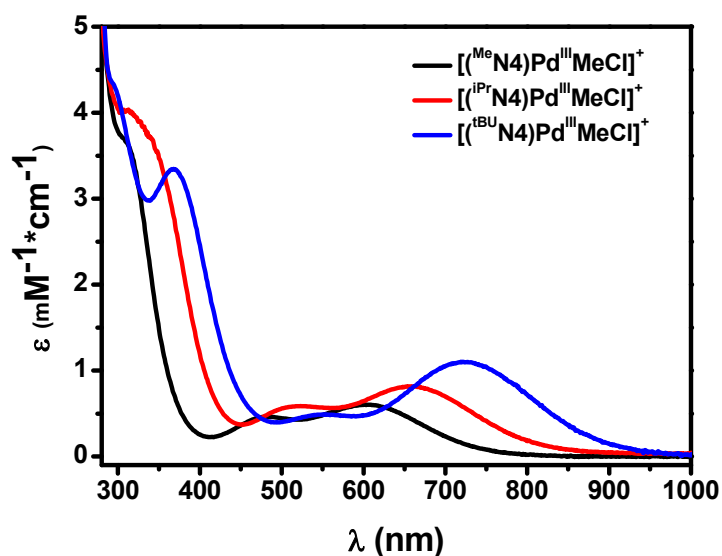


**Figure S23.** Overlay of UV-vis spectra for  $[(^R\text{N}4)\text{Pd}^{\text{III}}\text{MeCl}]^+$  ( $R = \text{Me}, \text{iPr}, \text{tBu}$ ).

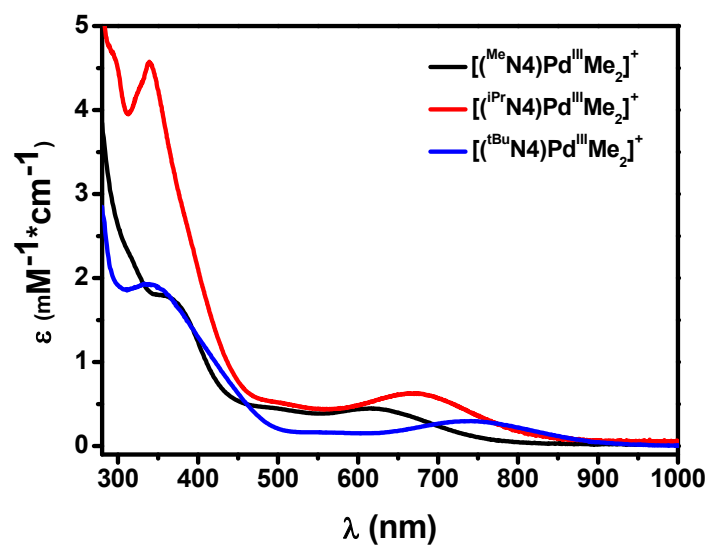


**Figure S24.** Overlay of UV-vis spectra of  $[(^R\text{N}4)\text{Pd}^{\text{III}}\text{Me}_2]^+$  ( $R = \text{Me}, \text{iPr}, \text{tBu}$ ).

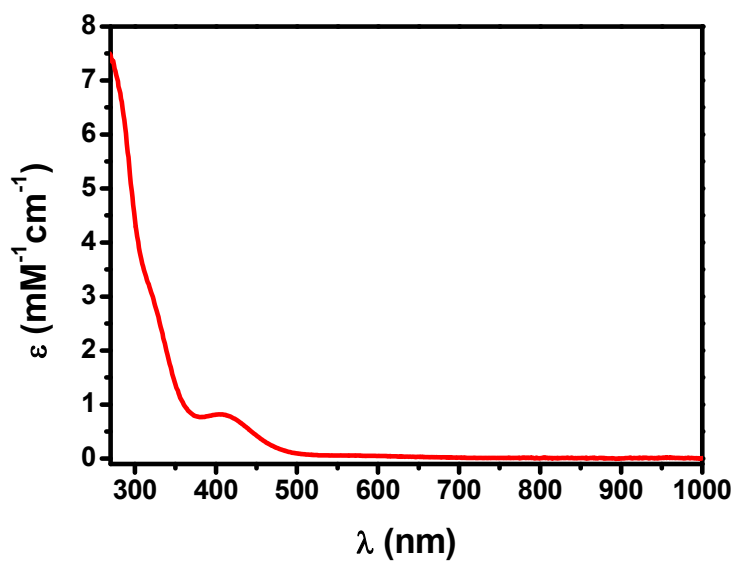


**Figure S25.** UV-vis spectrum of  $[(\text{MeCN})_4\text{Pd}^{\text{IV}}\text{MeCl}]^{2+}$  ( $1^{2+}$ ) in MeCN.

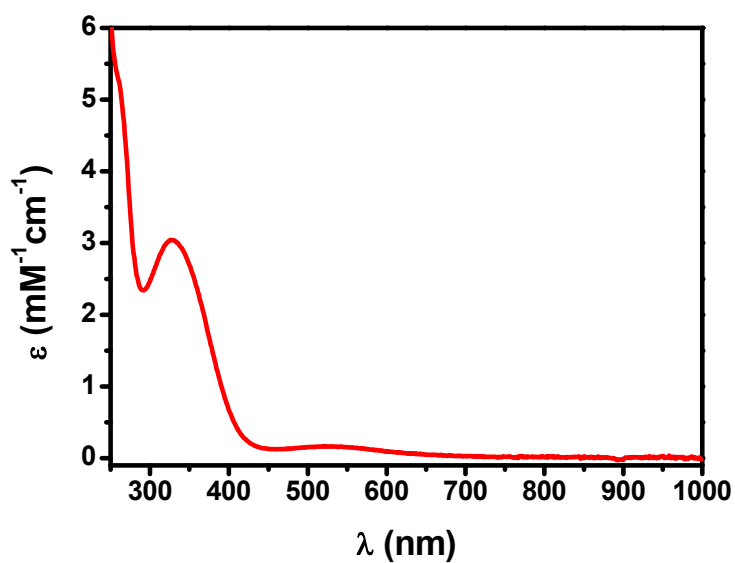


**Figure S26.** UV-vis spectrum of  $[(\text{MeCN})_4\text{Pd}^{\text{IV}}\text{Me}_2]^{2+}$  ( $3^{2+}$ ) in MeCN.

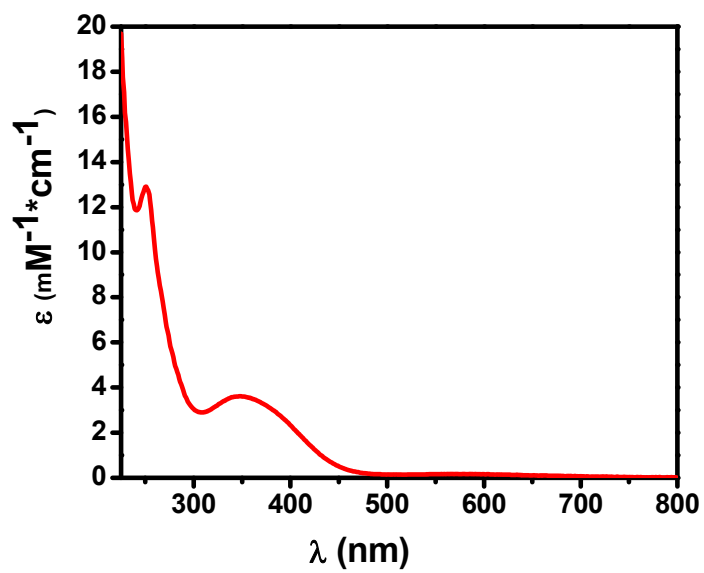


**Figure S27.** UV-vis spectrum of  $[(iPr_4N)Pd^{IV}Me_2]^{2+}$  ( $4^{2+}$ ) in MeCN.

### V. EPR spectra of $1^{+}$ - $4^{+}$ and $[(t^{\text{Bu}}\text{N}_4)\text{Pd}^{\text{III}}\text{MeCl}]^{+}$

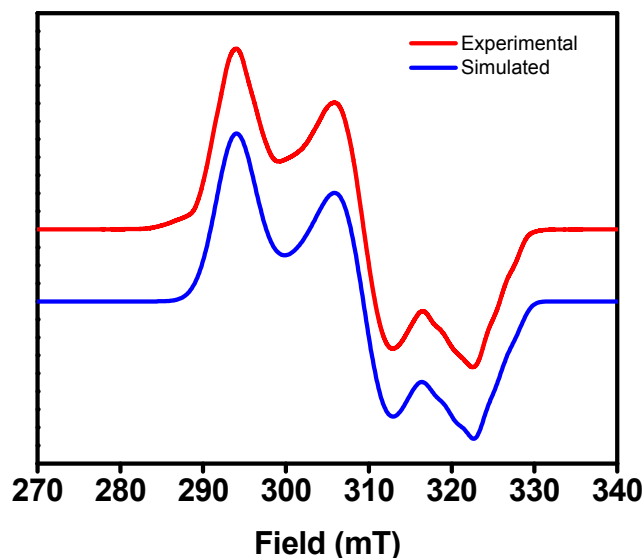


**Figure S28.** EPR spectrum of  $[(^{\text{Me}}\text{N}_4)\text{Pd}^{\text{III}}\text{MeCl}]\text{ClO}_4$  ( $[1^{+}]\text{ClO}_4$ ) in 3:1 PrCN:MeCN glass, 77 K. Frequency: 9099.911 MHz. Simulated spectrum parameters:  $g_x = 2.212$ ,  $g_y = 2.101$ ,  $g_z = 2.014$  ( $A_N = 23.0$  G).

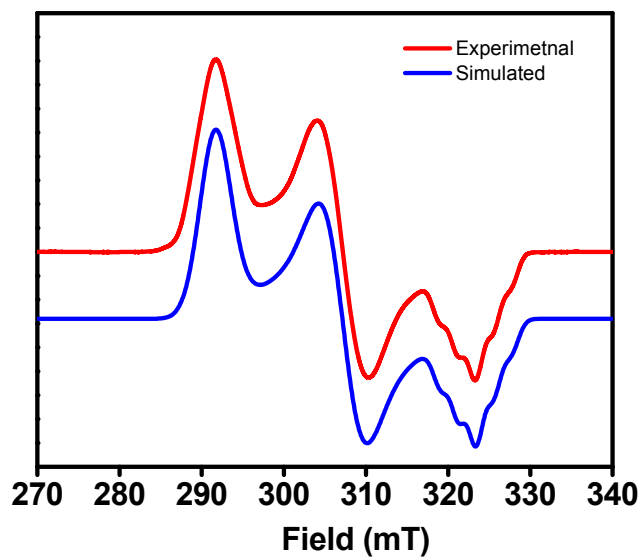


**Figure S29.** EPR spectrum of  $[(^{\text{iPr}}\text{N}_4)\text{Pd}^{\text{III}}\text{MeCl}]\text{ClO}_4$  ( $[2^{+}]\text{ClO}_4$ ) in 3:1 PrCN:MeCN glass, 77 K. Frequency: 9097.799 MHz. Simulated spectrum parameters:  $g_x = 2.228$ ,  $g_y = 2.115$ ,  $g_z = 2.011$  ( $A_N = 21.3$  G).

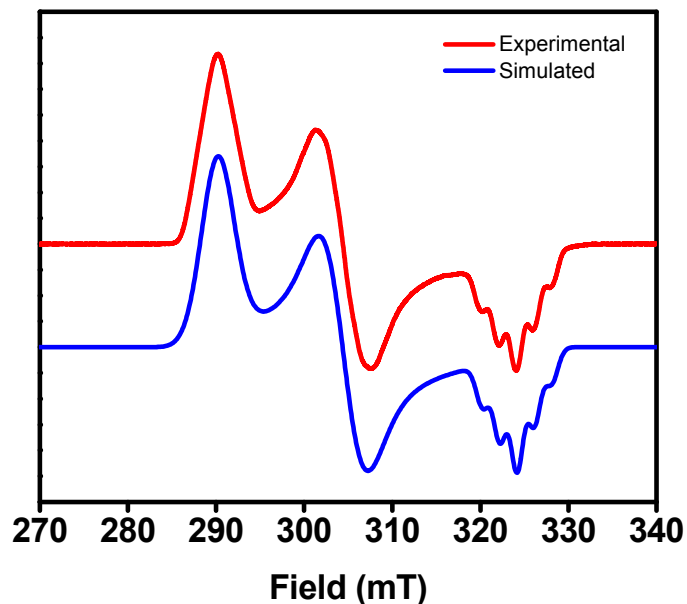


**Figure S30.** EPR spectrum of  $[(t\text{Bu}_4\text{N})\text{Pd}^{\text{III}}\text{MeCl}]\text{ClO}_4$  in 3:1 PrCN:MeCN glass, 77 K. Frequency: 9094.600 MHz. Simulated spectrum parameters:  $g_x = 2.239$ ,  $g_y = 2.134$ ,  $g_z = 2.005$  ( $A_N = 19.5$  G).

Note: In the previously reported EPR spectrum of  $[(t\text{Bu}_4\text{N})\text{Pd}^{\text{III}}\text{MeCl}]^+$ ,<sup>6</sup> the superhyperfine splitting was not resolved in frozen MeCN solution. However, the use of a glassing solvent mixture 3:1 PrCN:MeCN leads to EPR spectra with resolved superhyperfine coupling to the two axial N atoms.

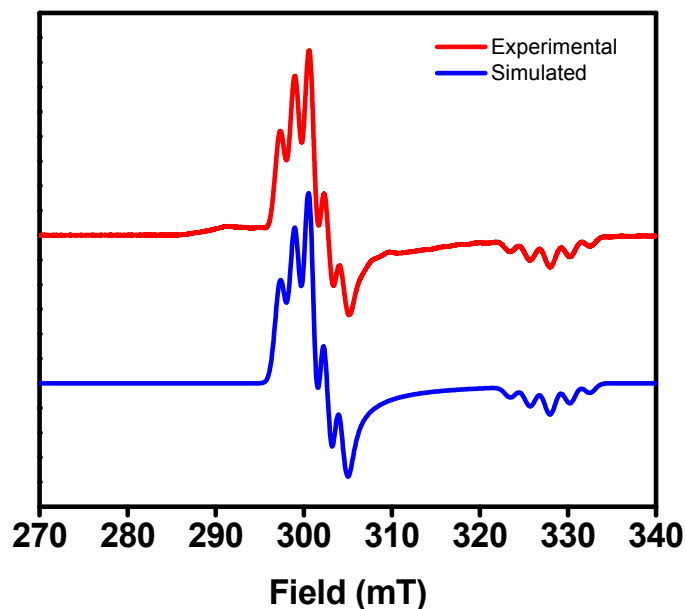


**Figure S31.** EPR spectrum of  $[(^{13}\text{C}4)\text{Pd}^{\text{III}}\text{Me}_2](\text{ClO}_4)$  ( $[3^+]\text{ClO}_4$ ) in 3:1 PrCN:MeCN glass, 77 K. Frequency: 9129.597 MHz. Simulated spectrum parameters:  $g_x = 2.168$  ( $A_N = 16.0$  G),  $g_y = 2.168$  ( $A_N = 16.0$  G),  $g_z = 1.989$  ( $A_N = 22.5$  G).

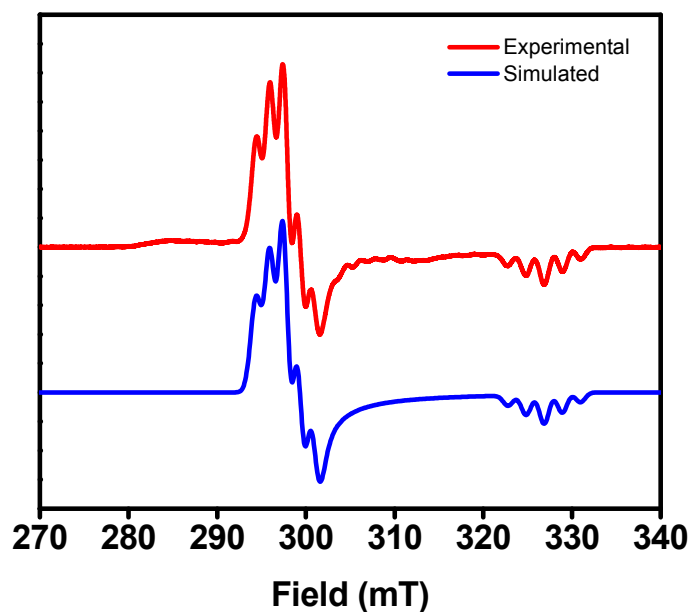


**Figure S32.** EPR spectrum of  $[(^{13}\text{Pr}4)\text{Pd}^{\text{III}}\text{Me}_2]\text{ClO}_4$  ( $[4^+]\text{ClO}_4$ ) in 3:1 PrCN:MeCN glass, 77 K. Frequency: 9097.611 MHz. Simulated spectrum parameters:  $g_x = 2.184$  ( $A_N = 15.0$  G),  $g_y = 2.184$  ( $A_N = 15.0$  G),  $g_z = 1.988$  ( $A_N = 20.4$  G).

VI. ORTEP and space filling models of  $1^{+}$ ,  $2^{+}$ ,  $3^{2+}$ , and  $4^{2+}$

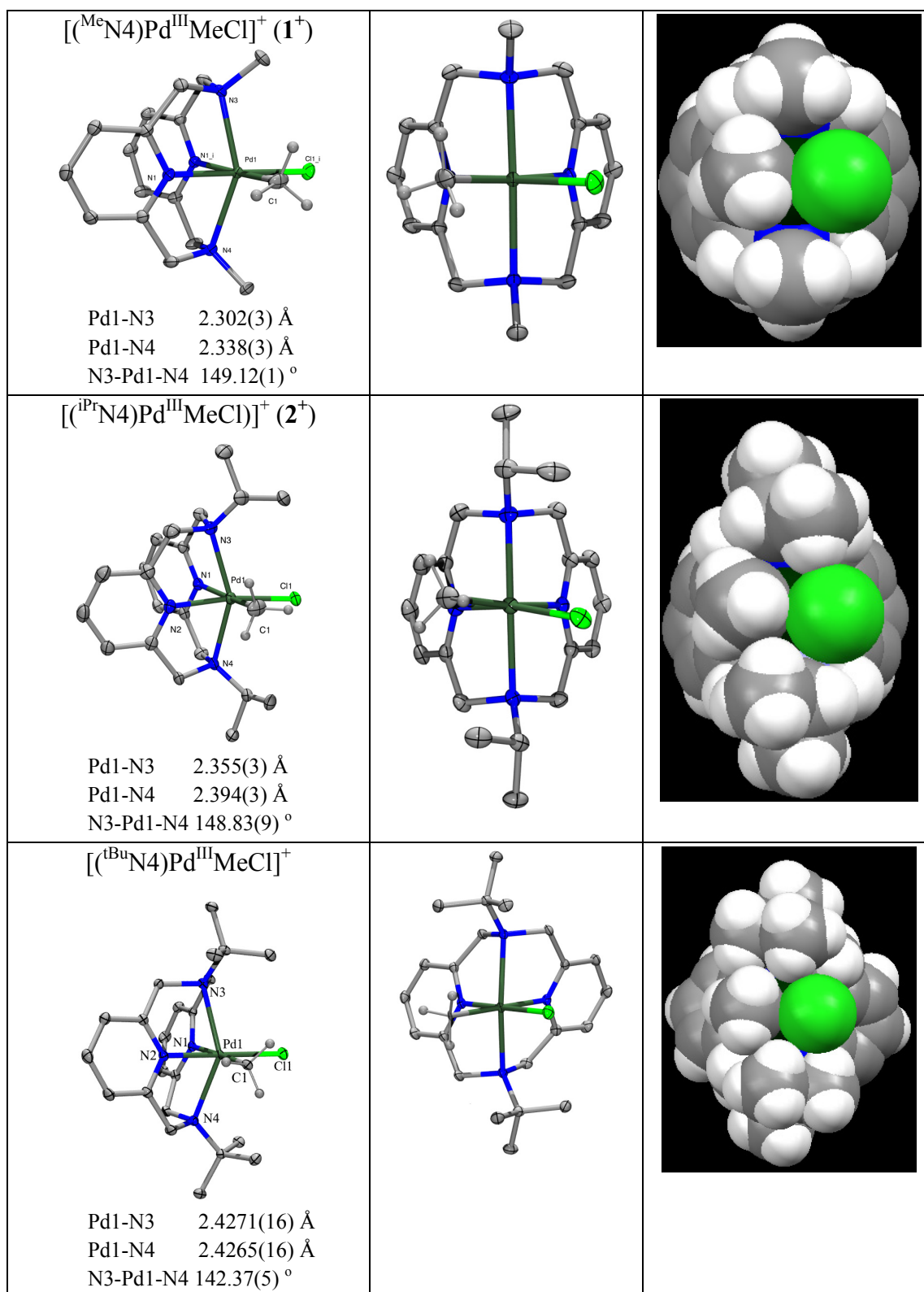
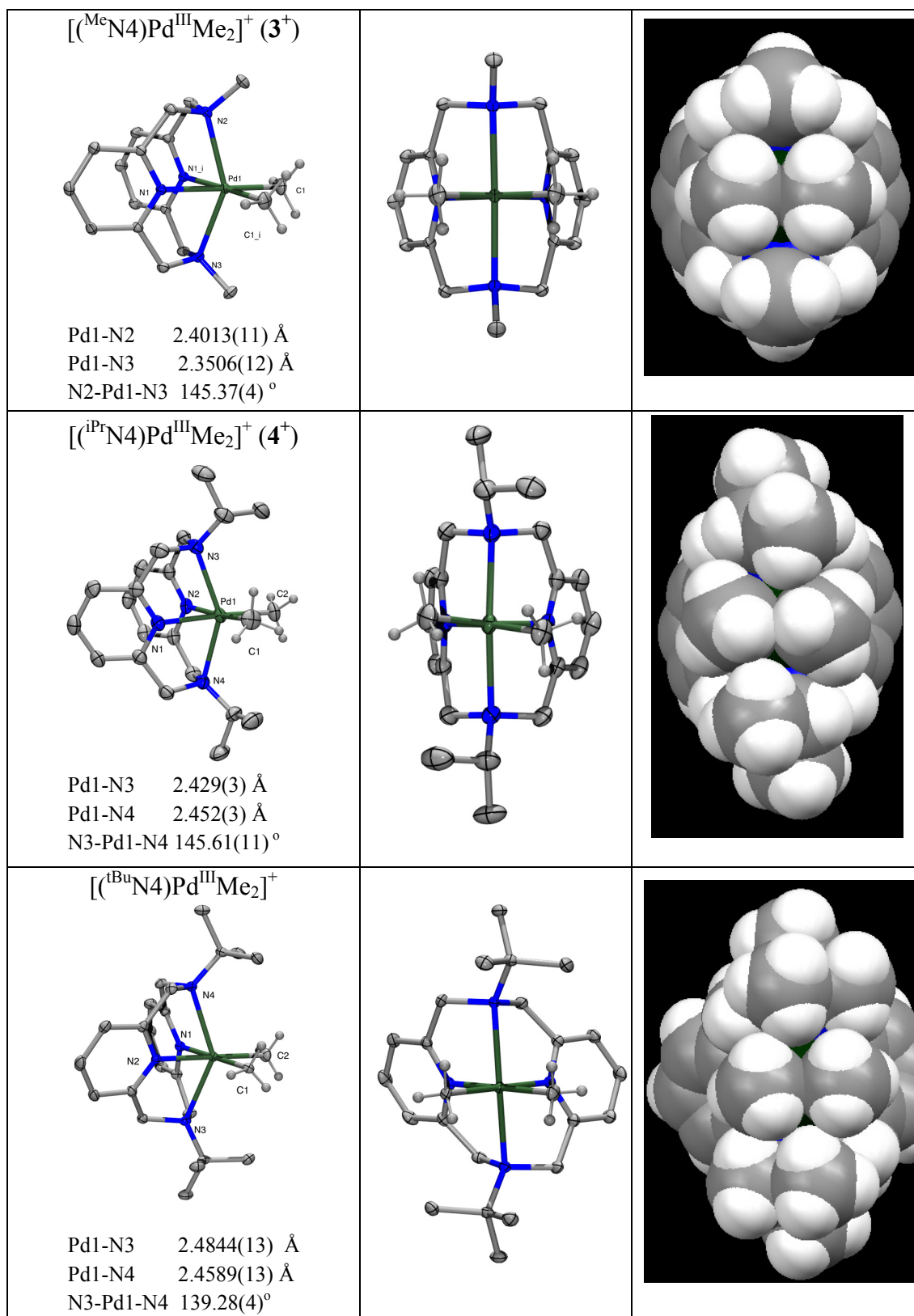
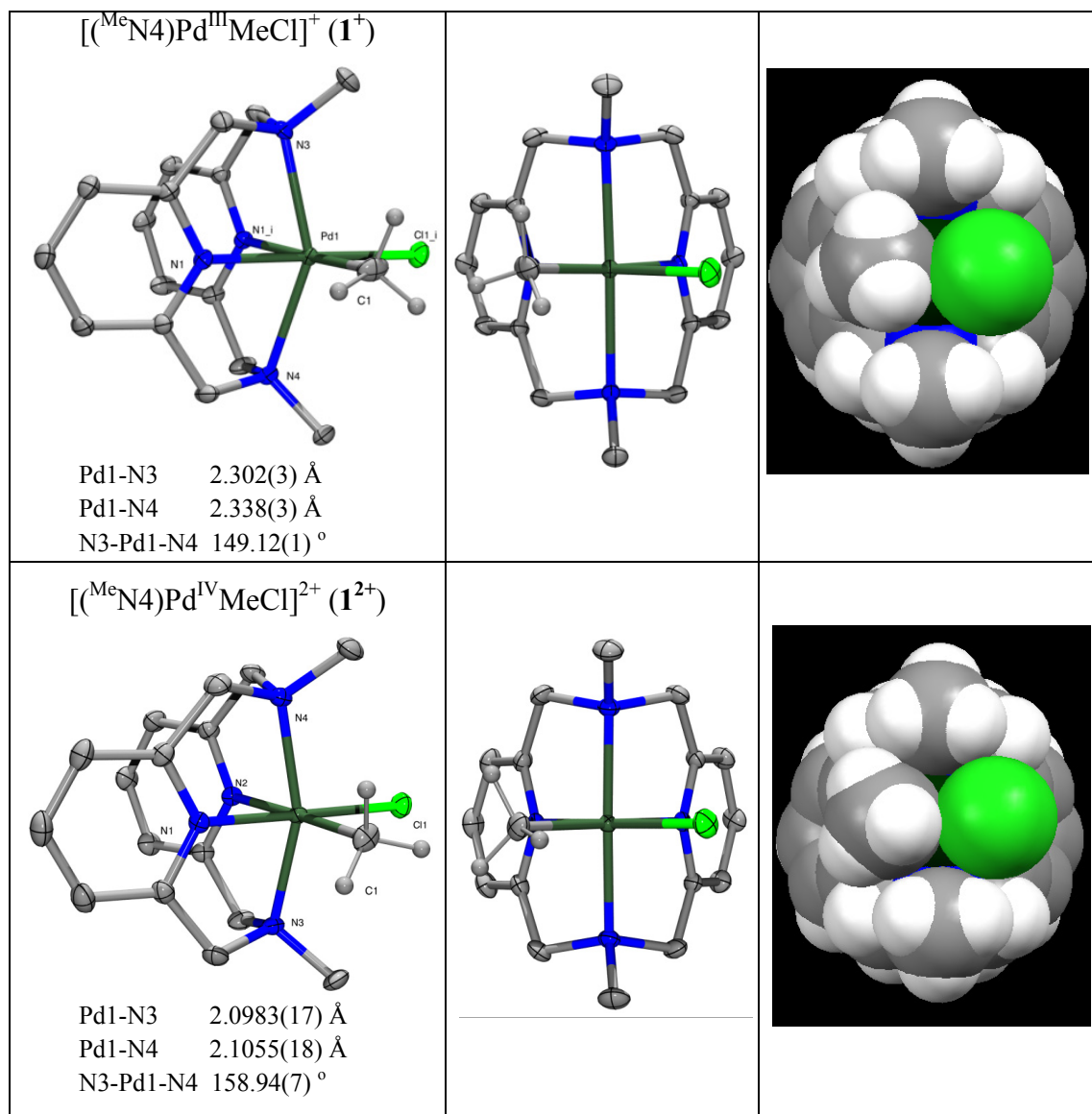


Figure S33. ORTEP diagrams and space filling models of  $[(^{\text{R}}\text{N4})\text{Pd}^{\text{III}}\text{MeCl}]^+$  complexes.



**Figure S34.** ORTEP diagrams and space filling models of  $[(^{\text{R}}\text{N4})\text{Pd}^{\text{III}}\text{Me}_2]^+$  complexes.



**Figure S35.** ORTEP diagrams and space filling models of  $\mathbf{1}^+$  and  $\mathbf{1}^{2+}$ .

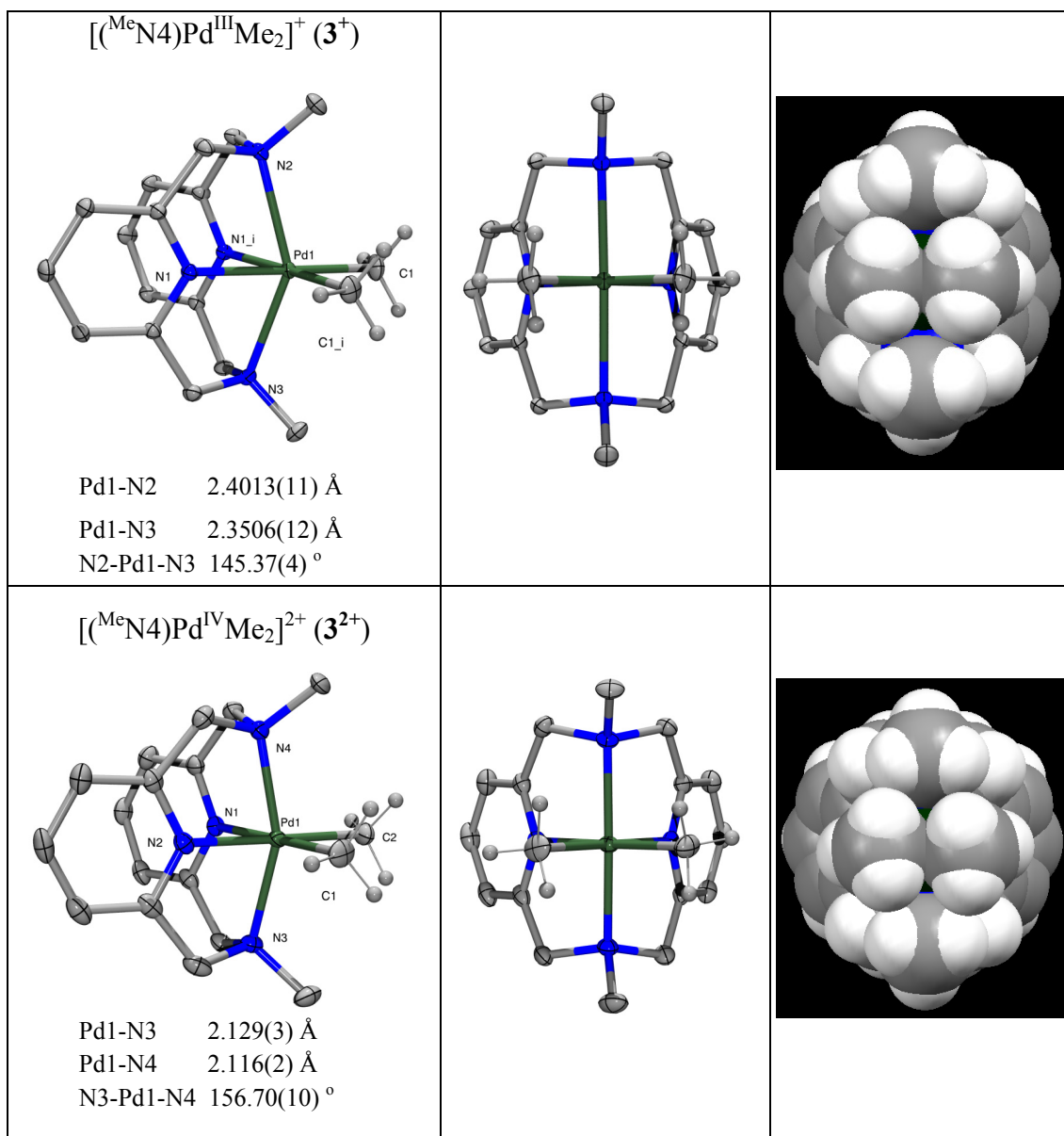


**Figure S36.** ORTEP diagrams and space filling models of  $\mathbf{3}^+$  and  $\mathbf{3}^{2+}$ .

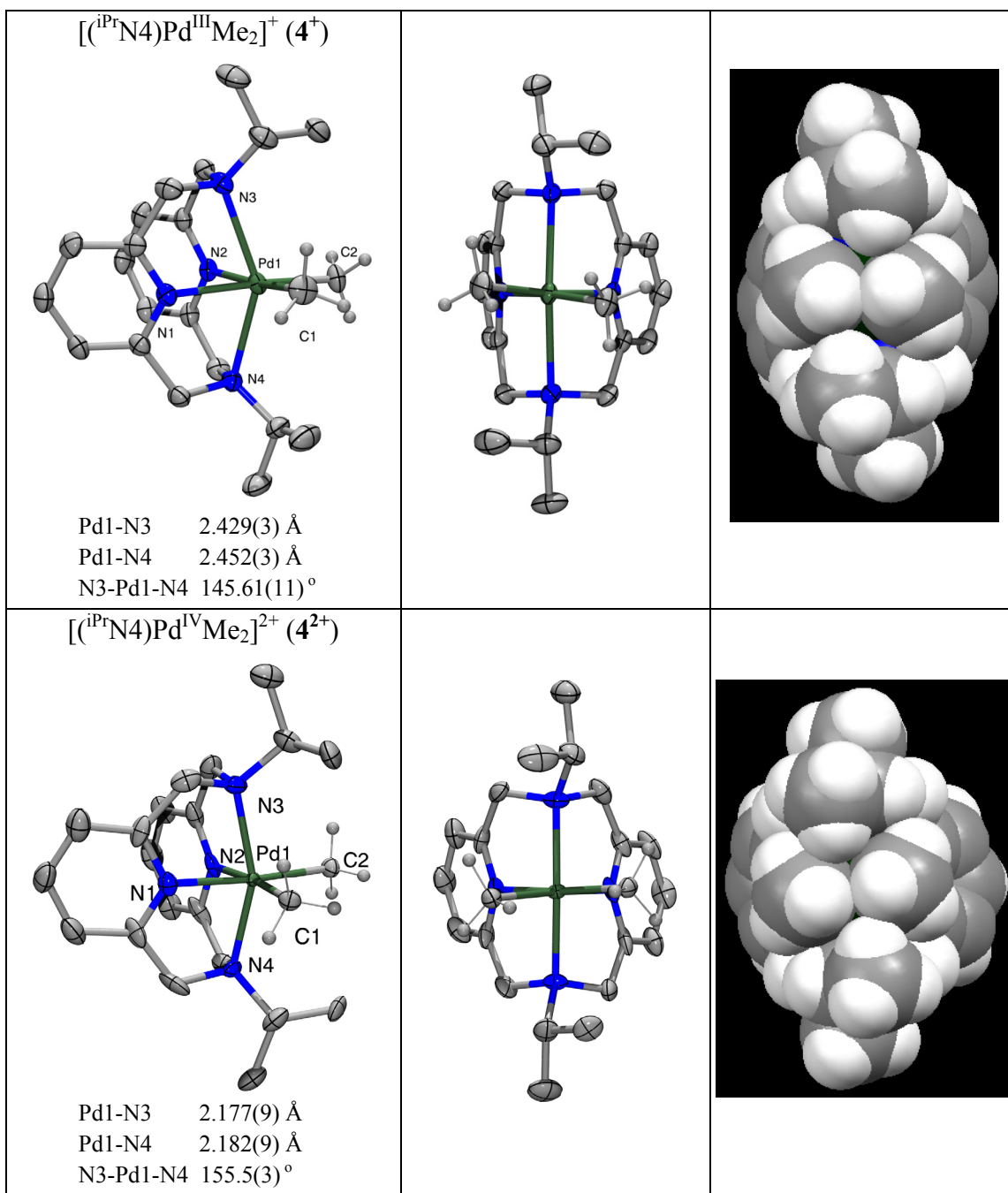


**Figure S37.** ORTEP diagrams and space filling models of  $4^+$  and  $4^{2+}$ .

## VII. Photolysis and thermolysis of $^R\text{N}_4\text{Pd}^{\text{III}}$ and $^R\text{N}_4\text{Pd}^{\text{IV}}$ complexes

*General procedure:* All preparations were performed in a nitrogen-filled glovebox. For each measurement,  $^R\text{N}_4\text{Pd}^{\text{III}}$  and  $^R\text{N}_4\text{Pd}^{\text{IV}}$  complexes (4-8 mg) were dissolved in degassed NMR solvents. In order to avoid the escape of the volatiles into the headspace, the NMR tubes were filled to the top for both photolysis and thermolysis experiments. All the NMR tubes were sealed with rubber septa and parafilm after loading the samples. For the photolysis experiments, the NMR tubes were placed in an ice bath and irradiated with two 100 W halogen lamps placed at a distance about 10 cm from the sample. For the thermolysis experiments, the NMR tubes were placed in a 70 °C mineral oil bath. Irradiation or heating was continued until no further changes were observed by  $^1\text{H}$  NMR. Formation of insoluble products was not observed during the course of photolysis and thermolysis. After the reaction was complete, dioxane (1  $\mu\text{L}$ , 11.7  $\mu\text{mol}$ ) was injected into the NMR sample as an internal standard to determine the product yields. The organic products such as  $\text{C}_2\text{H}_6$ ,  $\text{CH}_3\text{Cl}$ , TEMPO-Me,  $[\text{iPrN}_4\cdot\text{H}]^+$ , and  $[\text{iPrN}_4\cdot 2\text{H}]^{2+}$  were identified by comparison of  $^1\text{H}$  NMR with authentic samples and literature data.<sup>6</sup> The identity of the  $[(^{\text{Me}}\text{N}_4)\text{Pd}^{\text{II}}\text{Me}(\text{MeCN})]^+$ ,  $[(^{\text{iPr}}\text{N}_4)\text{Pd}^{\text{II}}\text{Me}(\text{MeCN})]^+$ ,  $[(^{\text{iPr}}\text{N}_4)\text{Pd}^{\text{II}}\text{Cl}(\text{MeCN})]^+$ , and  $[(^{\text{iPr}}\text{N}_4)\text{Pd}^{\text{II}}(\text{MeCN})_2]^{2+}$  products was determined by comparison of the signals in the NMR spectra with those of known  $[(^{\text{tBu}}\text{N}_4)\text{Pd}^{\text{II}}\text{Me}(\text{MeCN})]^+$ ,  $[(^{\text{tBu}}\text{N}_4)\text{Pd}^{\text{II}}\text{Cl}(\text{MeCN})]^+$ ,  $[(^{\text{tBu}}\text{N}_4)\text{Pd}^{\text{II}}(\text{MeCN})_2]^{2+}$  complexes and/or independently synthesized samples.  $[(^{\text{Me}}\text{N}_4)\text{Pd}^{\text{II}}\text{Cl}(\text{MeCN})]^+$  and  $[(^{\text{Me}}\text{N}_4)\text{Pd}^{\text{II}}(\text{MeCN})_2]^{2+}$  could not be independently synthesized and identified due to their instability. Product yields were determined by integration of the corresponding NMR peaks relative to the dioxane standard and calculated as  $[\text{moles of product}]/[\text{moles of } ^R\text{N}_4\text{Pd}^{\text{III}} \text{ or } ^R\text{N}_4\text{Pd}^{\text{IV}}] * 100\%$  and are reported as averages of 2-4 runs. A long delay time (150 s) was used to quantify the amount of products.

Ethane:  $^1\text{H}$  NMR ( $\text{CD}_3\text{CN}$ ),  $\delta$ : 0.85 (s).

Methane:  $^1\text{H}$  NMR ( $\text{CD}_3\text{CN}$ ),  $\delta$ : 0.20 (s).

Methylchloride:  $^1\text{H}$  NMR ( $\text{CD}_3\text{CN}$ ),  $\delta$ : 3.03 (s).

1-Methoxy-2,2,6,6-tetramethylpiperidine (Me-TEMPO):  $^1\text{H}$  NMR ( $\text{CD}_3\text{CN}$ ),  $\delta$  1.05 (s, 6H), 1.14 (s, 6H), 1.36-1.56 (m, 6H), 3.56 (s, 3H).

$^{\text{Me}}\text{N}_4$ :  $^1\text{H}$  NMR ( $\text{CD}_3\text{CN}$ ),  $\delta$  7.13 (t,  $J = 7.8$  Hz, 2 H, py-H), 6.74 (d,  $J = 7.8$  Hz, 4H, py-H), 3.72 (s, 8H,  $-\text{CH}_2-$ ), 2.65 (s, 6H, N- $\text{CH}_3$ ).

$[(^{\text{Me}}\text{N}_4\cdot\text{H})]^+$ :  $^1\text{H}$  NMR ( $\text{CD}_3\text{CN}$ ),  $\delta$  7.91 (t,  $J = 7.5$  Hz, 2 H, py-H), 7.35 (d,  $J = 7.5$  Hz, 4H, py-H), 4.08 (s, 8H,  $-\text{CH}_2-$ ), 2.62 (s, 6H, N- $\text{CH}_3$ ).

$[\text{Me}_4\text{N}_4\cdot 2\text{H}]^{2+}$ :  $^1\text{H}$  NMR ( $\text{CD}_3\text{CN}$ ),  $\delta$  7.45 (t,  $J = 7.8$  Hz, 2 H, py-H), 6.99 (d,  $J = 7.5$  Hz, 4H, py-H), 4.73 (d,  $J = 15.0$  Hz, 4H,  $-\text{CH}_2-$ ), 4.50 (d,  $J = 15.0$  Hz, 4H,  $-\text{CH}_2-$ ), 3.34 (s, 6H, N- $\text{CH}_3$ ).

$[\text{iPr}_4\text{N}_4]$ :  $^1\text{H}$  NMR ( $\text{CD}_3\text{CN}$ ),  $\delta$  7.08, (t,  $J = 7.8$  Hz, 2 H, py-H), 6.70 (d,  $J = 7.8$  Hz, 4H, py-H), 3.78 (s, 8H,  $-\text{CH}_2-$ ), 3.26 (m,  $J = 6.6$  Hz, 2H, *iPr*-CH), 1.22 (d,  $J = 6.6$  Hz, 12H, *iPr*- $\text{CH}_3$ ).

$[\text{iPr}_4\text{N}_4\cdot \text{H}]^+$ :  $^1\text{H}$  NMR ( $\text{CD}_3\text{CN}$ ),  $\delta$  7.97 (t,  $J = 7.5$  Hz, 2 H, py-H), 7.41 (d,  $J = 7.8$  Hz, 4H, py-H), 4.17 (br, 8H,  $-\text{CH}_2-$ ), 3.03 (m,  $J = 6.6$  Hz, 2H, *iPr*-CH), 1.03 (d,  $J = 6.3$  Hz, 12H, *iPr*- $\text{CH}_3$ ).

$[\text{iPr}_4\text{N}_4\cdot 2\text{H}]^+$ :  $^1\text{H}$  NMR ( $\text{CD}_3\text{CN}$ ),  $\delta$  7.51 (t,  $J = 7.8$  Hz, 2H, py-H), 7.07 (d,  $J = 7.8$  Hz, 4H, py-H), 4.71 (d,  $J = 14.7$  Hz, 4H,  $-\text{CH}_2-$ ), 4.29 (dd,  $J^1 = 15$  Hz,  $J^2 = 3.6$  Hz, 4H,  $-\text{CH}_2-$ ), 4.20 (m,  $J = 6.6$  Hz, *iPr*-CH), 1.57 (d,  $J = 6.6$  Hz, 12H, *iPr*- $\text{CH}_3$ ).

Note: The protonated ligands  $[\text{Me}_4\text{N}_4\cdot \text{H}]^+$ ,  $[\text{Me}_4\text{N}_4\cdot 2\text{H}]^{2+}$ ,  $[\text{iPr}_4\text{N}_4\cdot \text{H}]^+$ , and  $[\text{iPr}_4\text{N}_4\cdot 2\text{H}]^{2+}$  were synthesized by mixing the free ligand with 1 or 2 equiv of 1.0 M HCl.

$[(\text{Me}_4\text{N}_4)\text{Pd}^{\text{II}}\text{Me}(\text{MeCN})]^+$ :  $^1\text{H}$  NMR ( $\text{CD}_3\text{CN}$ ),  $\delta$  7.58 (br, py-H), 7.18 (br, Py-H), 5.60 (br,  $-\text{CH}_2-$ ), 4.94 (br,  $-\text{CH}_2-$ ), 4.21 (br,  $-\text{CH}_2-$ ), 2.72 (br, N- $\text{CH}_3$ ), 0.74 (s, Pd- $\text{CH}_3$ ).

$[(\text{iPr}_4\text{N}_4)\text{Pd}^{\text{II}}\text{Me}(\text{MeCN})]^+$ :  $^1\text{H}$  NMR ( $\text{CD}_3\text{CN}$ ),  $\delta$  7.49 (t,  $J = 7.5$  Hz, 2H, py-H), 7.08 (d,  $J = 7.4$  Hz, 4H, py-H), 5.90-5.40 (m, 4H, NCH<sub>2</sub>), 4.22 (d,  $J = 12.7$  Hz, 4H, NCH<sub>2</sub>), 3.33 (m,  $J = 6.6$  Hz, 2H, *iPr*-CH), 1.35-1.15 (m, 12H, *iPr*- $\text{CH}_3$ ), 0.52 (s, 1.5H, PdCH<sub>3</sub>), 0.32 (s, 1.5H, Pd- $\text{CH}_3$ ).

$[(\text{iPr}_4\text{N}_4)\text{Pd}^{\text{II}}\text{Cl}(\text{MeCN})]^+$ :  $^1\text{H}$  NMR ( $\text{CD}_3\text{CN}$ ),  $\delta$  7.64 (br, 2H, py-H), 7.14 (br, 4H, py-H), 6.1 (br,  $-\text{CH}_2-$ ), 4.7 (br,  $-\text{CH}_2-$ ), 3.9 (br,  $-\text{CH}_2-$ ), 1.53 (br, 12H, *iPr*- $\text{CH}_3$ ).

$[(\text{iPr}_4\text{N}_4)\text{Pd}^{\text{II}}(\text{MeCN})_2]^{2+}$ :  $^1\text{H}$  NMR ( $\text{CD}_3\text{CN}$ ),  $\delta$  7.64 (t, 2H, py-H,  $J = 7.8$  Hz), 7.16 (d, 4H, py-H,  $J = 7.8$  Hz), 4.74 (d, 4H, NCH<sub>2</sub>,  $J = 15.0$  Hz), 4.38 (d, 2H, NCH<sub>2</sub>,  $J = 15.0$  Hz), 4.33 (d, 2H, NCH<sub>2</sub>,  $J = 15.0$  Hz), 4.23 (m, 2H, *iPr*-CH,  $J = 6.9$  Hz), 1.53 (d, 12H, *iPr*- $\text{CH}_3$ ,  $J = 6.6$  Hz).

**Table S1.** Product yields during photolysis of  $[(^{\text{Me}}\text{N4})\text{Pd}^{\text{III}}\text{MeCl}]^+$  (**1**<sup>+</sup>),  $[(^{\text{iPr}}\text{N4})\text{Pd}^{\text{III}}\text{MeCl}]^+$  (**2**<sup>+</sup>),  $[(^{\text{Me}}\text{N4})\text{Pd}^{\text{III}}\text{Me}_2]^+$  (**3**<sup>+</sup>), and  $[(^{\text{iPr}}\text{N4})\text{Pd}^{\text{III}}\text{Me}_2]^+$  (**4**<sup>+</sup>).

Cmpd	C <sub>2</sub> H <sub>6</sub> , %	CH <sub>3</sub> Cl, %	CH <sub>4</sub> , %	TEMPO-Me, %	$[(^{\text{R}}\text{N4})\text{Pd}^{\text{II}}\text{Me}(\text{MeCN})]^+$ , % (R = Me or iPr)	$[(^{\text{R}}\text{N4})\text{Pd}^{\text{II}}\text{Cl}(\text{MeCN})]^+$ , % (R = Me or iPr)
<b>1</b> <sup>+</sup> <sup>a</sup>	14±1	5±1	5±1	NA	15±5	ND
<b>1</b> <sup>+</sup> <sup>b</sup>	0	0	0	80±9	0	ND
<b>2</b> <sup>+</sup> <sup>a</sup>	17±2	21±1	7±1	NA	25±4	41±1
<b>2</b> <sup>+</sup> <sup>b</sup>	0	0	0	99±1	0	99±1
<b>3</b> <sup>+</sup> <sup>a</sup>	30±3	NA	13±1	NA	47±3	NA
<b>3</b> <sup>+</sup> <sup>b</sup>	12±1	NA	7±2	47±3	26±2	NA
<b>4</b> <sup>+</sup> <sup>a</sup>	28±1	NA	9±2	NA	73±2	NA
<b>4</b> <sup>+</sup> <sup>b</sup>	19±1	NA	3±1	64±5	45±8	NA

<sup>a</sup> photolysis; <sup>b</sup> photolysis in the presence of 2 equiv TEMPO. NA – not applicable; ND – not detected.

**Table S2.** Product yields during thermolysis of  $[(^{\text{Me}}\text{N4})\text{Pd}^{\text{IV}}\text{MeCl}]^{2+}$  (**1**<sup>2+</sup>),  $[(^{\text{iPr}}\text{N4})\text{Pd}^{\text{IV}}\text{MeCl}]^{2+}$  (**2**<sup>2+</sup>),  $[(^{\text{Me}}\text{N4})\text{Pd}^{\text{IV}}\text{Me}_2]^{2+}$  (**3**<sup>2+</sup>), and  $[(^{\text{iPr}}\text{N4})\text{Pd}^{\text{IV}}\text{Me}_2]^{2+}$  (**4**<sup>2+</sup>).

Complex	C <sub>2</sub> H <sub>6</sub> , %	CH <sub>3</sub> Cl, %	CH <sub>4</sub> , %	TEMPO-Me, %	$[(^{\text{R}}\text{N4})\text{Pd}^{\text{II}}(\text{MeCN})_2]^+$ , % (R = Me or iPr)
<b>1</b> <sup>2+</sup> <sup>a</sup>	0	22±1	0	NA	ND
<b>1</b> <sup>2+</sup> <sup>b</sup>	0	22±1	<2	0	ND
<b>1</b> <sup>2+</sup> <sup>c</sup>	0	99±1	0	NA	( <sup>Me</sup> N4)Pd <sup>II</sup> Cl <sub>2</sub> , 99±1
<b>2</b> <sup>2+</sup> <sup>d</sup>	0	52±1	0	NA	39±1
<b>3</b> <sup>2+</sup> <sup>a</sup>	<1	NA	55±1	NA	ND
<b>4</b> <sup>2+</sup> <sup>e</sup>	54±1	NA	24±1	NA	19±1

<sup>a</sup> thermolysis at 70 °C; <sup>b</sup> thermolysis at 70 °C in presence of 2 equiv TEMPO; <sup>c</sup> reaction in presence of 2 equiv Et<sub>4</sub>NCl at RT. <sup>d</sup> reaction performed at RT. NA – not applicable; <sup>e</sup> thermolysis performed at 70 °C for 64 hours that also leads to formation of 88% of [<sup>iPr</sup>N4•H]<sup>+</sup>; ND – not detected.

**Table S3.** Product yields during photolysis of  $[(^{\text{Me}}\text{N4})\text{Pd}^{\text{IV}}\text{Me}_2]^{2+}$  ( $\mathbf{3}^{2+}$ ) and  $[(^{\text{iPr}}\text{N4})\text{Pd}^{\text{IV}}\text{Me}_2]^{2+}$  ( $\mathbf{4}^{2+}$ ).

Complex	C <sub>2</sub> H <sub>6</sub> , %	CH <sub>3</sub> Cl, %	CH <sub>4</sub> , %	TEMPO-Me, %	$[(^{\text{R}}\text{N4})\text{Pd}^{\text{II}}(\text{MeCN})_2]^+$ , % (R = Me or iPr)
$\mathbf{3}^{2+ \text{ a}}$	46±2	NA	6±1	NA	ND
$\mathbf{3}^{2+ \text{ b}}$	49±3	NA	6±1	42±3	ND
$\mathbf{4}^{2+ \text{ a}}$	54±1	NA	24±1	NA	45±2
$\mathbf{4}^{2+ \text{ b}}$	50±4	NA	16±2	79±3	65±3

<sup>a</sup> photolysis; <sup>b</sup> photolysis in the presence of 2 equiv TEMPO. NA – not applicable; ND – not detected.

Note: An appreciable amount of TEMPO-Me was observed during the photolysis of  $\mathbf{3}^{2+}$  or  $\mathbf{4}^{2+}$  in the presence of TEMPO. However the yield of ethane was not affected, suggesting that although radical side reactions may be present, yet they do not lead to C-C bond formation.

## Photolysis of (<sup>R</sup>N<sub>4</sub>)Pd<sup>III</sup> complexes

### 1) Photolysis of [(<sup>R</sup>N<sub>4</sub>)Pd<sup>III</sup>MeCl]<sup>+</sup> complexes

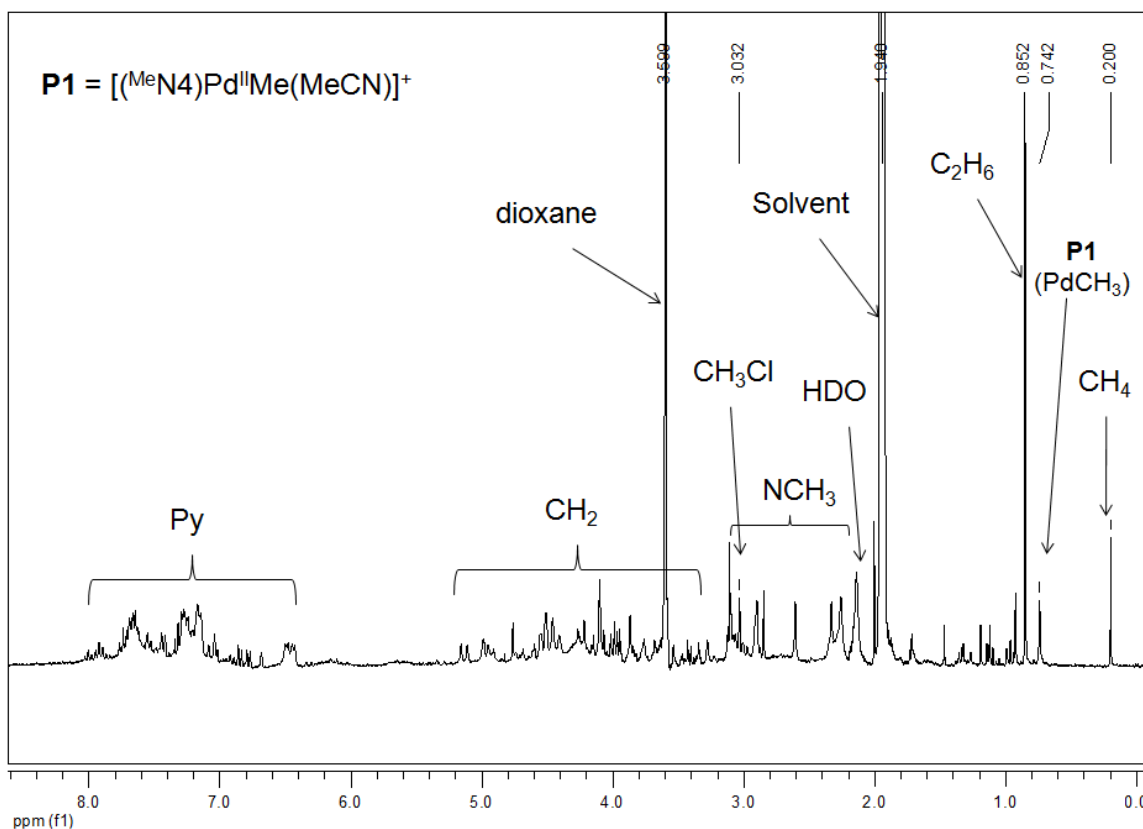
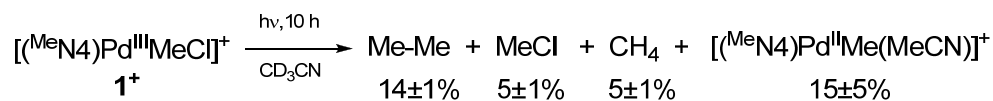


**Figure S38.** <sup>1</sup>H NMR spectrum of solution of **1**<sup>+</sup> in CD<sub>3</sub>CN after irradiation for 10 hours at 0 °C. [(<sup>Me</sup>eN<sub>4</sub>)Pd<sup>II</sup>Me(MeCN)]<sup>+</sup> was identified by comparison with an independently synthesized sample. However, [(<sup>Me</sup>eN<sub>4</sub>)Pd<sup>II</sup>Me(MeCN)]<sup>+</sup> and [(<sup>Me</sup>eN<sub>4</sub>)Pd<sup>II</sup>Cl(MeCN)]<sup>+</sup> are unstable and decompose to a mixture of unidentified Pd<sup>II</sup> products. Intergration of the entire aromatic region gives ~73% yield for all Pd<sup>II</sup> products. No free or protonated ligand was identified in the NMR spectrum.

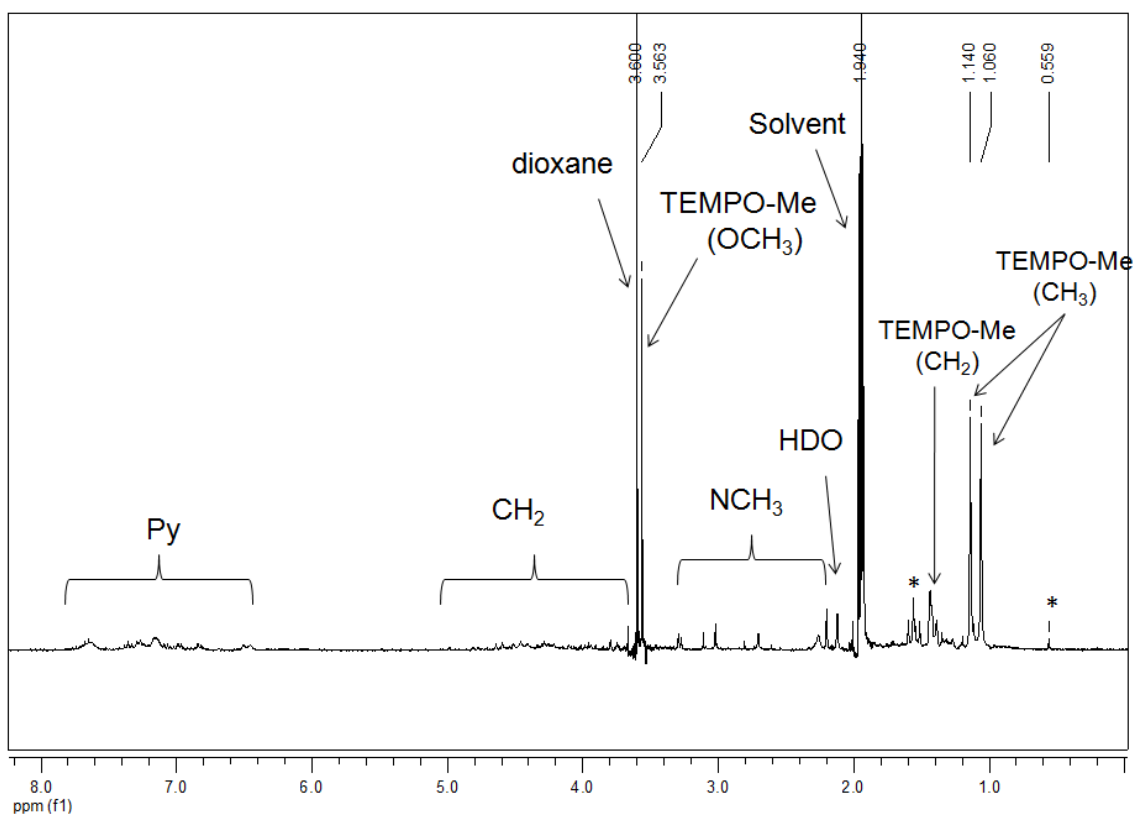
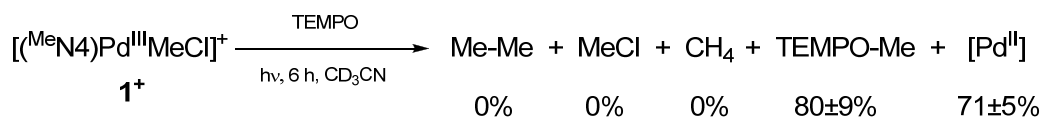


**Figure S39.** <sup>1</sup>H NMR spectrum of solution of **1**<sup>+</sup> in CD<sub>3</sub>CN after irradiation for 6 hours at 0 °C in the presence of 2 equiv TEMPO. The expected [<sup>(Me)</sup>N<sub>4</sub>Pd<sup>II</sup>Cl(MeCN)]<sup>+</sup> product is unstable and decomposes to a mixture of unidentified Pd<sup>II</sup> products. Integration of the entire aromatic region gives ~71% yield for all Pd<sup>II</sup> products. Peaks marked with asterisk are unidentified products.

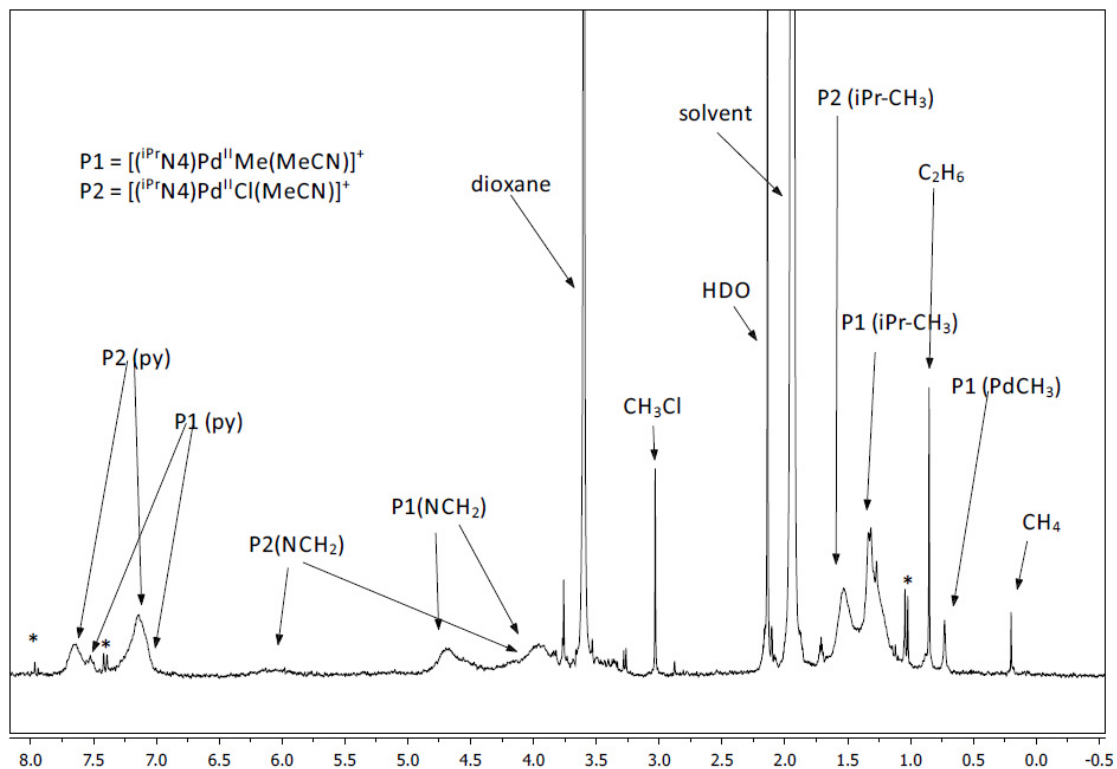
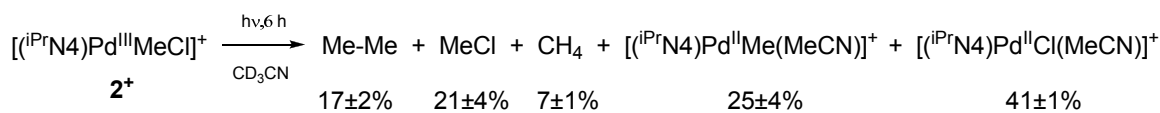


**Figure S40.**  $^1H$  NMR spectrum of a solution of  $\mathbf{2^+}$  in  $CD_3CN$  after irradiation for 6 hours at  $0^\circ C$ .  $[(iPr_4N)Pd^{II}Me(MeCN)]^+$  was identified by comparison with an independently synthesized sample.  $[(iPr_4N)Pd^{II}Cl(MeCN)]^+$  was identified by analogy with the previously reported  $[(tBu_4N)Pd^{II}Cl(MeCN)]^+$  complex.<sup>6</sup> Peaks marked with an asterisk correspond to  $[iPr_4N\cdot H]^+$ .

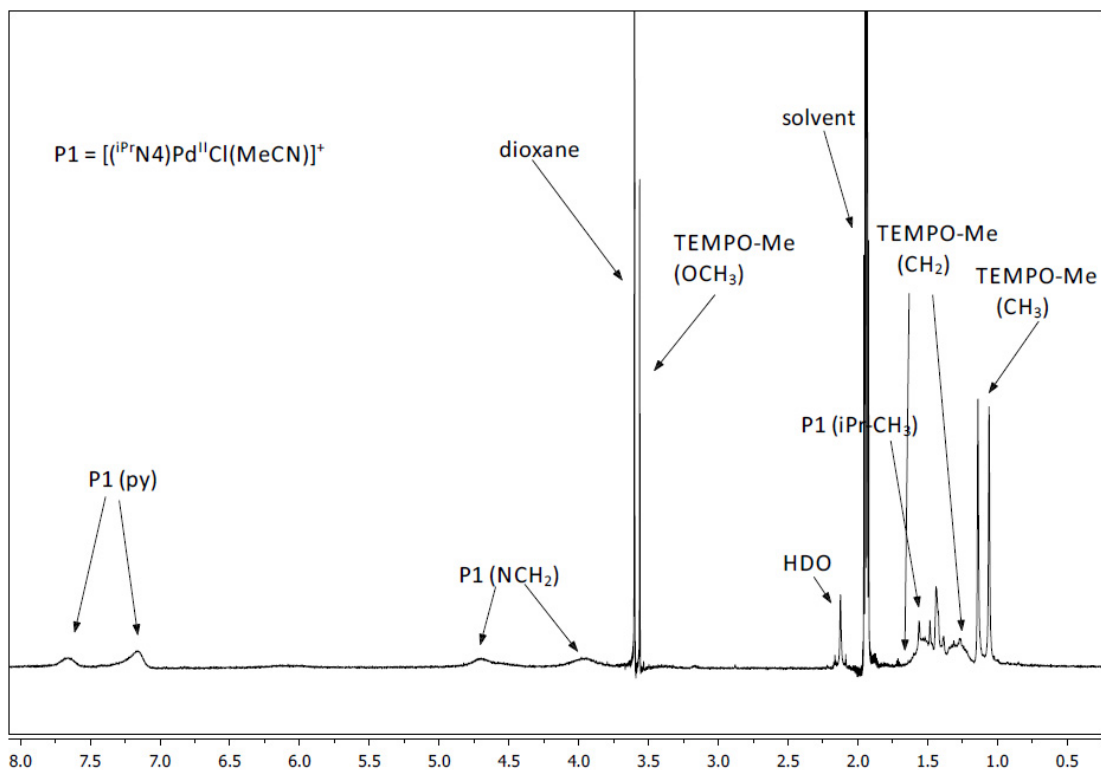
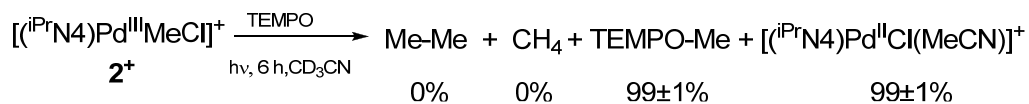


**Figure S41.** <sup>1</sup>H NMR spectrum of a solution of **2<sup>+</sup>** in CD<sub>3</sub>CN after irradiation for 6 hours at 0 °C in the presence of 2 equiv of TEMPO. [(iPr<sub>4</sub>N)Pd<sup>II</sup>Cl(MeCN)]<sup>+</sup> was identified by analogy with the previously reported [(<sup>t</sup>Bu<sub>4</sub>N)Pd<sup>II</sup>Cl(MeCN)]<sup>+</sup> complex.<sup>6</sup>

## 2) Photolysis of $[(^R\text{N}4)\text{Pd}^{\text{III}}\text{Me}_2]^+$ complexes

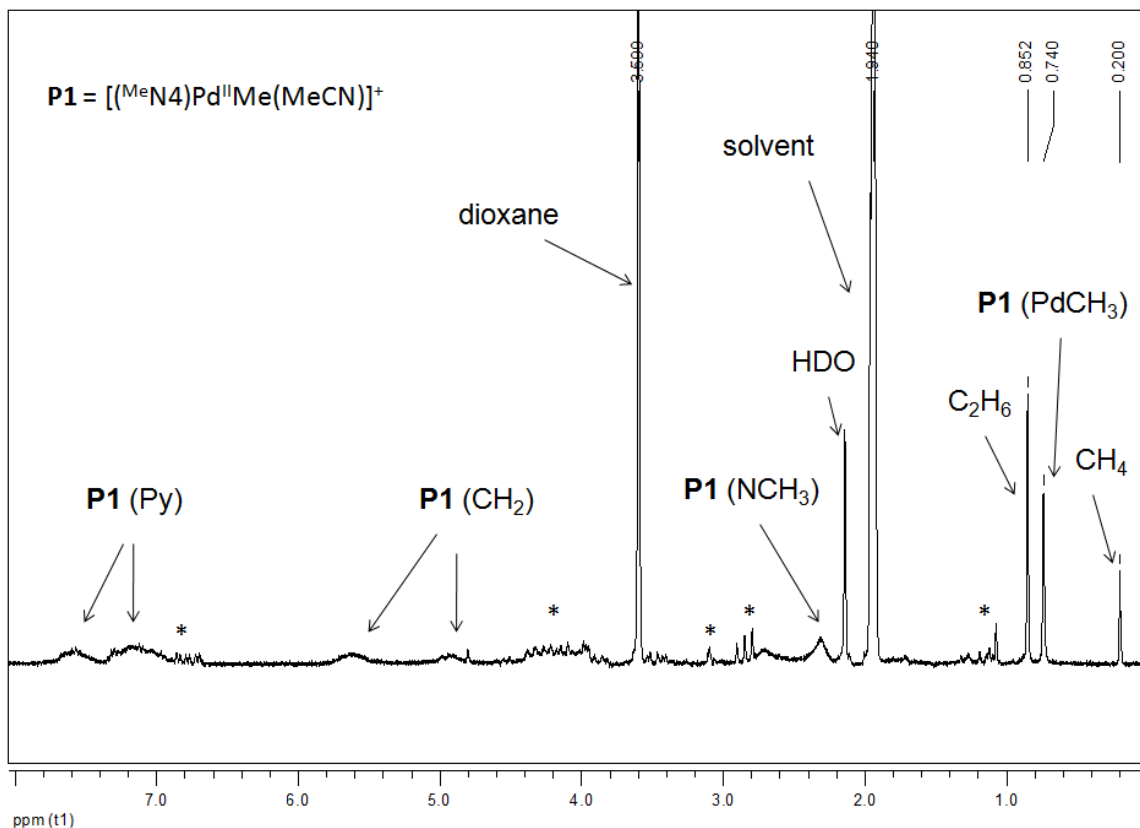
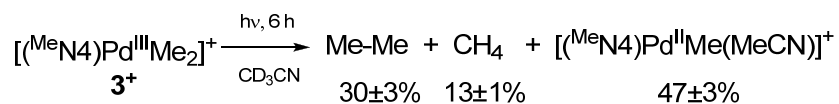


**Figure S42.**  $^1\text{H}$  NMR spectrum of solution of  $3^+$  in  $\text{CD}_3\text{CN}$  after irradiation for 6 hours at  $0^\circ\text{C}$ .  $[(^{\text{Me}}\text{N}4)\text{Pd}^{\text{II}}\text{Me}(\text{MeCN})]^+$  was identified by comparison with an independently synthesized sample. However,  $[(^{\text{Me}}\text{N}4)\text{Pd}^{\text{II}}\text{Me}(\text{MeCN})]^+$  is unstable and decomposes to a mixture of unidentified  $\text{Pd}^{\text{II}}$  products (marked with an asterisk). Integration of the entire aromatic region gives  $\sim 73\%$  yield for all  $\text{Pd}^{\text{II}}$  products. No free or protonated ligand was identified in the  $^1\text{H}$  NMR spectrum.

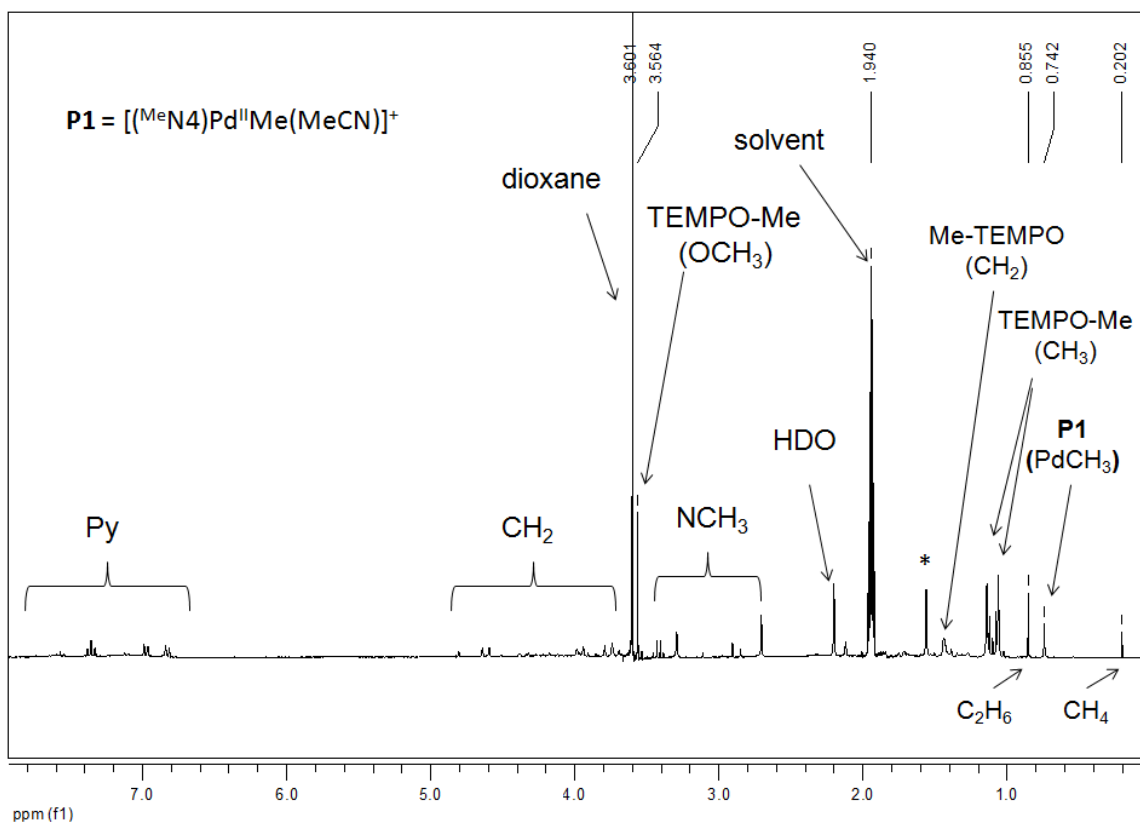
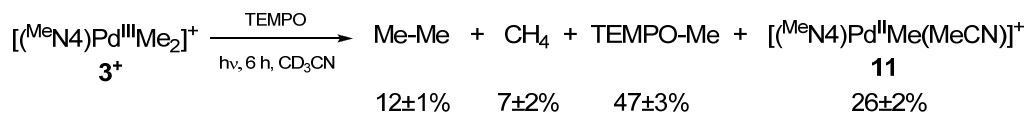


**Figure S43.**  $^1\text{H}$  NMR spectrum of solution of  $\mathbf{3}^+$  in  $\text{CD}_3\text{CN}$  after irradiation for 6 hours at  $0^\circ\text{C}$  in the presence of 2 eq. TEMPO. The identity and yield of  $[(\text{Me}^n\text{N}_4)\text{Pd}^{\text{II}}\text{Me}(\text{MeCN})]^+$  product was determined and calculated as described above. However, this species is unstable and decomposes to a mixture of unidentified  $\text{Pd}^{\text{II}}$  products. Integration of the entire aromatic region gives  $\sim 75\%$  yield for all  $\text{Pd}^{\text{II}}$  products. The peak marked with an asterisk was not identified.

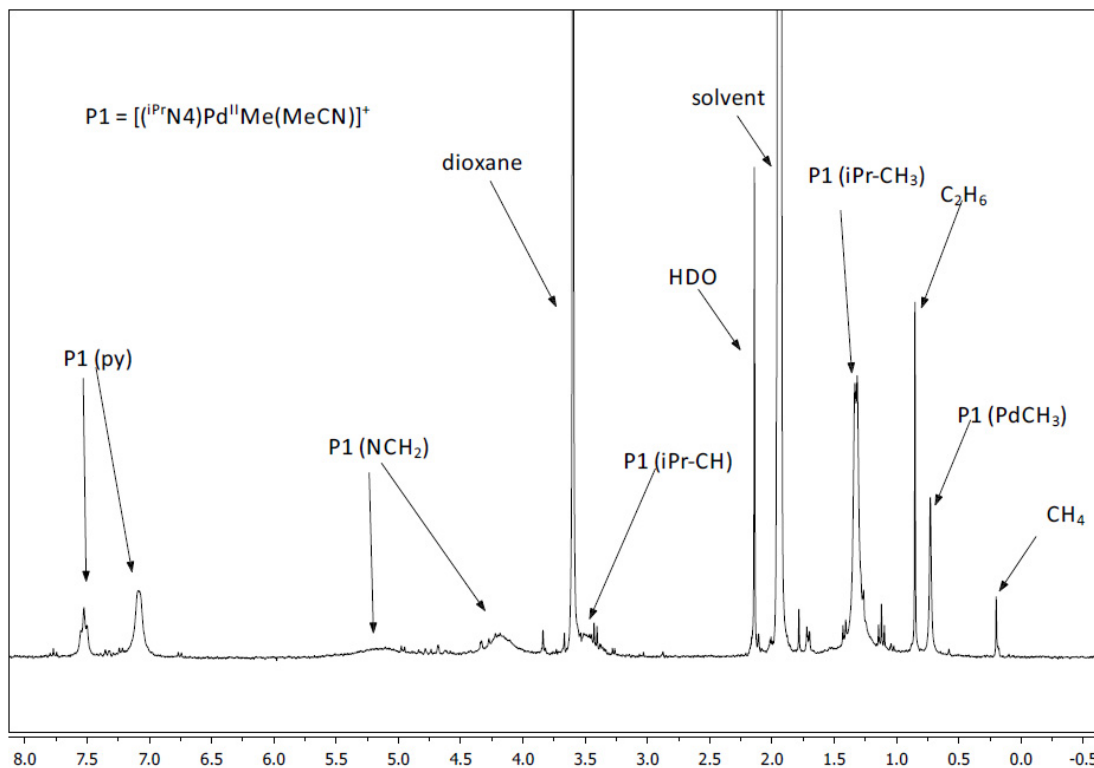
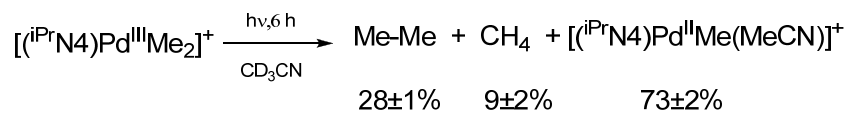


**Figure S44.** <sup>1</sup>H NMR spectrum of a solution of **4**<sup>+</sup> in CD<sub>3</sub>CN after irradiation for 6 hours at 0 °C. [(iPr<sub>4</sub>N)Pd<sup>II</sup>Me(MeCN)]<sup>+</sup> was identified by comparison with an independently synthesized sample.



## Thermolysis of (<sup>R</sup>N<sub>4</sub>)Pd<sup>IV</sup> complexes

### 1) Thermolysis of [(<sup>R</sup>N<sub>4</sub>)Pd<sup>IV</sup>MeCl]<sup>2+</sup> complexes

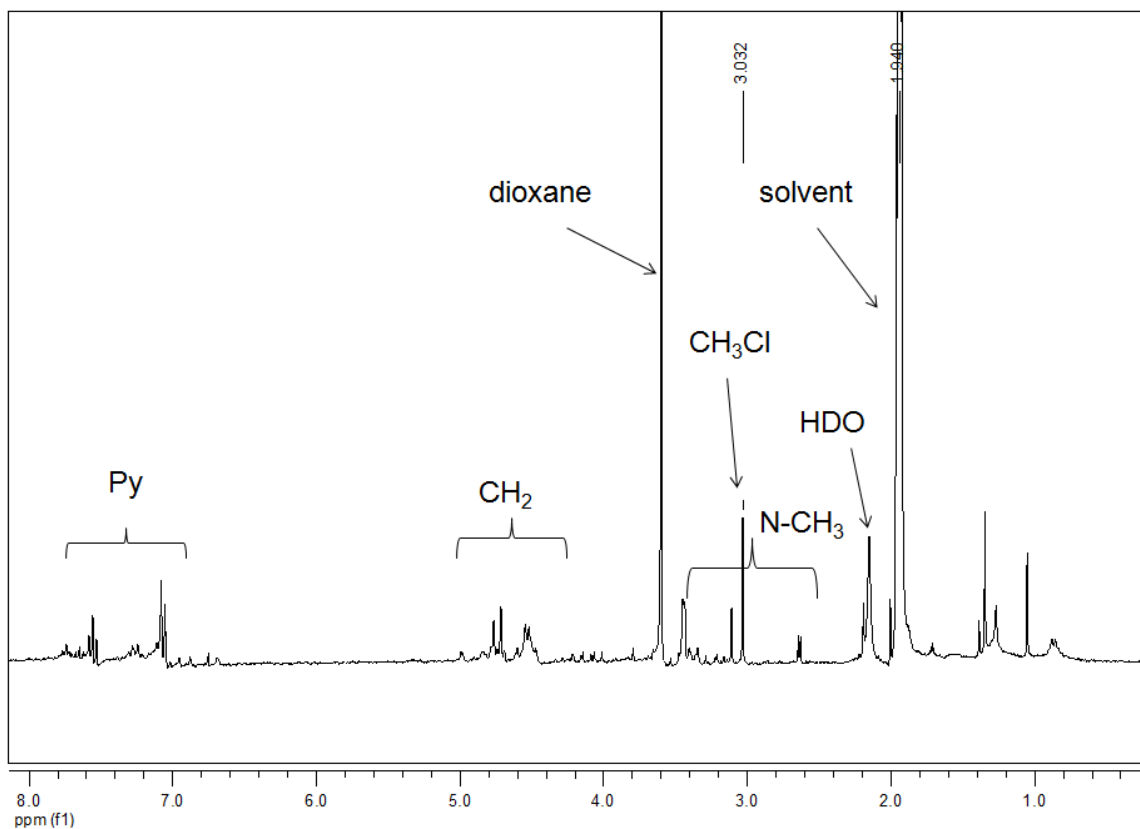
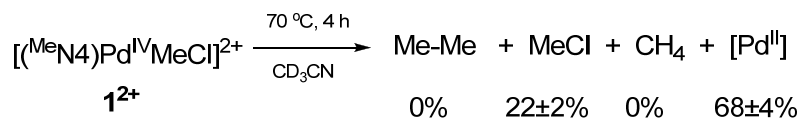


**Figure S46.** <sup>1</sup>H NMR spectrum of solution of **1**<sup>2+</sup> in CD<sub>3</sub>CN after heating at 70 °C for 4 hours in the absence of light. The expected [(<sup>Me</sup>N<sub>4</sub>)Pd<sup>II</sup>(MeCN)<sub>2</sub>]<sup>2+</sup> product is unstable and decomposes to a mixture of unidentified Pd<sup>II</sup> products. Intergration of the entire aromatic region gives ~68% overall yield for all Pd<sup>II</sup> products.

Note: Similar product yields were obtained in the presence of 2 equiv TEMPO.

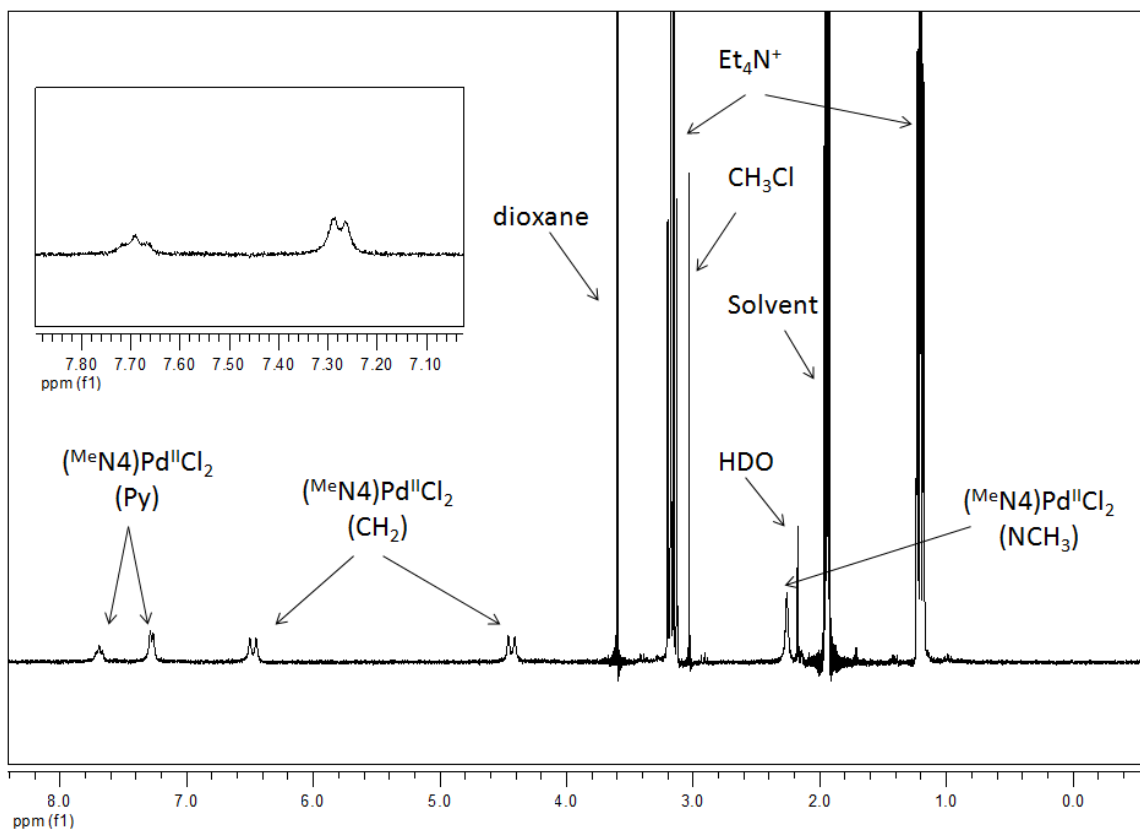
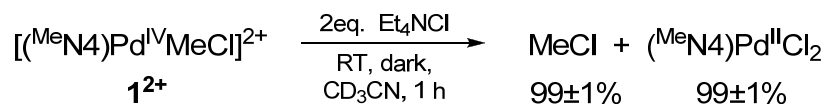


**Figure S47.**  $^1\text{H}$  NMR spectrum for  $[(\text{Me}_4\text{N})\text{Pd}^{\text{IV}}\text{MeCl}](\text{ClO}_4)_2$  with 2 equiv of  $\text{Et}_4\text{NCl}$  in  $\text{CD}_3\text{CN}$  after 1 hour at  $20^\circ\text{C}$ .  $(\text{Me}_4\text{N})\text{Pd}^{\text{II}}\text{Cl}_2$  was identified by comparison with an independently synthesized sample.

Note: Similar product yields were obtained in the presence of 2 equiv TEMPO.

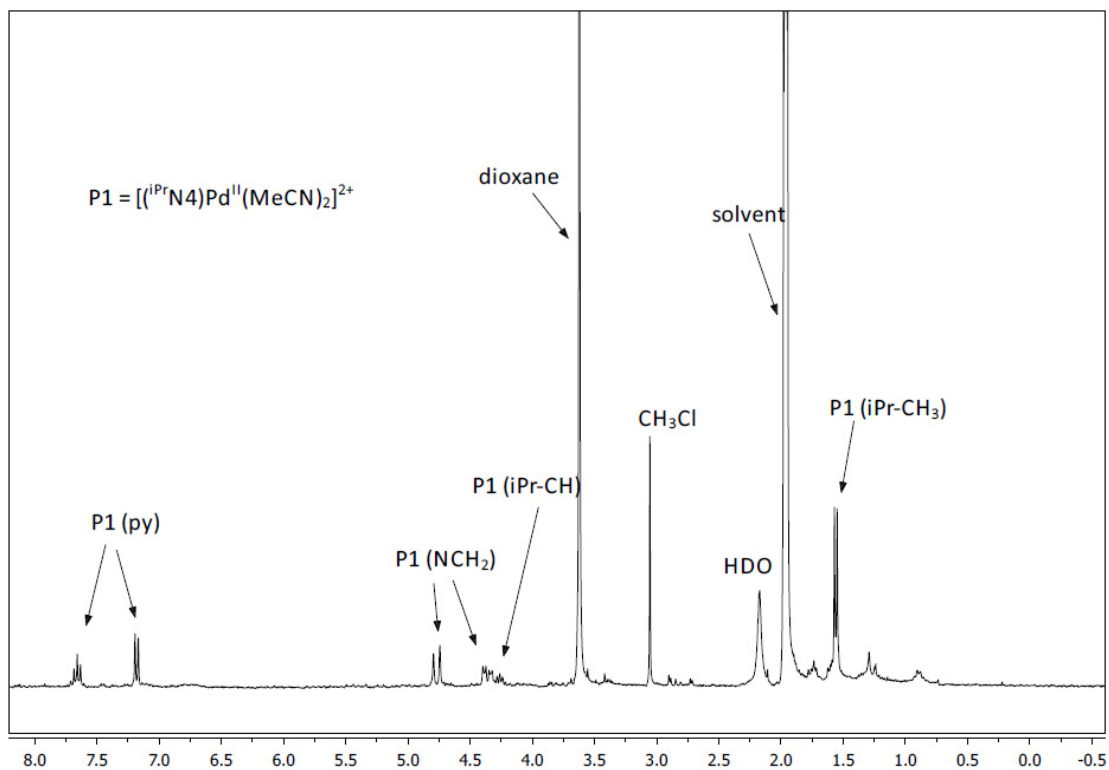
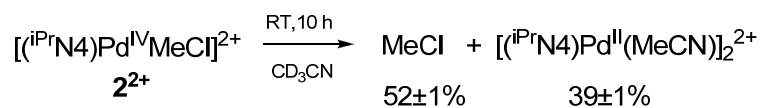


**Figure S48.** <sup>1</sup>H NMR spectrum of a solution of  $\mathbf{2^{2+}}$  in  $\text{CD}_3\text{CN}$  after 10 hours at RT.  $[(iPr_4N)Pd^{II}(MeCN)_2]^{2+}$  was identified by comparison with an independently synthesized sample.

Note: Similar product yields were obtained in the presence of 2 equiv TEMPO.

## 2) Thermolysis of $[(^R\text{N}4)\text{Pd}^{\text{IV}}\text{Me}_2]^+$ complexes

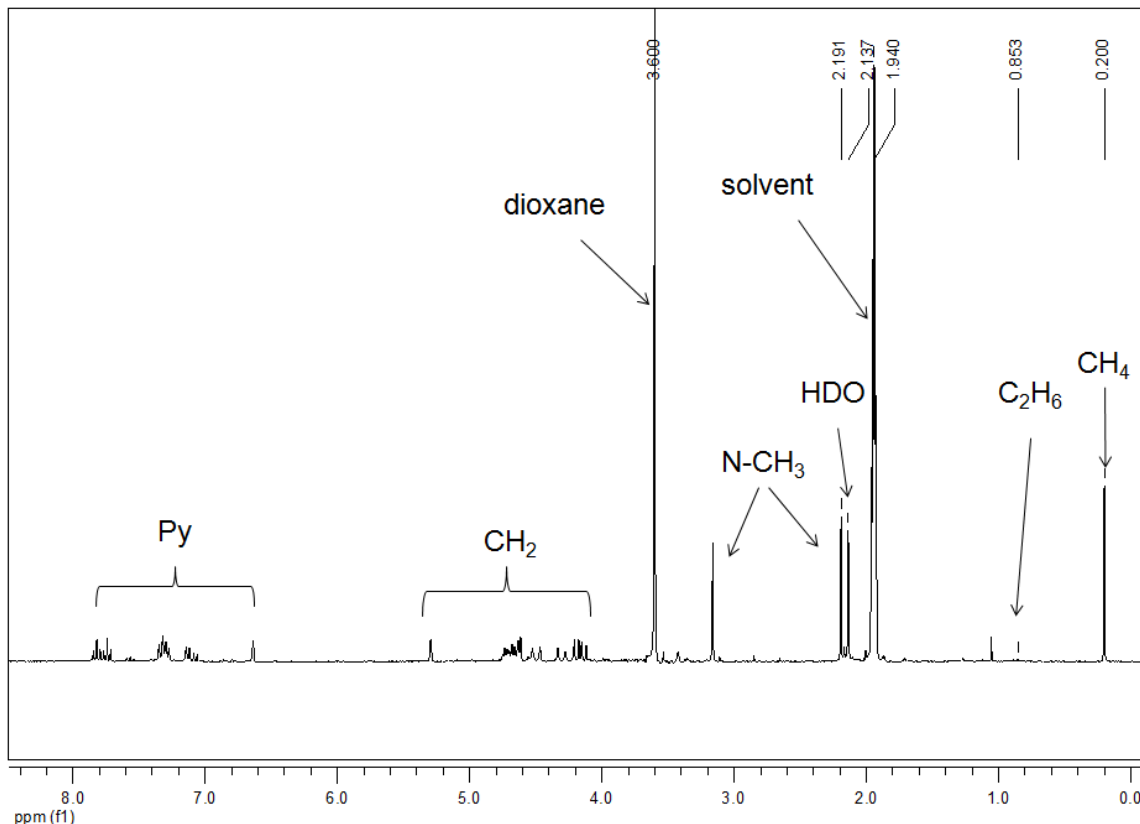
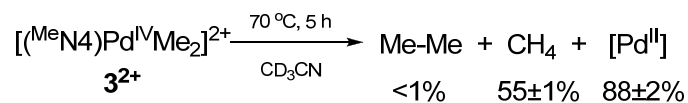


**Figure S49.**  $^1\text{H}$  NMR spectrum of solution of  $\mathbf{3}^{2+}$  in  $\text{CD}_3\text{CN}$  after heating at  $70\text{ }^\circ\text{C}$  for 5 hours in the absence of light.  $\mathbf{3}^{2+}$  likely undergoes unspecific thermal decomposition with formation of methane. Intergration of the entire aromatic region gives  $\sim 88\%$  yield for all  $\text{Pd}^{\text{II}}$  products.

Note: Similar product yields were obtained in the presence of 2 equiv TEMPO.

The dramatically reduced yield of ethane from  $\mathbf{3}^{2+}$  is likely due its symmetric structure and the rigid  $^R\text{N}4$  ligand that disfavord formation of a 5-coordinate intermediate needed for reductive elimination.

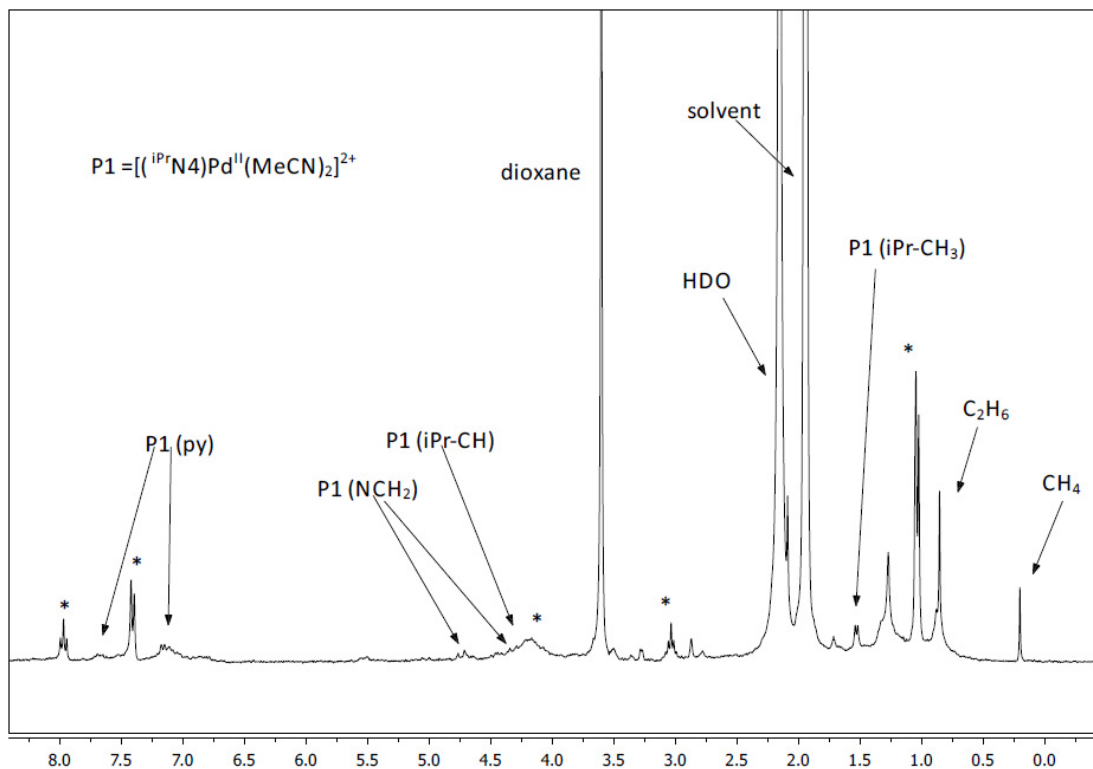
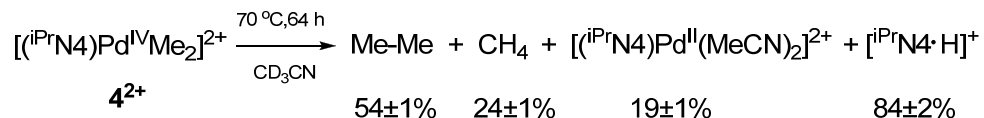


**Figure S50.** <sup>1</sup>H NMR spectrum of a solution of  $\mathbf{4}^{2+}$  in CD<sub>3</sub>CN after heating at 70 °C for 64 hours. [(<sup>i</sup>Pr<sub>4</sub>N<sub>4</sub>)Pd<sup>II</sup>(MeCN)<sub>2</sub>]<sup>2+</sup> was identified by comparison an independently synthesized sample. Peaks labelled with asterisk correspond to [<sup>i</sup>Pr<sub>4</sub>N<sub>4</sub>·H]<sup>+</sup>, which likely forms upon unspecific decomposition of the starting material and [(<sup>i</sup>Pr<sub>4</sub>N<sub>4</sub>)Pd<sup>II</sup>(MeCN)<sub>2</sub>]<sup>2+</sup>.

Note: Similar product yields were obtained in the presence of 2 equiv TEMPO.

### Photolysis of $[(^R\text{N}4)\text{Pd}^{\text{IV}}\text{Me}_2]^{2+}$ complexes

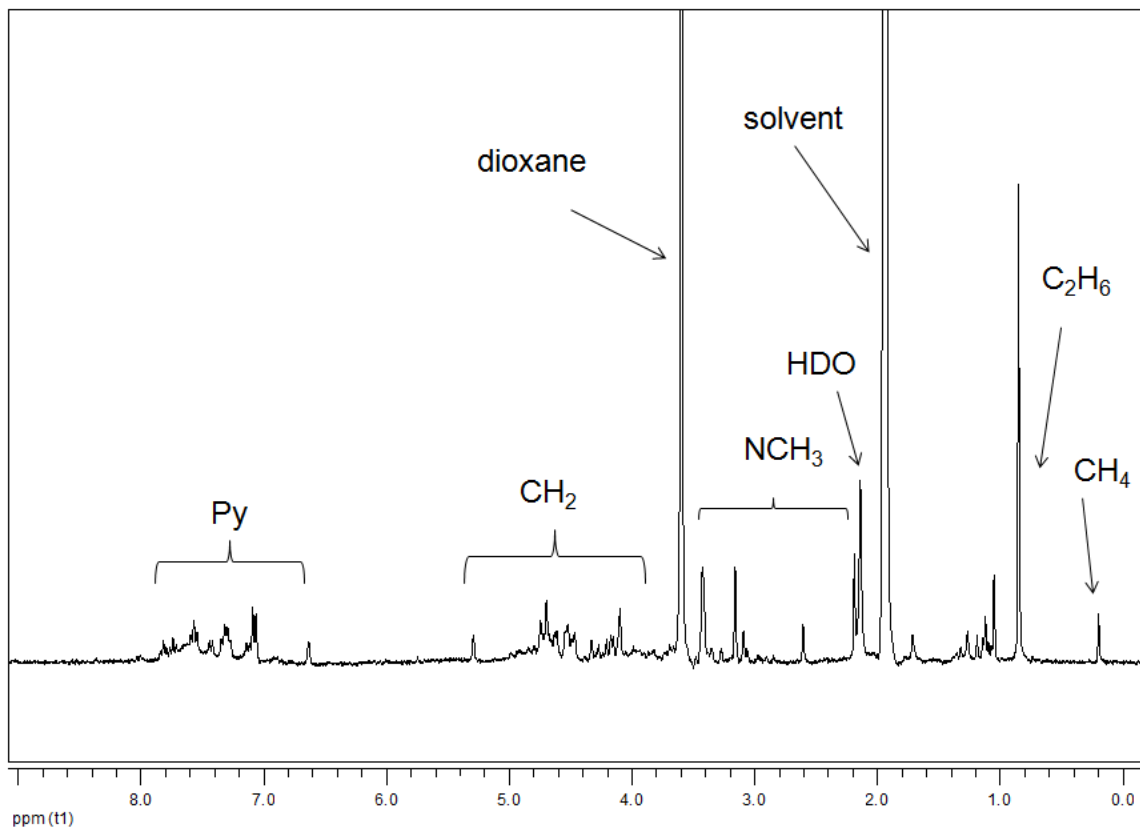
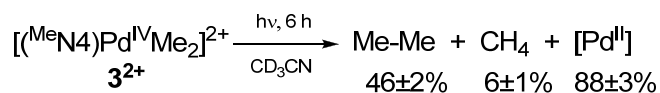


**Figure S51.**  $^1\text{H}$  NMR spectrum of solution of  $3^{2+}$  in  $\text{CD}_3\text{CN}$  after irradiation for 6 hours at  $0\text{ }^\circ\text{C}$ . The expected  $[(^{\text{Me}}\text{N}4)\text{Pd}^{\text{II}}(\text{MeCN})_2]^{2+}$  product is unstable and decomposes to a mixture of unidentified  $\text{Pd}^{\text{II}}$  products. Intergration of the entire aromatic region gives  $\sim 88\%$  overall yield for all  $\text{Pd}^{\text{II}}$  products.

Note: A similar yield of ethane was obtained in presence of 2 equiv TEMPO, suggesting a non-radical mechanism of ethane formation.

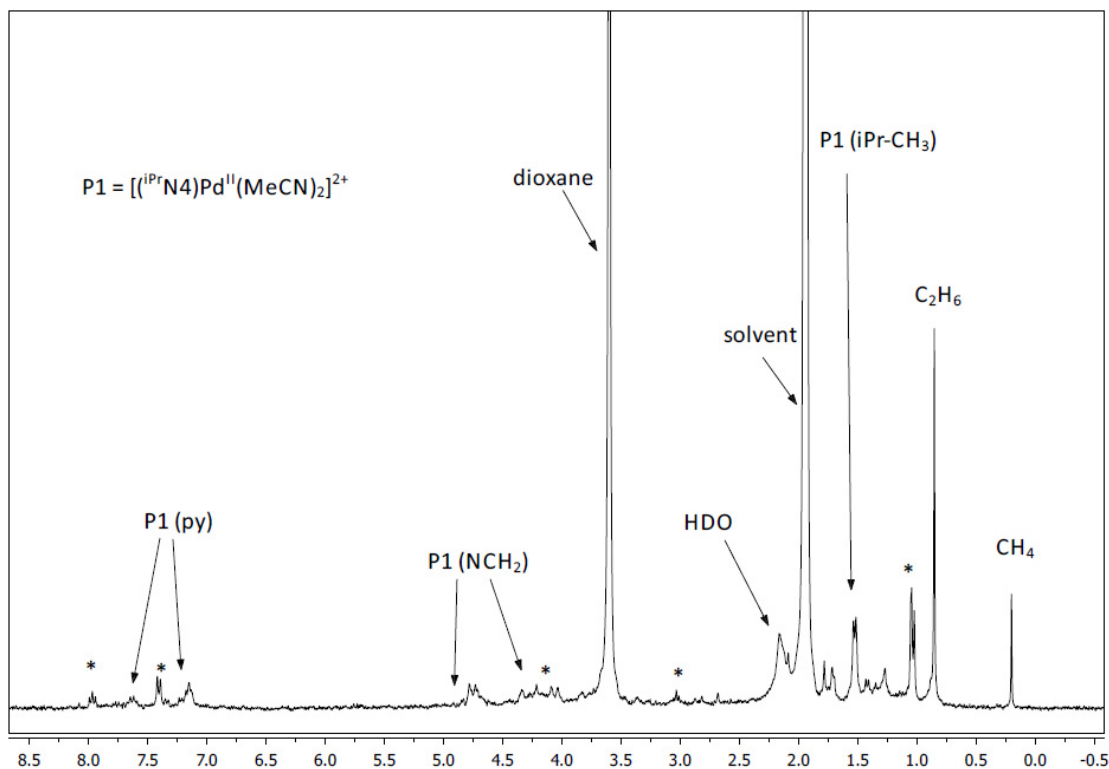
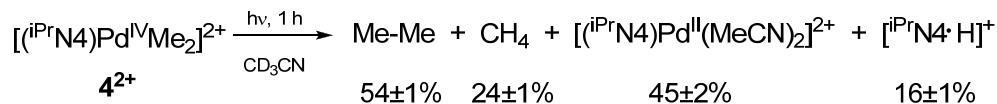


**Figure S52.**  $^1H$  NMR spectrum of a solution of  $4^{2+}$  in  $CD_3CN$  after irradiation for 1 hour at  $0\text{ }^\circ C$ .  $[(iPrN4)Pd^{II}(MeCN)_2]^{2+}$  was identified by comparison with an independently synthesized sample. Peaks labelled with asterisk correspond to  $[iPrN4\cdot H]^+$ , which likely forms upon decomposition of  $[(iPrN4)Pd^{II}(MeCN)_2]^{2+}$ .

Note: A similar yield of ethane was obtained in presence of 2 equiv TEMPO, suggesting a non-radical mechanism of ethane formation.

## Synthesis of $[(^R\text{N}4)\text{Pd}^{\text{II}}\text{Me}(\text{MeCN})]^+$ and $[(^i\text{PrN}4)\text{Pd}^{\text{II}}(\text{MeCN})_2]^{2+}$ complexes

### 1) Synthesis of $[(^{\text{Me}}\text{N}4)\text{Pd}^{\text{II}}\text{Me}(\text{MeCN})]^+$

Under  $\text{N}_2$ , 2-4 mg of  $(^{\text{Me}}\text{N}4)\text{Pd}^{\text{II}}\text{MeCl}$  (**1**) were dissolved in 1 mL  $\text{CD}_3\text{CN}$  and treated with 1 or 2 equiv of  $\text{NaBPh}_4$ ,  $\text{KPF}_6$ , or  $\text{NaBF}_4$ . The reaction mixture was transferred to an NMR tube and monitored by NMR.  $[(^{\text{Me}}\text{N}4)\text{Pd}^{\text{II}}\text{Me}(\text{MeCN})]^+$  was identified by comparison with the analogous complex  $[(^{\text{tBu}}\text{N}4)\text{Pd}^{\text{II}}\text{Me}(\text{MeCN})]^+$ .<sup>6</sup> In all cases,  $[(^{\text{Me}}\text{N}4)\text{Pd}^{\text{II}}\text{Me}(\text{MeCN})]^+$  was generated within 10 min, followed by its decomposition to methane and unidentified  $\text{Pd}^{\text{II}}$  complexes.

Treatment of  $(^{\text{Me}}\text{N}4)\text{Pd}^{\text{II}}\text{MeCl}$  with  $\text{AgBF}_4$  or  $\text{AgOTf}$  were also performed, following a reported procedure,<sup>10</sup> yet the  $\text{Ag}^+$  ions caused the oxidation of the  $\text{Pd}^{\text{II}}$  centers and formation of a complicated mixture of Pd products.

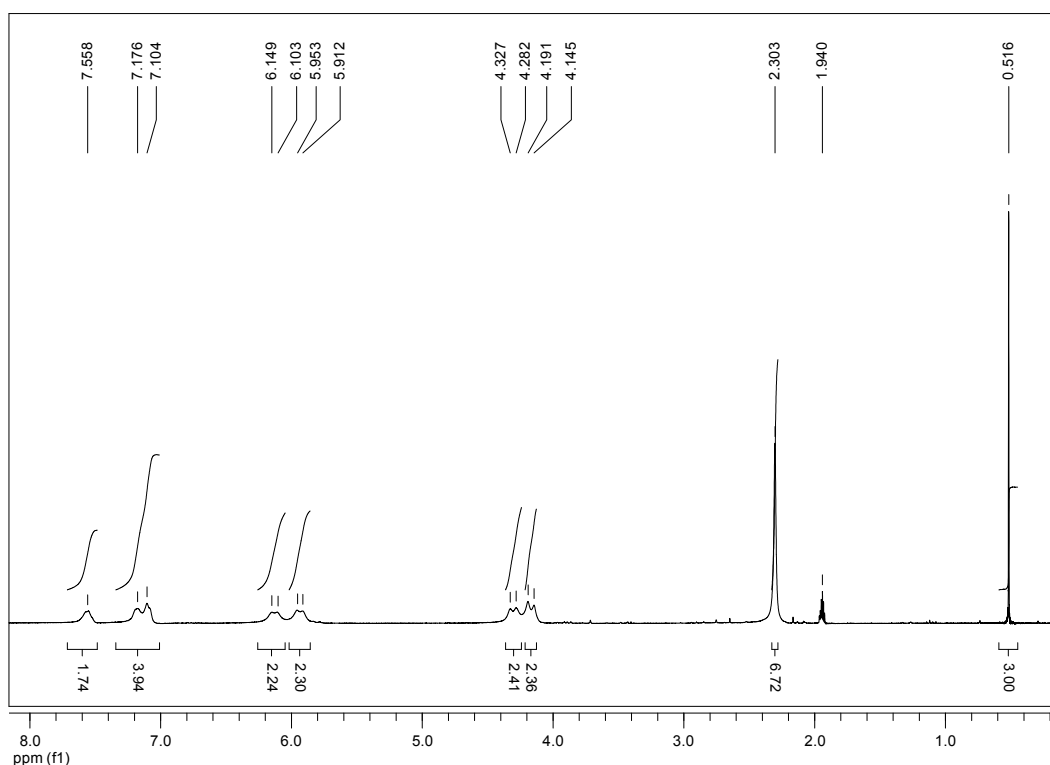


**Figure S53.**  $^1\text{H}$  NMR spectrum of  $(^{\text{Me}}\text{N}4)\text{Pd}^{\text{II}}\text{MeCl}$  (**1**) in  $\text{CD}_3\text{CN}$  before addition of  $\text{KPF}_6$ .  $^1\text{H}$  NMR (300MHz,  $\text{CD}_3\text{CN}$ ):  $\delta$  7.56 (br, 2H, py-H), 7.14 (br m, 4H, py-H), 6.13 (d,  $J = 13.8$  Hz, 2H,  $-\text{CH}_2-$ ), 5.93 (d,  $J = 12.3$  Hz, 2H,  $-\text{CH}_2-$ ), 4.30 (d,  $J = 13.5$  Hz, 2H,  $-\text{CH}_2-$ ), 4.17 (d,  $J = 13.8$  Hz, 2H,  $-\text{CH}_2-$ ), 2.30 (s, 6H, N- $\text{CH}_3$ ), 0.52 (s, 3H, Pd- $\text{CH}_3$ ).

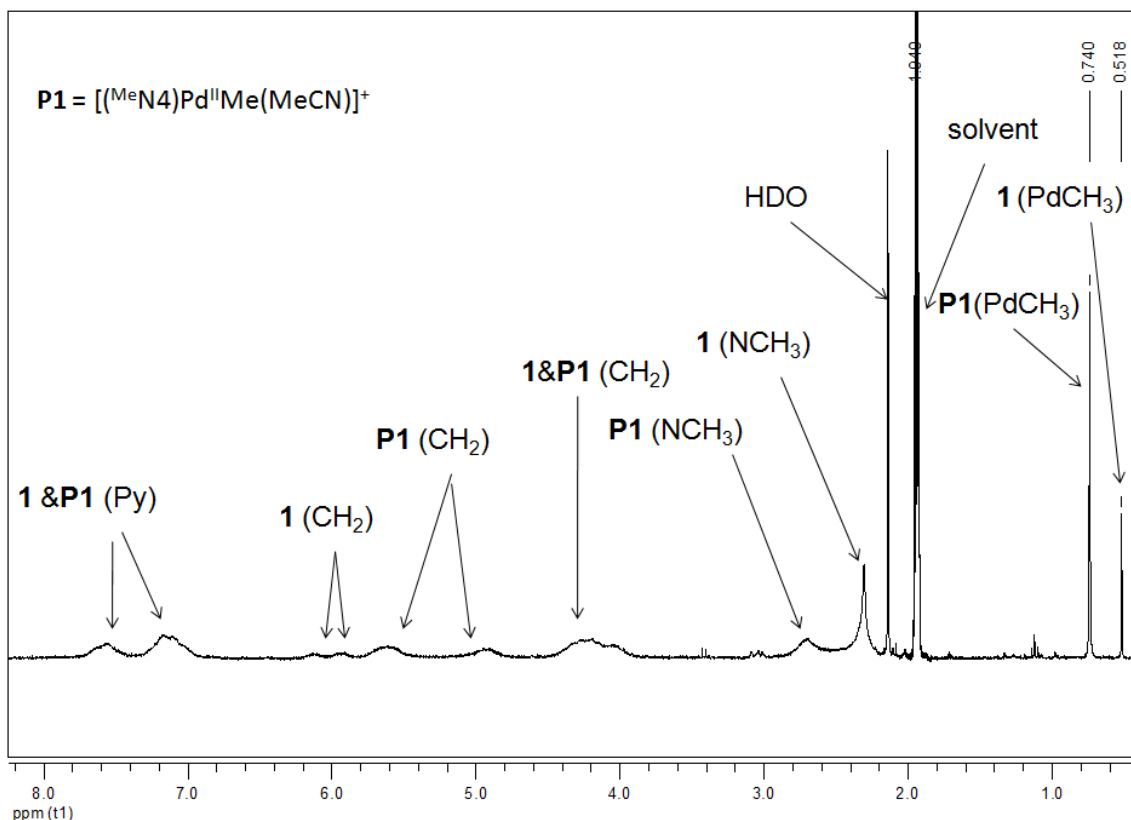


**Figure S54.**  $^1\text{H}$  NMR spectrum of the reaction mixture of **1** and 2 equiv  $\text{KPF}_6$  after 10 min in  $\text{CD}_3\text{CN}$ .  $^1\text{H}$  NMR (300MHz,  $\text{CD}_3\text{CN}$ ):  $\delta$  7.58 (br, py-H), 7.18 (br, Py-H), 5.60 (br,  $-\text{CH}_2-$ ), 4.94 (br,  $-\text{CH}_2-$ ), 4.21 (br,  $-\text{CH}_2-$ ), 2.72 (br, N- $\text{CH}_3$ ), 0.74 (s, Pd- $\text{CH}_3$ ).

## 2) Attempts to synthesize $[(\text{Me}^e\text{N4})\text{Pd}^{\text{II}}(\text{MeCN})_2]^{2+}$

Two methods were employed synthesize  $[(\text{Me}^e\text{N4})\text{Pd}^{\text{II}}(\text{MeCN})_2]^{2+}$ : 1) treatment of  $(\text{Me}^e\text{N4})\text{Pd}^{\text{II}}\text{Cl}_2$  with 2 equiv of  $\text{AgOTf}$  or  $\text{AgBF}_4$ ; and 2) treatment of  $\text{Me}^e\text{N4}$  with 1 equiv of  $[\text{Pd}^{\text{II}}(\text{MeCN})_4](\text{BF}_4)_2$ . In either case, Pd black formed quickly along with several unidentified products, as observed by NMR.

### 3) Synthesis of $[(iPr_4N)Pd^{II}Me(MeCN)]^+$

Under  $N_2$ ,  $(iPr_4N)Pd^{II}MeCl$  (26 mg, 0.054 mmol) was dissolved in 2 mL  $CD_3CN$ .  $AgOTf$  (14 mg, 0.054 mmol) in 2 mL of  $CD_3CN$  was added to give a yellow suspension. The solution was stirred at RT under  $N_2$  in dark for 4 hours. The solution was filtered and then immediately analyzed by NMR. Attempts to isolate the  $[(iPr_4N)Pd^{II}Me(MeCN)]^+$  product were unsuccessful.

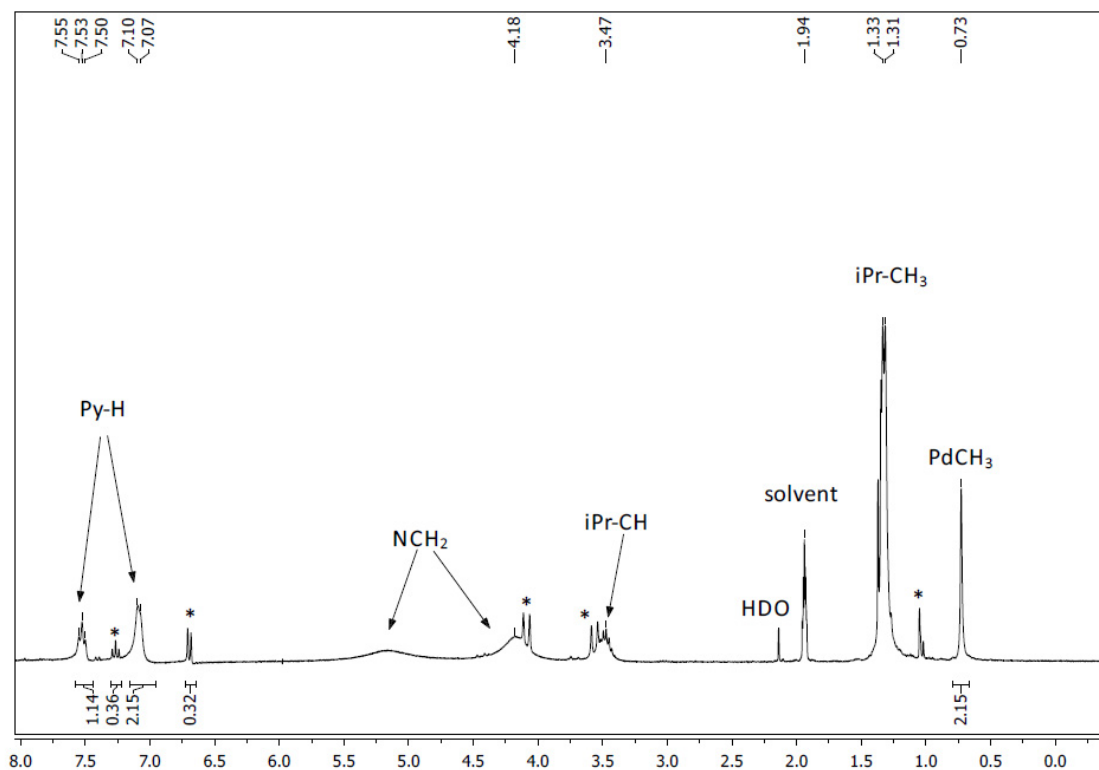


**Figure S55.**  $^1H$  NMR spectrum of a solution of  $[(iPr_4N)Pd^{II}Me(MeCN)]^+$  in  $CD_3CN$ . Peaks marked with an asterisk correspond to the  $iPr_4N$  ligand.

$^1H$  NMR (300MHz,  $CD_3CN$ ):  $\delta$  7.52 (br, py-H), 7.07 (br, Py-H), 5.2(br,  $-CH_2-$ ), 4.2 (br,  $-CH_2-$ ), 3.5 (br, iPr-CH), 1.33 (d, iPr- $CH_3$ ), 0.73 (s, Pd-Me)

#### 4) Synthesis of $[(iPrN4)Pd^{II}(MeCN)_2]^{2+}$

$[Pd(MeCN)_4](BF_4)_2$  (8.0 mg, 0.018 mmol) and  $iPrN4$  (5.8 mg, 0.018 mmol) were dissolved in 1 mL  $CD_3CN$ , the solution was stirred at RT in dark for 20 minutes, and the NMR was recorded. Attempts to isolate the  $[(iPrN4)Pd^{II}Me(MeCN)]^+$  product were unsuccessful likely due to its instability.

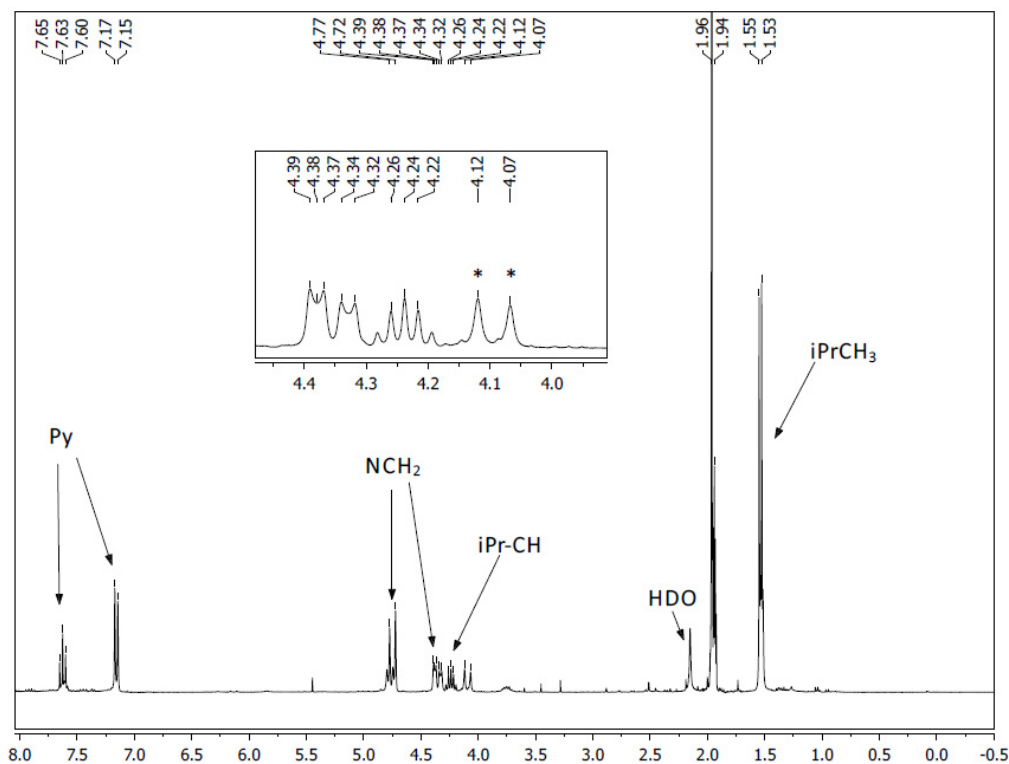
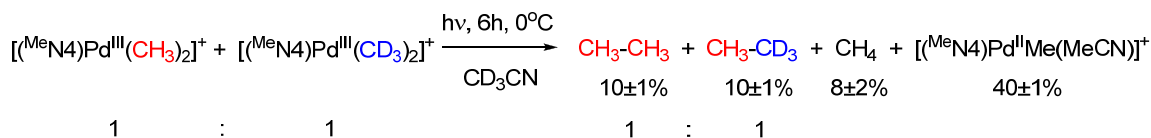


**Figure S56.**  $^1H$  NMR spectrum of a solution of  $[(iPrN4)Pd^{II}(MeCN)_2]^{2+}$  in  $CD_3CN$ . Peaks marked with asterisk were not identified.  $^1H$  NMR (300 MHz,  $CD_3CN$ ):  $\delta$  7.64 (t, 2H, py-H,  $J = 7.8$  Hz), 7.16 (d, 4H, py-H,  $J = 7.8$  Hz), 4.74 (d, 4H, NCH<sub>2</sub>,  $J = 15.0$  Hz), 4.38 (d, 2H, NCH<sub>2</sub>,  $J = 15.0$  Hz), 4.33 (d, 2H, NCH<sub>2</sub>,  $J = 15.0$  Hz) 4.23 (m, 2H,  $iPr-CH$ ,  $J = 6.9$  Hz), 1.53 (d, 12H,  $iPr-CH_3$ ,  $J = 6.6$  Hz).

## VIII. Crossover reactivity studies

### 1) Photolysis of a 1:1 mixture of $[(^R\text{N4})\text{Pd}^{\text{III}}(\text{CH}_3)_2](\text{ClO}_4)$ and $[(^R\text{N4})\text{Pd}^{\text{III}}(\text{CD}_3)_2](\text{ClO}_4)$

Similar to the above described photolysis experiment, under  $\text{N}_2$  atmosphere,  $[(^{\text{Me}}\text{N4})\text{Pd}^{\text{III}}(\text{CH}_3)_2]\text{ClO}_4$ ,  $[\text{I}^+]\text{ClO}_4$ , (2.8 mg, 5.6  $\mu\text{mol}$ ) and  $[(^{\text{Me}}\text{N4})\text{Pd}^{\text{III}}(\text{CD}_3)_2]\text{ClO}_4$ ,  $[\text{I}^{+d_6}]\text{ClO}_4$ , (2.8 mg, 5.5  $\mu\text{mol}$ ) were dissolved in 2.4mL  $\text{CD}_3\text{CN}$  solution and 2.0mmg of 1,3,5-trimethoxybenzene was added as an internal standard. The NMR tube was filled to the top and was sealed with a septum. Then NMR tubes were placed in an ice bath and irradiated with two 100 W halogen lamps placed at a distance about 10 cm from the sample. and the reaction was analyzed periodically by  $^1\text{H}$  NMR until no starting material was left. The ratio of  $\text{CH}_3\text{CH}_3$  and  $\text{CH}_3\text{CD}_3$  remained  $\sim 1:1$  at each time point. Although the yield of  $\text{CD}_3\text{CD}_3$  could not be determined by NMR, since the typical yield of ethane of pure  $[(^{\text{Me}}\text{N4})\text{Pd}^{\text{III}}\text{Me}_2]\text{ClO}_4$  in similar reaction is about 30%, the yield of  $\text{CD}_3\text{CD}_3$  can be estimated to be 10%. Therefore, the overall yield of  $\text{CH}_3\text{CH}_3$ :  $\text{CH}_3\text{CD}_3$ :  $\text{CD}_3\text{CD}_3$  is 1: 1: 1 as expected. A similar reaction was performed for a 1:1 mixture of  $[(^{\text{iPr}}\text{N4})\text{Pd}^{\text{III}}(\text{CH}_3)_2]^+$  and  $[(^{\text{iPr}}\text{N4})\text{Pd}^{\text{III}}(\text{CD}_3)_2]^+$ , to also yield a  $\sim 1:1$  ratio of  $\text{CH}_3\text{CH}_3$ : $\text{CH}_3\text{CD}_3$ .



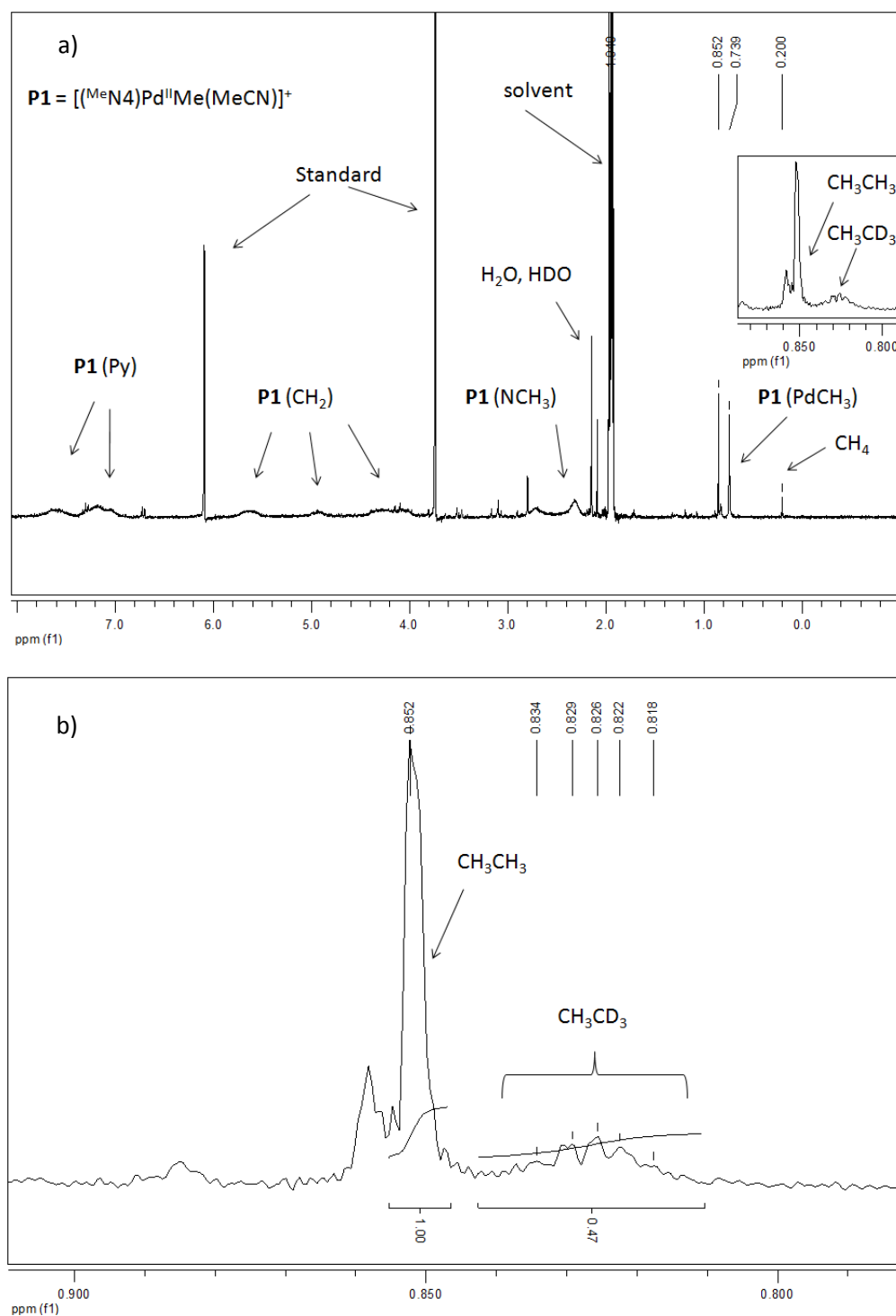


**Figure S57.**  $^1\text{H}$  NMR spectrum of a solution of 1:1 mixture of  $[\mathbf{1}^+]\text{ClO}_4$  and  $[\mathbf{1}^+-d_6]\text{ClO}_4$  in  $\text{CD}_3\text{CN}$  after irradiation for 6 hour at  $0^\circ\text{C}$ . a) full region; b) zoom-in region showing the  $\text{CH}_3\text{CH}_3$  and  $\text{CH}_3\text{CD}_3$  peaks.

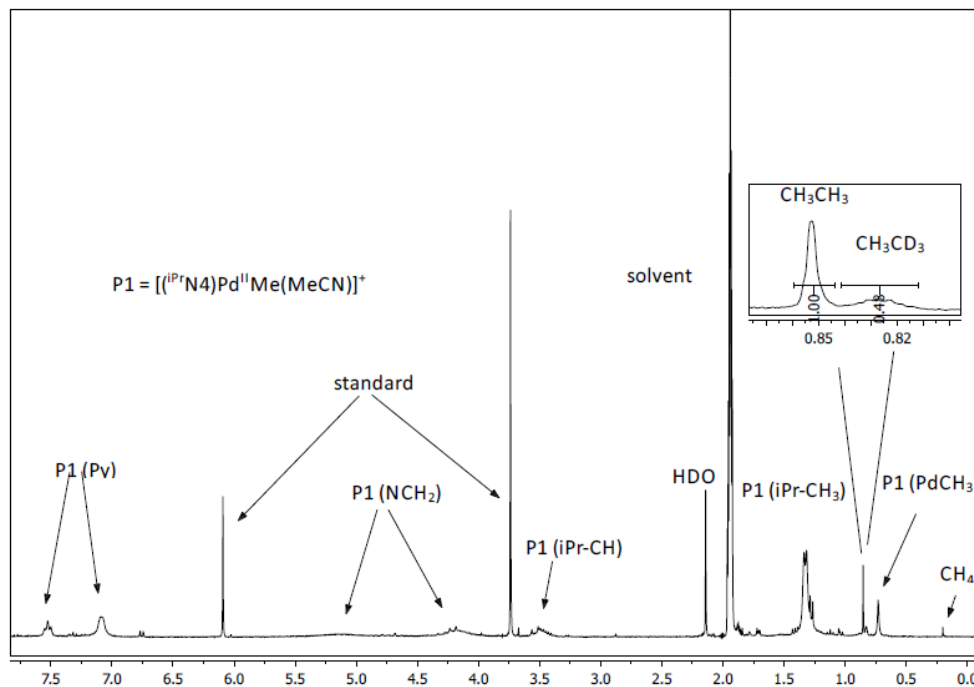
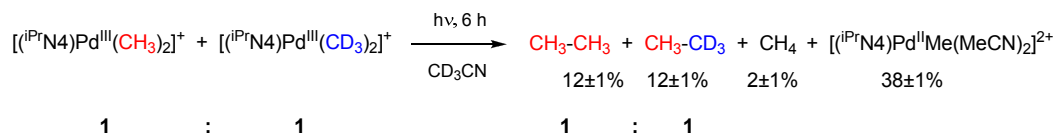


**Figure S58.** <sup>1</sup>H NMR spectrum of a solution of 1:1 [(<sup>i</sup>Pr<sub>4</sub>N)Pd<sup>III</sup>Me<sub>2</sub>]<sup>1+</sup>-[(<sup>i</sup>Pr<sub>4</sub>N)Pd<sup>III</sup>(CD<sub>3</sub>)<sub>2</sub>]<sup>1+</sup> in CD<sub>3</sub>CN after irradiation for 6 hours at 0 °C. 1,3,5-trimethoxybenzene was used as internal standard. [(<sup>i</sup>Pr<sub>4</sub>N)Pd<sup>II</sup>(Me)(MeCN)<sub>2</sub>]<sup>2+</sup> was identified by comparison of <sup>1</sup>H NMR spectrum with an authentic sample synthesized independently. The integration was based on the doublet at 0.73 ppm. Peaks labelled with asterisk belong to [<sup>i</sup>Pr<sub>4</sub>N•H]<sup>+</sup>, which was identified by comparison of <sup>1</sup>H NMR spectrum with an authentic sample synthesized independently.



### IX. X-ray structure characterization of $[1^+]\text{ClO}_4$ , $[2^+]\text{ClO}_4$ , $[3^+]\text{ClO}_4$ , $[4^+]\text{ClO}_4$ , $[1^{2+}](\text{ClO}_4)_2$ , $[3^{2+}](\text{PF}_6)_2$ , and $[4^{2+}](\text{PF}_6)_2$ .

*General information:* Crystals of x-ray diffraction quality were obtained by slow ether vapor diffusion into the corresponding acetonitrile or  $\text{CH}_2\text{Cl}_2$  solution of  $[1^+]\text{ClO}_4$ ,  $[2^+]\text{ClO}_4$ ,  $[3^+]\text{ClO}_4$ ,  $[4^+]\text{ClO}_4$ ,  $[1^{2+}](\text{ClO}_4)_2$ ,  $[3^{2+}](\text{PF}_6)_2$ , and  $[4^{2+}](\text{PF}_6)_2$ . Suitable crystals of appropriate dimensions were mounted on Mitgen loops in random orientations. Preliminary examination and data collection were performed using a Bruker Kappa Apex-II Charge Coupled Device (CCD) Detector system single crystal X-Ray diffractometer equipped with an Oxford Cryostream LT device. Data were collected using graphite monochromated Mo  $K\alpha$  radiation ( $\lambda = 0.71073 \text{ \AA}$ ) from a fine focus sealed tube X-Ray source. Preliminary unit cell constants were determined with a set of 36 narrow frame scans. Typical data sets consist of a combination of  $\omega$  and  $\phi$  scan frames with typical scan width of  $0.5^\circ$  and counting time of 15-30 seconds/frame at a crystal to detector distance of  $\sim 4.0 \text{ cm}$ . The collected frames were integrated using an orientation matrix determined from the narrow frame scans. Apex II and SAINT software packages (*Bruker Analytical X-Ray, Madison, WI, 2008*) were used for data collection and data integration. Analysis of the integrated data did not show any decay. Final cell constants were determined by global refinement of reflections from the complete data set. Data were corrected for systematic errors using SADABS (*Bruker Analytical X-Ray, Madison, WI, 2008*) based on the Laue symmetry using equivalent reflections.

Structure solutions and refinement were carried out using the SHELXTL- PLUS software package (*Sheldrick, G. M. (2008), Bruker-SHELXTL, Acta Cryst. A64,112-122*). The structures were refined with full matrix least-squares refinement by minimizing  $\sum w(F_o^2 - F_c^2)^2$ . All non-hydrogen atoms were refined anisotropically to convergence. Typically, H atoms are added at the calculated positions in the final refinement cycles.

Acknowledgement: Funding from the National Science Foundation (MRI, CHE-0420497) for the purchase of the ApexII diffractometer is acknowledged.

## X-ray structure determinations of [1<sup>+</sup>]ClO<sub>4</sub>

**Table S4.** Crystal data and structure refinement for lm26410.

Identification code	l26410/lt/FT-111710PdIIIMeCl	
Empirical formula	C <sub>19</sub> H <sub>26</sub> Cl <sub>2</sub> N <sub>5</sub> O <sub>4</sub> Pd	
Formula weight	565.75	
Temperature	100(2) K	
Wavelength	0.71073 Å	
Crystal system	Orthorhombic	
Space group	Pnma	
Unit cell dimensions	a = 13.6407(8) Å	α = 90°.
	b = 9.5515(5) Å	β = 90°.
	c = 17.0852(8) Å	γ = 90°.
Volume	2226.0(2) Å <sup>3</sup>	
Z	4	
Density (calculated)	1.688 Mg/m <sup>3</sup>	
Absorption coefficient	1.110 mm <sup>-1</sup>	
F(000)	1148	
Crystal size	0.22 x 0.15 x 0.14 mm <sup>3</sup>	
Theta range for data collection	1.91 to 32.75°.	
Index ranges	-20 ≤ h ≤ 20, -14 ≤ k ≤ 14, -26 ≤ l ≤ 25	
Reflections collected	41610	
Independent reflections	4309 [R(int) = 0.0453]	
Completeness to theta = 25.00°	100.0 %	
Absorption correction	Semi-empirical from equivalents	
Max. and min. transmission	0.8619 and 0.7946	
Refinement method	Full-matrix least-squares on F <sup>2</sup>	
Data / restraints / parameters	4309 / 0 / 167	
Goodness-of-fit on F <sup>2</sup>	1.272	
Final R indices [I > 2σ(I)]	R1 = 0.0399, wR2 = 0.0869	
R indices (all data)	R1 = 0.0469, wR2 = 0.0892	
Largest diff. peak and hole	0.675 and -1.368 e.Å <sup>-3</sup>	

**Table S5.** Bond lengths [Å] for lm26410.

Pd(1)-C(1)#1	2.021(11)	C(3)-C(4)	1.388(4)
Pd(1)-C(1)	2.021(11)	C(3)-H(3A)	0.9500
Pd(1)-N(1)	2.086(2)	C(4)-C(5)	1.383(4)
Pd(1)-N(1)#1	2.087(2)	C(4)-H(4A)	0.9500
Pd(1)-N(3)	2.301(3)	C(5)-C(6)	1.385(4)
Pd(1)-N(4)	2.339(3)	C(5)-H(5A)	0.9500
Pd(1)-Cl(1)	2.343(3)	C(6)-C(7)	1.502(4)
Pd(1)-Cl(1)#1	2.343(3)	C(7)-H(7A)	0.9900
C(1)-H(1A)	0.9800	C(7)-H(7B)	0.9900
C(1)-H(1B)	0.9800	C(8)-H(8A)	0.9900
C(1)-H(1C)	0.9800	C(8)-H(8B)	0.9900
N(1)-C(2)	1.338(3)	C(9)-H(9A)	0.9602
N(1)-C(6)	1.342(3)	C(9)-H(9B)	0.9600
N(3)-C(9)	1.468(5)	C(10)-H(10A)	0.9601
N(3)-C(7)#1	1.486(3)	C(10)-H(10B)	0.9599
N(3)-C(7)	1.486(3)	Cl(2)-O(2)	1.420(3)
N(4)-C(8)	1.477(3)	Cl(2)-O(1)	1.438(3)
N(4)-C(8)#1	1.477(3)	Cl(2)-O(3)#2	1.440(3)
N(4)-C(10)	1.477(4)	Cl(2)-O(3)	1.440(3)
C(2)-C(3)	1.384(4)	N(1S)-C(1S)	1.143(6)
C(2)-C(8)	1.509(3)	C(1S)-C(2S)	1.448(6)

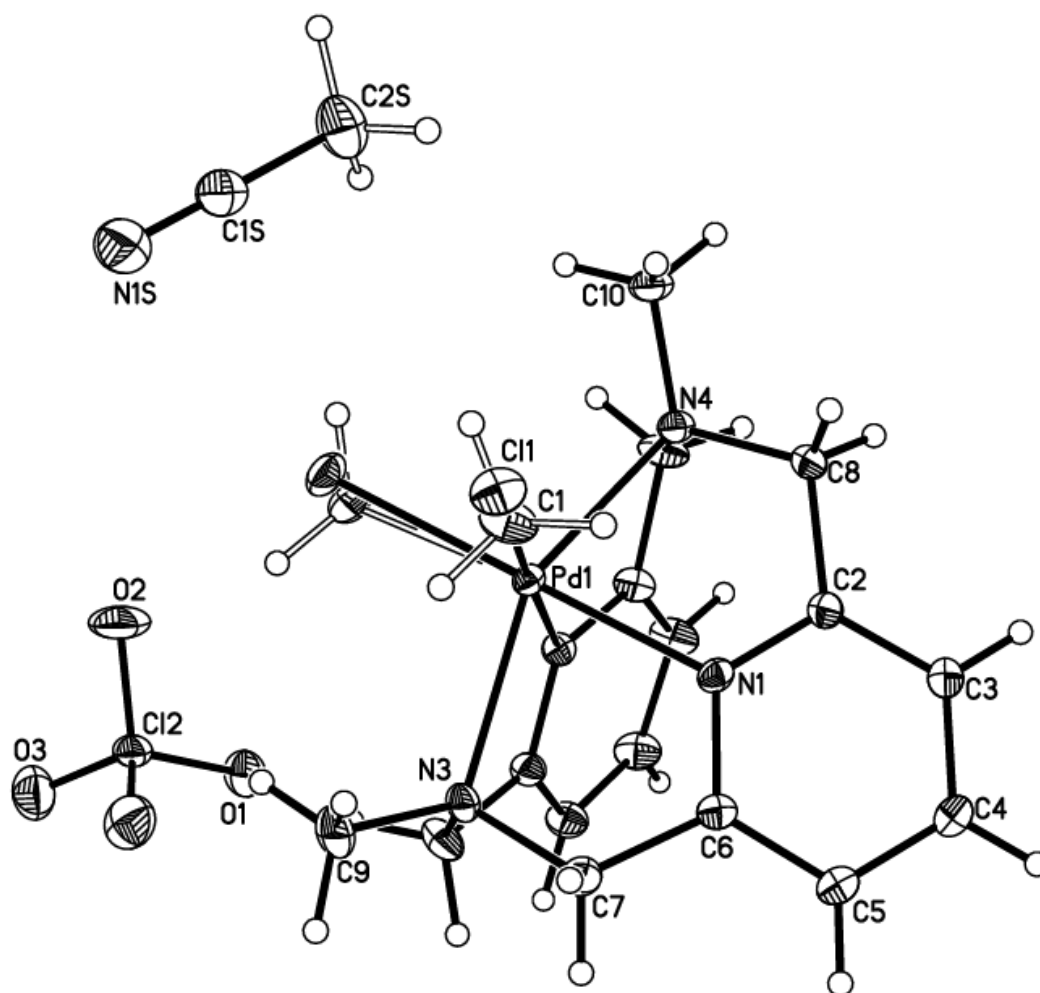


**Figure S60.** Projection view of [1<sup>+</sup>]ClO<sub>4</sub> with 50% thermal ellipsoids.

Note: All H atoms were added in their calculated positions and were treated using appropriate riding models. The Me group and the Cl atom bonded to the Pd atom are disordered over the two sites and were refined as 50% occupancy atoms.

## X-ray structure determinations of [2<sup>+</sup>]ClO<sub>4</sub>

**Table S6.** Crystal data and structure refinement for lm24710.

Identification code	l24710t5/lt/QFR-012-NB4-pp38	
Empirical formula	C21 H31 Cl2 N4 O4 Pd	
Formula weight	580.80	
Temperature	100(2) K	
Wavelength	0.71073 Å	
Crystal system	Monoclinic	
Space group	P2 <sub>1</sub> /c	
Unit cell dimensions	a = 13.7580(12) Å	α = 90°.
	b = 10.9028(9) Å	β = 102.449(5)°.
	c = 15.9177(13) Å	γ = 90°.
Volume	2331.5(3) Å <sup>3</sup>	
Z	4	
Density (calculated)	1.655 Mg/m <sup>3</sup>	
Absorption coefficient	1.061 mm <sup>-1</sup>	
F(000)	1188	
Crystal size	0.36 x 0.16 x 0.08 mm <sup>3</sup>	
Theta range for data collection	2.28 to 30.64°.	
Index ranges	-19 ≤ h ≤ 19, 0 ≤ k ≤ 15, 0 ≤ l ≤ 22	
Reflections collected	7130	
Independent reflections	7137 [R(int) = 0.0000]	
Completeness to theta = 25.00°	99.7 %	
Absorption correction	Semi-empirical from equivalents	
Max. and min. transmission	0.9228 and 0.7038	
Refinement method	Full-matrix least-squares on F <sup>2</sup>	
Data / restraints / parameters	7137 / 55 / 328	
Goodness-of-fit on F <sup>2</sup>	1.137	
Final R indices [I > 2σ(I)]	R1 = 0.0378, wR2 = 0.0756	
R indices (all data)	R1 = 0.0496, wR2 = 0.0817	
Largest diff. peak and hole	0.982 and -0.857 e.Å <sup>-3</sup>	

**Table S7.** Bond lengths [ $\text{\AA}$ ] for lm24710.

Pd(1)-C(1)	2.035(3)	C(5)-H(5)	0.9500
Pd(1)-N(2)	2.067(3)	C(6)-C(7)	1.508(4)
Pd(1)-N(1)	2.120(3)	C(7)-H(7A)	0.9900
Pd(1)-N(3)	2.355(3)	C(7)-H(7B)	0.9900
Pd(1)-Cl(1)	2.3713(9)	C(8)-C(9)	1.492(5)
Pd(1)-N(4)	2.394(3)	C(8)-H(8A)	0.9900
Cl(2)-O(2')	1.387(6)	C(8)-H(8B)	0.9900
Cl(2)-O(3)	1.395(5)	C(9)-C(10)	1.388(5)
Cl(2)-O(1)	1.414(3)	C(10)-C(11)	1.386(6)
Cl(2)-O(1')	1.414(3)	C(10)-H(10)	0.9500
Cl(2)-O(2)	1.427(6)	C(11)-C(12)	1.380(5)
Cl(2)-O(3')	1.429(6)	C(11)-H(11)	0.9500
Cl(2)-O(4')	1.429(5)	C(12)-C(13)	1.387(5)
Cl(2)-O(4)	1.435(5)	C(12)-H(12)	0.9500
N(1)-C(2)	1.335(4)	C(13)-C(14)	1.507(5)
N(1)-C(6)	1.340(4)	C(14)-H(14A)	0.9900
N(2)-C(9)	1.333(4)	C(14)-H(14B)	0.9900
N(2)-C(13)	1.337(4)	C(15)-H(15A)	0.9900
N(3)-C(8)	1.492(4)	C(15)-H(15B)	0.9900
N(3)-C(7)	1.496(4)	C(16)-C(17)	1.526(5)
N(3)-C(16)	1.506(4)	C(16)-C(18)	1.526(6)
N(4)-C(15)	1.477(4)	C(16)-H(16)	1.0000
N(4)-C(14)	1.478(4)	C(17)-H(17A)	0.9800
N(4)-C(19)	1.507(4)	C(17)-H(17B)	0.9800
C(1)-H(1A)	0.9800	C(17)-H(17C)	0.9800
C(1)-H(1B)	0.9800	C(18)-H(18A)	0.9800
C(1)-H(1C)	0.9800	C(18)-H(18B)	0.9800
C(2)-C(3)	1.388(4)	C(18)-H(18C)	0.9800
C(2)-C(15)	1.507(5)	C(19)-C(20)	1.498(5)
C(3)-C(4)	1.380(5)	C(19)-C(21)	1.523(5)
C(3)-H(3)	0.9500	C(19)-H(19)	1.0000
C(4)-C(5)	1.390(5)	C(20)-H(20A)	0.9800
C(4)-H(4)	0.9500	C(20)-H(20B)	0.9800
C(5)-C(6)	1.377(4)	C(20)-H(20C)	0.9800

C(21)-H(21A)	0.9800	C(21)-H(21C)	0.9800
C(21)-H(21B)	0.9800		

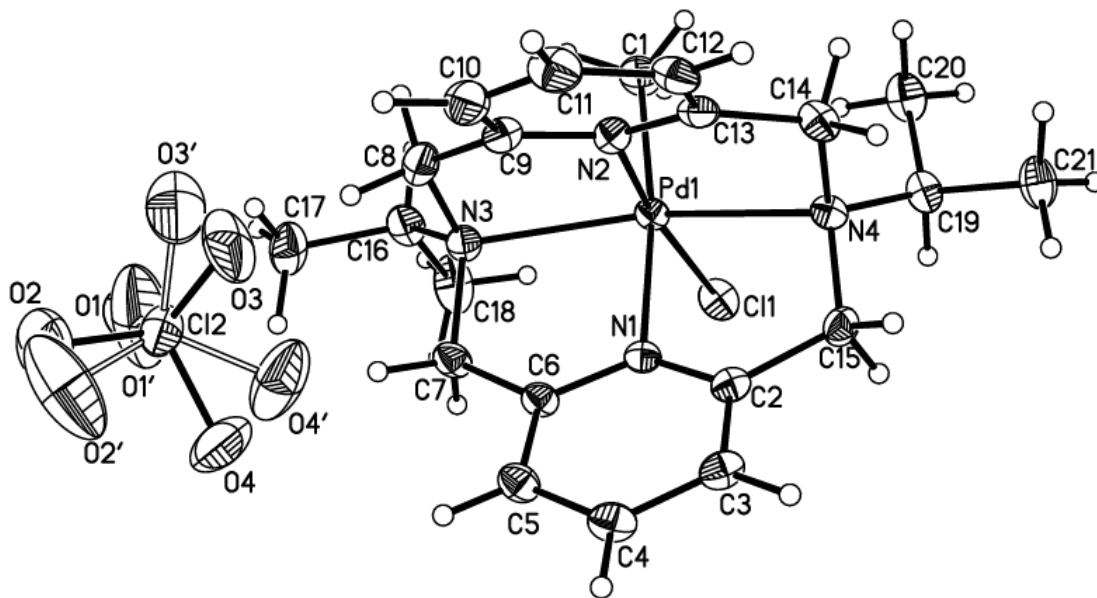


**Figure S61.** Projection view of [2<sup>+</sup>]ClO<sub>4</sub> with 50% thermal ellipsoids.

## X-ray structure determinations of [3<sup>+</sup>]ClO<sub>4</sub>

**Table S8.** Crystal data and structure refinement for Im5911.

Identification code	15911/lr/FT-041811-PdIII Me <sub>2</sub>	
Empirical formula	C <sub>20</sub> H <sub>29</sub> Cl N <sub>5</sub> O <sub>4</sub> Pd	
Formula weight	545.33	
Temperature	100(2) K	
Wavelength	0.71073 Å	
Crystal system	Orthorhombic	
Space group	Pnma	
Unit cell dimensions	a = 13.7422(9) Å	α = 90°.
	b = 9.5335(6) Å	β = 90°.
	c = 17.2691(10) Å	γ = 90°.
Volume	2262.4(2) Å <sup>3</sup>	
Z	4	
Density (calculated)	1.601 Mg/m <sup>3</sup>	
Absorption coefficient	0.975 mm <sup>-1</sup>	
F(000)	1116	
Crystal size	0.28 x 0.25 x 0.17 mm <sup>3</sup>	
Theta range for data collection	1.89 to 40.40°.	
Index ranges	-22 ≤ h ≤ 24, -17 ≤ k ≤ 17, -31 ≤ l ≤ 31	
Reflections collected	60880	
Independent reflections	7449 [R(int) = 0.0367]	
Completeness to theta = 25.00°	100.0 %	
Absorption correction	Semi-empirical from equivalents	
Max. and min. transmission	0.8502 and 0.7753	
Refinement method	Full-matrix least-squares on F <sup>2</sup>	
Data / restraints / parameters	7449 / 0 / 157	
Goodness-of-fit on F <sup>2</sup>	1.074	
Final R indices [I > 2σ(I)]	R1 = 0.0242, wR2 = 0.0577	
R indices (all data)	R1 = 0.0322, wR2 = 0.0608	
Largest diff. peak and hole	1.353 and -0.518 e.Å <sup>-3</sup>	

**Table S9.** Bond lengths [Å] for lm5911.

Pd(1)-C(1)	2.0432(10)	C(4)-C(5)	1.3928(15)
Pd(1)-C(1)#1	2.0433(10)	C(4)-H(4)	0.9500
Pd(1)-N(1)#1	2.1393(7)	C(5)-C(6)	1.3854(13)
Pd(1)-N(1)	2.1393(7)	C(5)-H(5)	0.9500
Pd(1)-N(3)	2.3506(12)	C(6)-C(7)	1.5091(13)
Pd(1)-N(2)	2.4013(11)	C(7)-H(7A)	0.9900
N(1)-C(2)	1.3398(12)	C(7)-H(7B)	0.9900
N(1)-C(6)	1.3413(11)	C(8)-H(8A)	0.9900
N(2)-C(9)	1.4725(18)	C(8)-H(8B)	0.9900
N(2)-C(7)#1	1.4768(11)	C(9)-H(9A)	0.9800
N(2)-C(7)	1.4768(11)	C(9)-H(9B)	0.9800
N(3)-C(10)	1.4732(16)	C(10)-H(10A)	0.9800
N(3)-C(8)	1.4820(11)	C(10)-H(10B)	0.9800
N(3)-C(8)#1	1.4821(11)	Cl(1)-O(3)	1.4260(14)
C(1)-H(1A)	0.9800	Cl(1)-O(1)	1.4398(8)
C(1)-H(1B)	0.9800	Cl(1)-O(1)#1	1.4398(8)
C(1)-H(1C)	0.9800	Cl(1)-O(2)	1.4404(11)
C(2)-C(3)	1.3890(13)	N(1S)-C(1S)	1.135(2)
C(2)-C(8)	1.5036(12)	C(1S)-C(2S)	1.450(2)
C(3)-C(4)	1.3847(14)	C(2S)-H(2SA)	0.9799
C(3)-H(3)	0.9500	C(2S)-H(2SB)	0.9800

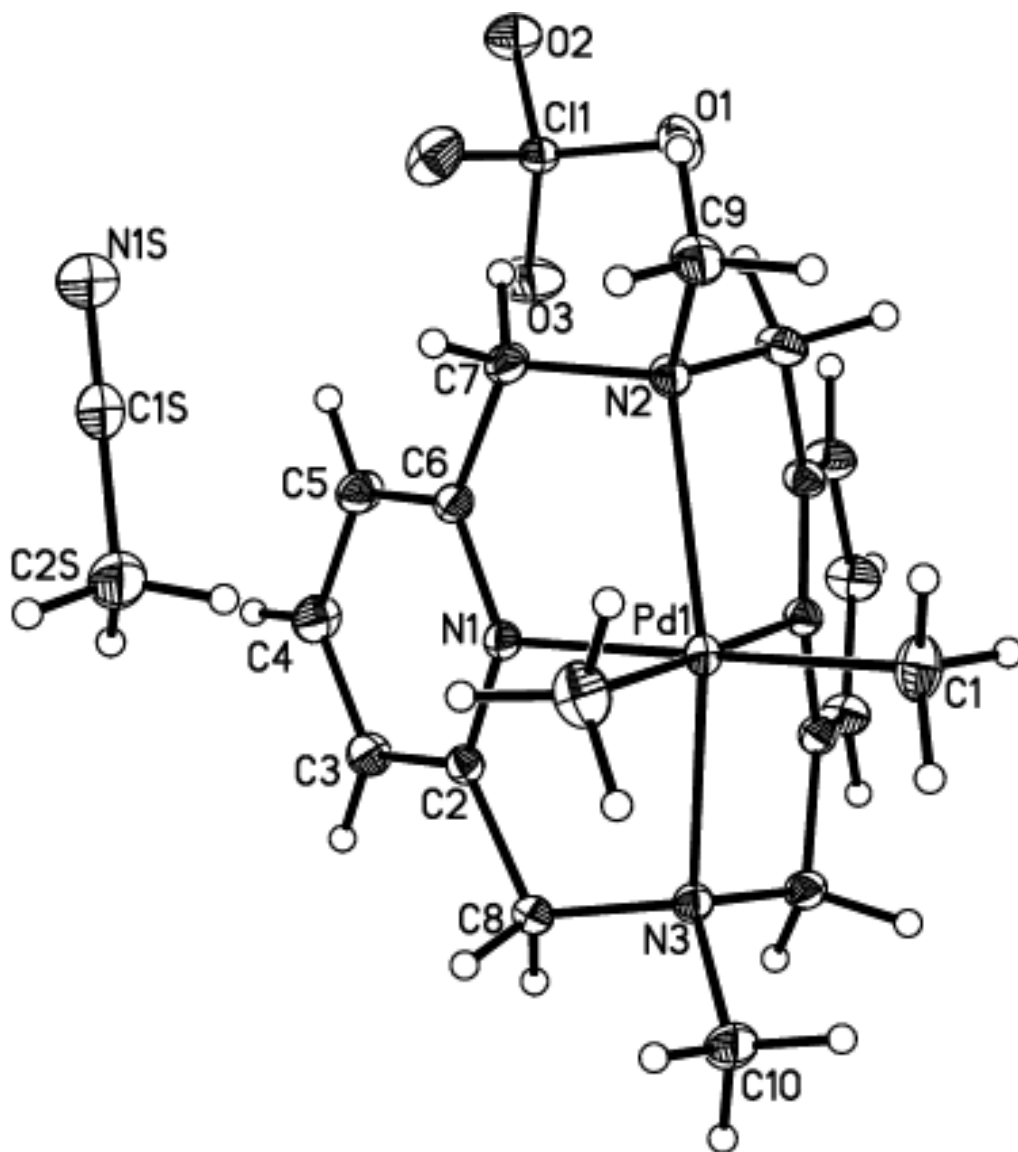


**Figure S62.** Projection view of  $[3^+]\text{ClO}_4$  with 50% thermal ellipsoids.

## X-ray structure determinations of [4<sup>+</sup>]ClO<sub>4</sub>

**Table S10.** Crystal data and structure refinement for lm6211.

Identification code	l6211/lt/Fengrui	
Empirical formula	C <sub>46</sub> H <sub>71</sub> Cl <sub>2</sub> N <sub>9</sub> O <sub>8</sub> Pd <sub>2</sub>	
Formula weight	1161.81	
Temperature	100(2) K	
Wavelength	0.71073 Å	
Crystal system	Monoclinic	
Space group	P2 <sub>1</sub> /n	
Unit cell dimensions	a = 13.8856(8) Å	α = 90°.
	b = 15.1803(8) Å	β = 92.908(3)°.
	c = 24.4154(13) Å	γ = 90°.
Volume	5139.8(5) Å <sup>3</sup>	
Z	4	
Density (calculated)	1.501 Mg/m <sup>3</sup>	
Absorption coefficient	0.863 mm <sup>-1</sup>	
F(000)	2400	
Crystal size	0.231 x 0.196 x 0.114 mm <sup>3</sup>	
Theta range for data collection	1.726 to 27.617°.	
Index ranges	-18 ≤ h ≤ 18, -19 ≤ k ≤ 19, -31 ≤ l ≤ 31	
Reflections collected	197720	
Independent reflections	11894 [R(int) = 0.0597]	
Completeness to theta = 25.000°	99.9 %	
Absorption correction	Semi-empirical from equivalents	
Max. and min. transmission	0.9081 and 0.8256	
Refinement method	Full-matrix least-squares on F <sup>2</sup>	
Data / restraints / parameters	11894 / 605 / 689	
Goodness-of-fit on F <sup>2</sup>	1.053	
Final R indices [I > 2σ(I)]	R1 = 0.0420, wR2 = 0.1113	
R indices (all data)	R1 = 0.0591, wR2 = 0.1256	
Extinction coefficient	0	
Largest diff. peak and hole	1.778 and -1.512 e.Å <sup>-3</sup>	

**Table S11.** Bond lengths [Å] and for lm6211.

Pd(1)-C(1)	2.033(4)	C(1)-H(1B)	0.9800
Pd(1)-C(2)	2.042(4)	C(1)-H(1C)	0.9800
Pd(1)-N(2)	2.132(3)	C(2)-H(2A)	0.9800
Pd(1)-N(1)	2.165(3)	C(2)-H(2B)	0.9800
Pd(1)-N(3)	2.428(3)	C(2)-H(2C)	0.9800
Pd(1)-N(4)	2.453(3)	C(3)-H(3A)	0.9800
Pd(2)-C(4)	2.051(4)	C(3)-H(3B)	0.9800
Pd(2)-C(3)	2.061(4)	C(3)-H(3C)	0.9800
Pd(2)-N(6)	2.125(3)	C(4)-H(4A)	0.9800
Pd(2)-N(5)	2.128(3)	C(4)-H(4B)	0.9800
Pd(2)-N(7)	2.401(3)	C(4)-H(4C)	0.9800
Pd(2)-N(8)	2.401(3)	C(5)-C(6)	1.384(5)
N(1)-C(9)	1.334(5)	C(5)-C(18)	1.497(5)
N(1)-C(5)	1.342(5)	C(6)-C(7)	1.379(6)
N(2)-C(16)	1.340(5)	C(6)-H(6)	0.9500
N(2)-C(12)	1.347(5)	C(7)-C(8)	1.377(6)
N(3)-C(11)	1.480(5)	C(7)-H(7)	0.9500
N(3)-C(10)	1.485(5)	C(8)-C(9)	1.392(6)
N(3)-C(19)	1.501(5)	C(8)-H(8)	0.9500
N(4)-C(18)	1.480(5)	C(9)-C(10)	1.497(6)
N(4)-C(17)	1.484(5)	C(10)-H(10A)	0.9900
N(4)-C(20)	1.506(5)	C(10)-H(10B)	0.9900
N(5)-C(29)	1.335(5)	C(11)-C(12)	1.509(5)
N(5)-C(25)	1.340(5)	C(11)-H(11A)	0.9900
N(6)-C(36)	1.337(5)	C(11)-H(11B)	0.9900
N(6)-C(32)	1.341(5)	C(12)-C(13)	1.379(5)
N(7)-C(31)	1.480(5)	C(13)-C(14)	1.381(6)
N(7)-C(30)	1.483(5)	C(13)-H(13)	0.9500
N(7)-C(39)	1.507(5)	C(14)-C(15)	1.381(6)
N(8)-C(37)	1.479(5)	C(14)-H(14)	0.9500
N(8)-C(38)	1.480(5)	C(15)-C(16)	1.384(5)
N(8)-C(42)	1.502(5)	C(15)-H(15)	0.9500
C(1)-H(1A)	0.9800	C(16)-C(17)	1.498(6)

C(17)-H(17A)	0.9900	C(31)-H(31B)	0.9900
C(17)-H(17B)	0.9900	C(32)-C(33)	1.384(5)
C(18)-H(18A)	0.9900	C(33)-C(34)	1.387(6)
C(18)-H(18B)	0.9900	C(33)-H(33)	0.9500
C(19)-C(22)	1.516(6)	C(34)-C(35)	1.381(6)
C(19)-C(21)	1.527(7)	C(34)-H(34)	0.9500
C(19)-H(19)	1.0000	C(35)-C(36)	1.380(6)
C(20)-C(23)	1.502(7)	C(35)-H(35)	0.9500
C(20)-C(24)	1.526(6)	C(36)-C(37)	1.513(6)
C(20)-H(20)	1.0000	C(37)-H(37A)	0.9900
C(21)-H(21A)	0.9800	C(37)-H(37B)	0.9900
C(21)-H(21B)	0.9800	C(38)-H(38A)	0.9900
C(21)-H(21C)	0.9800	C(38)-H(38B)	0.9900
C(22)-H(22A)	0.9800	C(39)-C(41)	1.514(6)
C(22)-H(22B)	0.9800	C(39)-C(40)	1.519(6)
C(22)-H(22C)	0.9800	C(39)-H(39)	1.0000
C(23)-H(23A)	0.9800	C(40)-H(40A)	0.9800
C(23)-H(23B)	0.9800	C(40)-H(40B)	0.9800
C(23)-H(23C)	0.9800	C(40)-H(40C)	0.9800
C(24)-H(24A)	0.9800	C(41)-H(41A)	0.9800
C(24)-H(24B)	0.9800	C(41)-H(41B)	0.9800
C(24)-H(24C)	0.9800	C(41)-H(41C)	0.9800
C(25)-C(26)	1.380(5)	C(42)-C(43)	1.512(7)
C(25)-C(38)	1.509(5)	C(42)-C(44)	1.528(6)
C(26)-C(27)	1.383(5)	C(42)-H(42)	1.0000
C(26)-H(26)	0.9500	C(43)-H(43A)	0.9800
C(27)-C(28)	1.377(6)	C(43)-H(43B)	0.9800
C(27)-H(27)	0.9500	C(43)-H(43C)	0.9800
C(28)-C(29)	1.385(5)	C(44)-H(44A)	0.9800
C(28)-H(28)	0.9500	C(44)-H(44B)	0.9800
C(29)-C(30)	1.503(5)	C(44)-H(44C)	0.9800
C(30)-H(30A)	0.9900	N(1S)-C(1S)	1.120(6)
C(30)-H(30B)	0.9900	C(1S)-C(2S)	1.463(8)
C(31)-C(32)	1.508(5)	C(2S)-H(2S1)	0.9800
C(31)-H(31A)	0.9900	C(2S)-H(2S2)	0.9800

C(2S)-H(2S3)	0.9800	Cl(2)-O(5)	1.421(3)
Cl(1)-O(4)	1.420(4)	Cl(2)-O(6)	1.428(3)
Cl(1)-O(3)	1.421(4)	Cl(2)-O(8)	1.431(4)
Cl(1)-O(1)	1.430(4)	Cl(2)-O(7)	1.431(3)
Cl(1)-O(2)	1.437(4)	Cl(2')-O(7')	1.409(4)
Cl(1')-O(3')	1.419(4)	Cl(2')-O(8')	1.423(4)
Cl(1')-O(4')	1.422(4)	Cl(2')-O(6')	1.437(4)
Cl(1')-O(1')	1.424(4)	Cl(2')-O(5')	1.439(4)
Cl(1')-O(2')	1.436(4)		

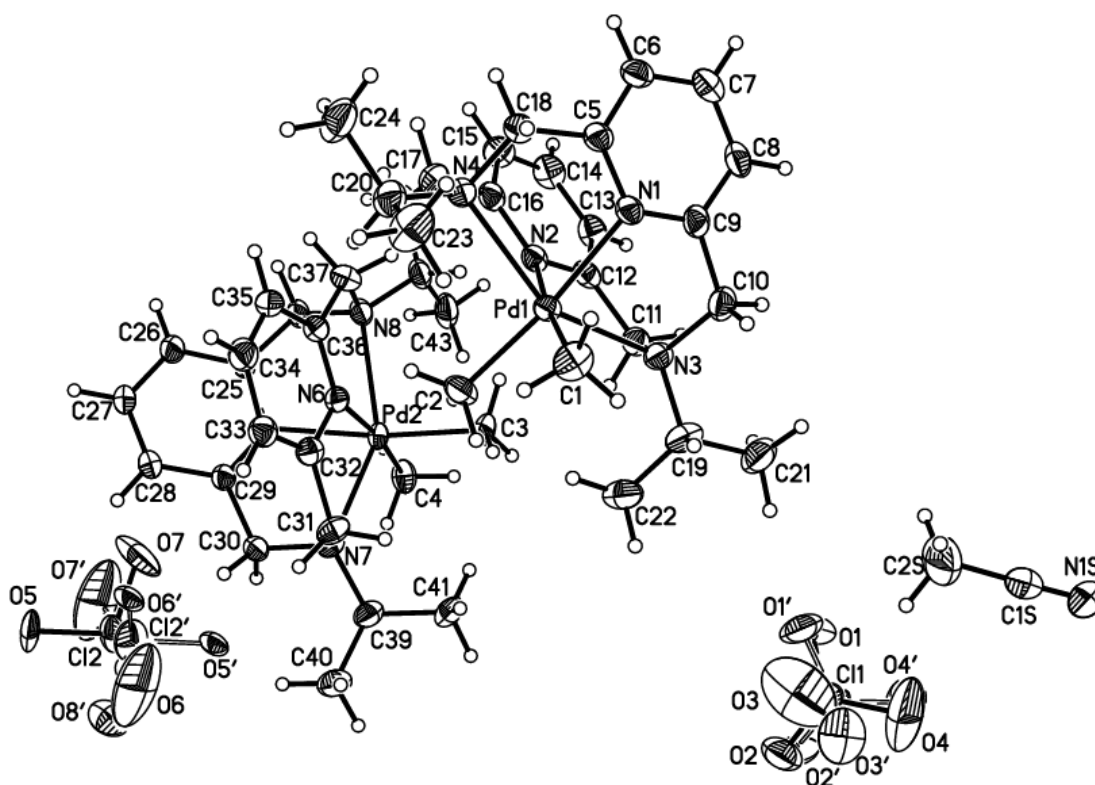


**Figure S63.** Projection view of  $[4^+]\text{ClO}_4$  with 50% thermal ellipsoids-disorder atoms and H atoms omitted.

## X-ray structure determination of $[1^{2+}](ClO_4)_2$

**Table S12.** Crystal data and structure refinement for lm9111.

Identification code	19111/lt/FT-063011-PdIVMeCl	
Empirical formula	C <sub>19</sub> H <sub>26</sub> Cl <sub>3</sub> N <sub>5</sub> O <sub>8</sub> Pd	
Formula weight	665.20	
Temperature	100(2) K	
Wavelength	0.71073 Å	
Crystal system	Monoclinic	
Space group	P2 <sub>1</sub> /n	
Unit cell dimensions	a = 10.7755(7) Å	α = 90°.
	b = 12.5823(9) Å	β = 101.389(3)°.
	c = 19.1881(12) Å	γ = 90°.
Volume	2550.3(3) Å <sup>3</sup>	
Z	4	
Density (calculated)	1.732 Mg/m <sup>3</sup>	
Absorption coefficient	1.096 mm <sup>-1</sup>	
F(000)	1344	
Crystal size	0.47 x 0.37 x 0.26 mm <sup>3</sup>	
Theta range for data collection	1.95 to 31.00°.	
Index ranges	-15 ≤ h ≤ 15, -18 ≤ k ≤ 18, -27 ≤ l ≤ 27	
Reflections collected	246996	
Independent reflections	8130 [R(int) = 0.0334]	
Completeness to theta = 31.00°	100.0 %	
Absorption correction	Semi-empirical from equivalents	
Max. and min. transmission	0.7615 and 0.6280	
Refinement method	Full-matrix least-squares on F <sup>2</sup>	
Data / restraints / parameters	8130 / 0 / 329	
Goodness-of-fit on F <sup>2</sup>	1.055	
Final R indices [I > 2σ(I)]	R1 = 0.0326, wR2 = 0.0905	
R indices (all data)	R1 = 0.0355, wR2 = 0.0931	
Largest diff. peak and hole	1.193 and -1.606 e.Å <sup>-3</sup>	

**Table S13.** Bond lengths [Å] for lm9111.

Pd(1)-N(1)	1.9658(17)	C(4)-H(4)	0.9500
Pd(1)-N(2)	2.0633(17)	C(5)-C(6)	1.389(3)
Pd(1)-C(1)	2.072(2)	C(5)-H(5)	0.9500
Pd(1)-N(3)	2.0983(17)	C(6)-C(7)	1.488(3)
Pd(1)-N(4)	2.1055(18)	C(7)-H(7A)	0.9900
Pd(1)-Cl(1)	2.2917(6)	C(7)-H(7B)	0.9900
Cl(2)-O(4)	1.405(2)	C(8)-C(9)	1.503(3)
Cl(2)-O(3)	1.411(2)	C(8)-H(8A)	0.9900
Cl(2)-O(1)	1.429(2)	C(8)-H(8B)	0.9900
Cl(2)-O(2)	1.446(2)	C(9)-C(10)	1.384(3)
Cl(3)-O(7)	1.410(2)	C(10)-C(11)	1.394(3)
Cl(3)-O(8)	1.430(2)	C(10)-H(10)	0.9500
Cl(3)-O(6)	1.4305(19)	C(11)-C(12)	1.397(3)
Cl(3)-O(5)	1.433(2)	C(11)-H(11)	0.9500
N(1)-C(6)	1.336(3)	C(12)-C(13)	1.386(3)
N(1)-C(2)	1.342(3)	C(12)-H(12)	0.9500
N(2)-C(9)	1.329(3)	C(13)-C(14)	1.505(3)
N(2)-C(13)	1.333(3)	C(14)-H(14A)	0.9900
N(3)-C(16)	1.490(3)	C(14)-H(14B)	0.9900
N(3)-C(7)	1.508(3)	C(15)-H(15A)	0.9900
N(3)-C(8)	1.516(3)	C(15)-H(15B)	0.9900
N(4)-C(17)	1.494(3)	C(16)-H(16A)	0.9800
N(4)-C(15)	1.509(3)	C(16)-H(16B)	0.9800
N(4)-C(14)	1.516(3)	C(16)-H(16C)	0.9800
C(1)-H(1A)	0.9800	C(17)-H(17A)	0.9800
C(1)-H(1B)	0.9800	C(17)-H(17B)	0.9800
C(1)-H(1C)	0.9800	C(17)-H(17C)	0.9800
C(2)-C(3)	1.380(3)	N(1S)-C(1S)	1.130(5)
C(2)-C(15)	1.494(3)	C(1S)-C(2S)	1.432(5)
C(3)-C(4)	1.386(4)	C(2S)-H(2S1)	0.9800
C(3)-H(3)	0.9500	C(2S)-H(2S2)	0.9800
C(4)-C(5)	1.385(4)	C(2S)-H(2S3)	0.9800

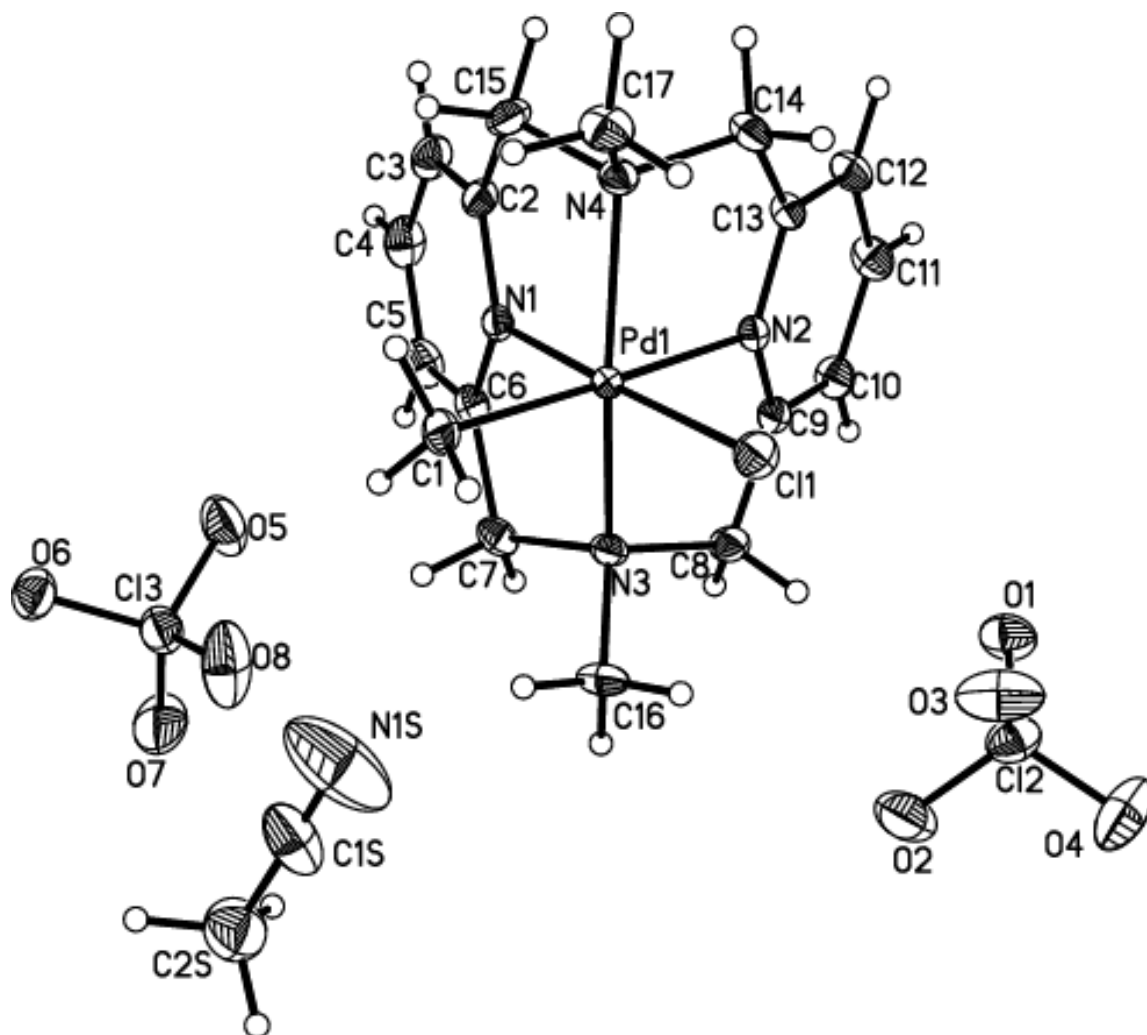


**Figure S64.** Projection view of [1<sup>2+</sup>](ClO<sub>4</sub>)<sub>2</sub> with 50% thermal ellipsoids.

### X-ray structure determinations of $[3^{2+}](PF_6)_2$

**Table S14.** Crystal data and structure refinement for lm5311.

Identification code	15311/lt/FT-041211-PdIVMe2	
Empirical formula	C <sub>20</sub> H <sub>29</sub> F <sub>12</sub> N <sub>5</sub> P <sub>2</sub> Pd	
Formula weight	735.82	
Temperature	100(2) K	
Wavelength	0.71073 Å	
Crystal system	Triclinic	
Space group	P-1	
Unit cell dimensions	a = 8.3484(8) Å	$\alpha = 75.555(5)^\circ$ .
	b = 10.5436(10) Å	$\beta = 78.534(6)^\circ$ .
	c = 16.3188(15) Å	$\gamma = 77.041(5)^\circ$ .
Volume	1340.0(2) Å <sup>3</sup>	
Z	2	
Density (calculated)	1.824 Mg/m <sup>3</sup>	
Absorption coefficient	0.917 mm <sup>-1</sup>	
F(000)	736	
Crystal size	0.22 x 0.15 x 0.08 mm <sup>3</sup>	
Theta range for data collection	2.03 to 27.61°.	
Index ranges	-10 ≤ h ≤ 10, -13 ≤ k ≤ 13, -21 ≤ l ≤ 21	
Reflections collected	34391	
Independent reflections	6090 [R(int) = 0.0503]	
Completeness to theta = 25.00°	99.3 %	
Absorption correction	Semi-empirical from equivalents	
Max. and min. transmission	0.9327 and 0.8216	
Refinement method	Full-matrix least-squares on F <sup>2</sup>	
Data / restraints / parameters	6090 / 0 / 366	
Goodness-of-fit on F <sup>2</sup>	1.035	
Final R indices [I > 2σ(I)]	R1 = 0.0357, wR2 = 0.0801	
R indices (all data)	R1 = 0.0515, wR2 = 0.0863	
Largest diff. peak and hole	1.874 and -0.696 e.Å <sup>-3</sup>	

**Table S15.** Bond lengths [Å] for lm5311.

Pd(1)-C(2)	2.039(3)	C(9)-C(10)	1.497(5)
Pd(1)-C(1)	2.042(3)	C(9)-H(9A)	0.9900
Pd(1)-N(1)	2.054(2)	C(9)-H(9B)	0.9900
Pd(1)-N(2)	2.058(3)	C(10)-C(11)	1.376(5)
Pd(1)-N(4)	2.116(2)	C(11)-C(12)	1.393(5)
Pd(1)-N(3)	2.129(3)	C(11)-H(11)	0.9500
N(1)-C(3)	1.328(4)	C(12)-C(13)	1.391(5)
N(1)-C(7)	1.337(4)	C(12)-H(12)	0.9500
N(2)-C(14)	1.328(4)	C(13)-C(14)	1.387(4)
N(2)-C(10)	1.334(4)	C(13)-H(13)	0.9500
N(3)-C(17)	1.492(4)	C(14)-C(15)	1.502(4)
N(3)-C(9)	1.513(4)	C(15)-H(15A)	0.9900
N(3)-C(8)	1.513(4)	C(15)-H(15B)	0.9900
N(4)-C(18)	1.486(4)	C(16)-H(16A)	0.9900
N(4)-C(16)	1.513(4)	C(16)-H(16B)	0.9900
N(4)-C(15)	1.526(4)	C(17)-H(17A)	0.9800
C(1)-H(1A)	0.9800	C(17)-H(17B)	0.9800
C(1)-H(1B)	0.9800	C(17)-H(17C)	0.9800
C(1)-H(1C)	0.9800	C(18)-H(18A)	0.9800
C(2)-H(2A)	0.9800	C(18)-H(18B)	0.9800
C(2)-H(2B)	0.9800	C(18)-H(18C)	0.9800
C(2)-H(2C)	0.9800	P(1)-F(1)	1.585(2)
C(3)-C(4)	1.387(4)	P(1)-F(3)	1.586(2)
C(3)-C(16)	1.498(4)	P(1)-F(2)	1.588(2)
C(4)-C(5)	1.379(5)	P(1)-F(5)	1.589(2)
C(4)-H(4)	0.9500	P(1)-F(6)	1.590(2)
C(5)-C(6)	1.391(5)	P(1)-F(4)	1.590(2)
C(5)-H(5)	0.9500	P(2)-F(10)	1.583(2)
C(6)-C(7)	1.377(4)	P(2)-F(8)	1.585(2)
C(6)-H(6)	0.9500	P(2)-F(7)	1.594(2)
C(7)-C(8)	1.507(4)	P(2)-F(9)	1.594(2)
C(8)-H(8A)	0.9900	P(2)-F(12)	1.594(2)
C(8)-H(8B)	0.9900	P(2)-F(11)	1.611(2)

N(1S)-C(1S)	1.130(5)	C(2S)-H(2S3)	0.9800
C(1S)-C(2S)	1.450(5)		
C(2S)-H(2S1)	0.9800		
C(2S)-H(2S2)	0.9800		

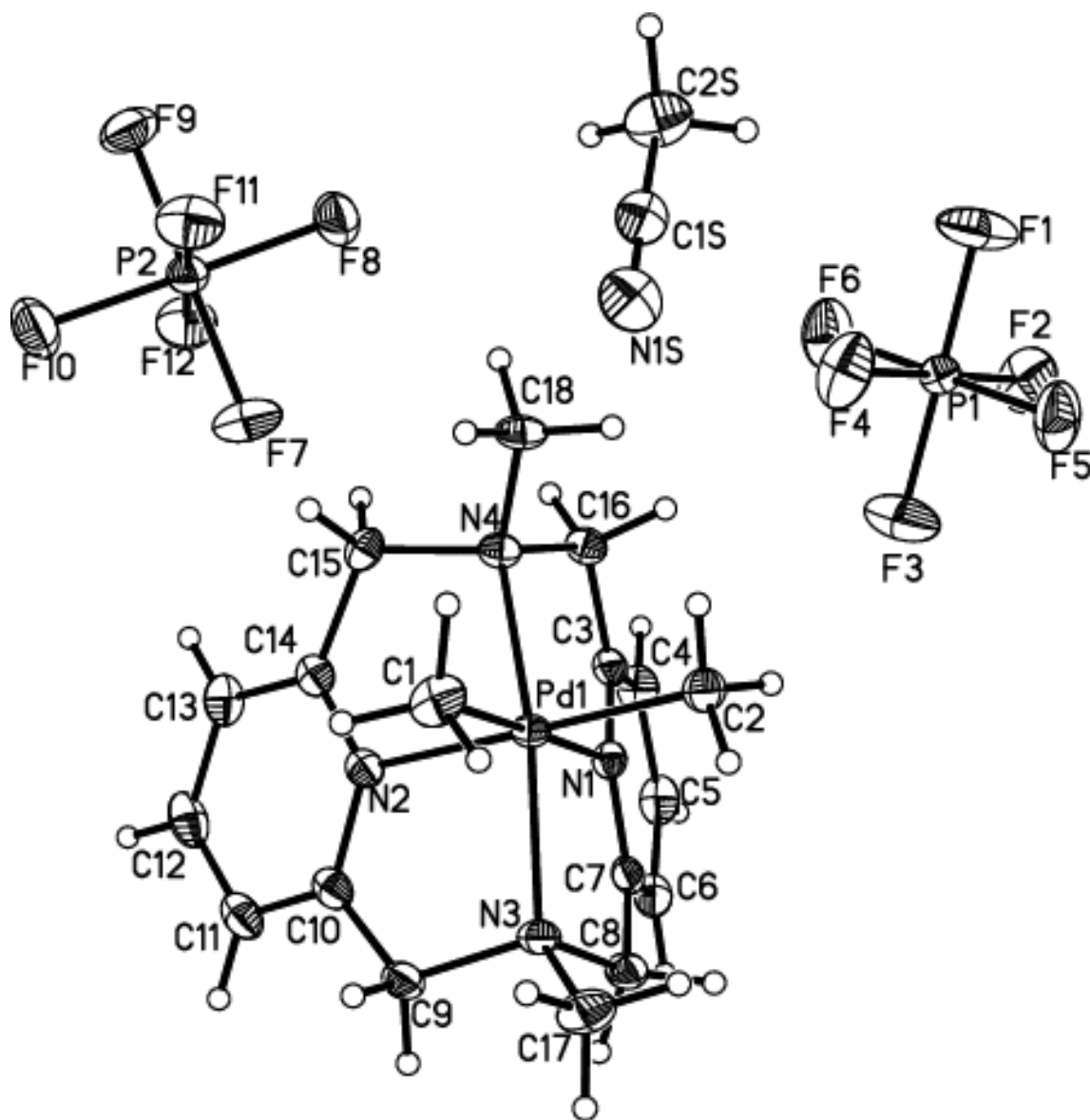


**Figure S65.** Projection view of [3<sup>2+</sup>](PF<sub>6</sub>)<sub>2</sub> with 50% thermal ellipsoids.

### X-ray structure determinations of [4<sup>2+</sup>](PF<sub>6</sub>)<sub>2</sub>

**Table S16.** Crystal data and structure refinement for lm14311.

Identification code	114311/Fengrui/iPrN4Pd(IV)pp11	
Empirical formula	C <sub>22</sub> H <sub>34</sub> F <sub>12</sub> N <sub>4</sub> P <sub>2</sub> Pd	
Formula weight	750.87	
Temperature	100(2) K	
Wavelength	0.71073 Å	
Crystal system	Monoclinic	
Space group	P2 <sub>1</sub> /c	
Unit cell dimensions	a = 10.0272(13) Å	α = 90°.
	b = 18.844(2) Å	β = 90.694(7)°.
	c = 15.044(2) Å	γ = 90°.
Volume	2842.4(6) Å <sup>3</sup>	
Z	4	
Density (calculated)	1.755 Mg/m <sup>3</sup>	
Absorption coefficient	0.866 mm <sup>-1</sup>	
F(000)	1512	
Crystal size	0.33 x 0.17 x 0.13 mm <sup>3</sup>	
Theta range for data collection	1.73 to 25.34°.	
Index ranges	-12 ≤ h ≤ 12, -23 ≤ k ≤ 23, -15 ≤ l ≤ 18	
Reflections collected	16961	
Independent reflections	5195 [R(int) = 0.0621]	
Completeness to theta = 25.34°	99.8 %	
Absorption correction	Semi-empirical from equivalents	
Max. and min. transmission	0.8980 and 0.7632	
Refinement method	Full-matrix least-squares on F <sup>2</sup>	
Data / restraints / parameters	5195 / 154 / 358	
Goodness-of-fit on F <sup>2</sup>	1.097	
Final R indices [I > 2σ(I)]	R1 = 0.0906, wR2 = 0.2158	
R indices (all data)	R1 = 0.1090, wR2 = 0.2259	
Largest diff. peak and hole	1.514 and -1.168 e.Å <sup>-3</sup>	

**Table S17.** Bond lengths [Å] for lm14311.

Pd(1)-C(2)	2.026(10)	C(9)-C(10)	1.484(19)
Pd(1)-N(1)	2.036(9)	C(9)-H(9A)	0.9900
Pd(1)-N(2)	2.047(9)	C(9)-H(9B)	0.9900
Pd(1)-C(1)	2.056(11)	C(10)-C(11)	1.407(17)
Pd(1)-N(3)	2.178(9)	C(11)-C(12)	1.38(2)
Pd(1)-N(4)	2.181(9)	C(11)-H(11)	0.9500
N(1)-C(3)	1.331(15)	C(12)-C(13)	1.40(2)
N(1)-C(7)	1.351(16)	C(12)-H(12)	0.9500
N(2)-C(10)	1.312(16)	C(13)-C(14)	1.364(17)
N(2)-C(14)	1.384(16)	C(13)-H(13)	0.9500
N(3)-C(8)	1.490(16)	C(14)-C(15)	1.485(19)
N(3)-C(9)	1.518(15)	C(15)-H(15A)	0.9900
N(3)-C(17)	1.541(14)	C(15)-H(15B)	0.9900
N(4)-C(16)	1.491(15)	C(16)-H(16A)	0.9900
N(4)-C(15)	1.497(15)	C(16)-H(16B)	0.9900
N(4)-C(20)	1.558(14)	C(17)-C(18)	1.505(5)
C(1)-H(1A)	0.9800	C(17)-C(19)	1.511(5)
C(1)-H(1B)	0.9800	C(17)-H(17)	1.0000
C(1)-H(1C)	0.9800	C(18)-H(18A)	0.9800
C(2)-H(2A)	0.9800	C(18)-H(18B)	0.9800
C(2)-H(2B)	0.9800	C(18)-H(18C)	0.9800
C(2)-H(2C)	0.9800	C(19)-H(19A)	0.9800
C(3)-C(4)	1.382(18)	C(19)-H(19B)	0.9800
C(3)-C(16)	1.486(19)	C(19)-H(19C)	0.9800
C(4)-C(5)	1.40(2)	C(20)-C(21)	1.474(17)
C(4)-H(4)	0.9500	C(20)-C(22)	1.538(19)
C(5)-C(6)	1.39(2)	C(20)-H(20)	1.0000
C(5)-H(5)	0.9500	C(21)-H(21A)	0.9800
C(6)-C(7)	1.362(18)	C(21)-H(21B)	0.9800
C(6)-H(6)	0.9500	C(21)-H(21C)	0.9800
C(7)-C(8)	1.497(18)	C(22)-H(22A)	0.9800
C(8)-H(8A)	0.9900	C(22)-H(22B)	0.9800
C(8)-H(8B)	0.9900	C(22)-H(22C)	0.9800

P(1)-F(5)	1.584(8)	P(1')-F(2')	1.580(16)
P(1)-F(2)	1.588(8)	P(1')-F(5')	1.580(16)
P(1)-F(1)	1.590(8)	P(1')-F(1')	1.584(16)
P(1)-F(6)	1.598(8)	P(1')-F(3')	1.597(16)
P(1)-F(4)	1.597(8)	P(1')-F(4')	1.598(16)
P(1)-F(3)	1.604(8)	P(1')-F(6')	1.598(16)
P(2)-F(8)	1.583(9)	P(2')-F(8')	1.578(16)
P(2)-F(11)	1.585(9)	P(2')-F(11')	1.580(16)
P(2)-F(7)	1.587(9)	P(2')-F(7')	1.585(16)
P(2)-F(9)	1.588(9)	P(2')-F(9')	1.597(16)
P(2)-F(12)	1.592(10)	P(2')-F(12')	1.598(16)
P(2)-F(10)	1.599(9)	P(2')-F(10')	1.599(16)

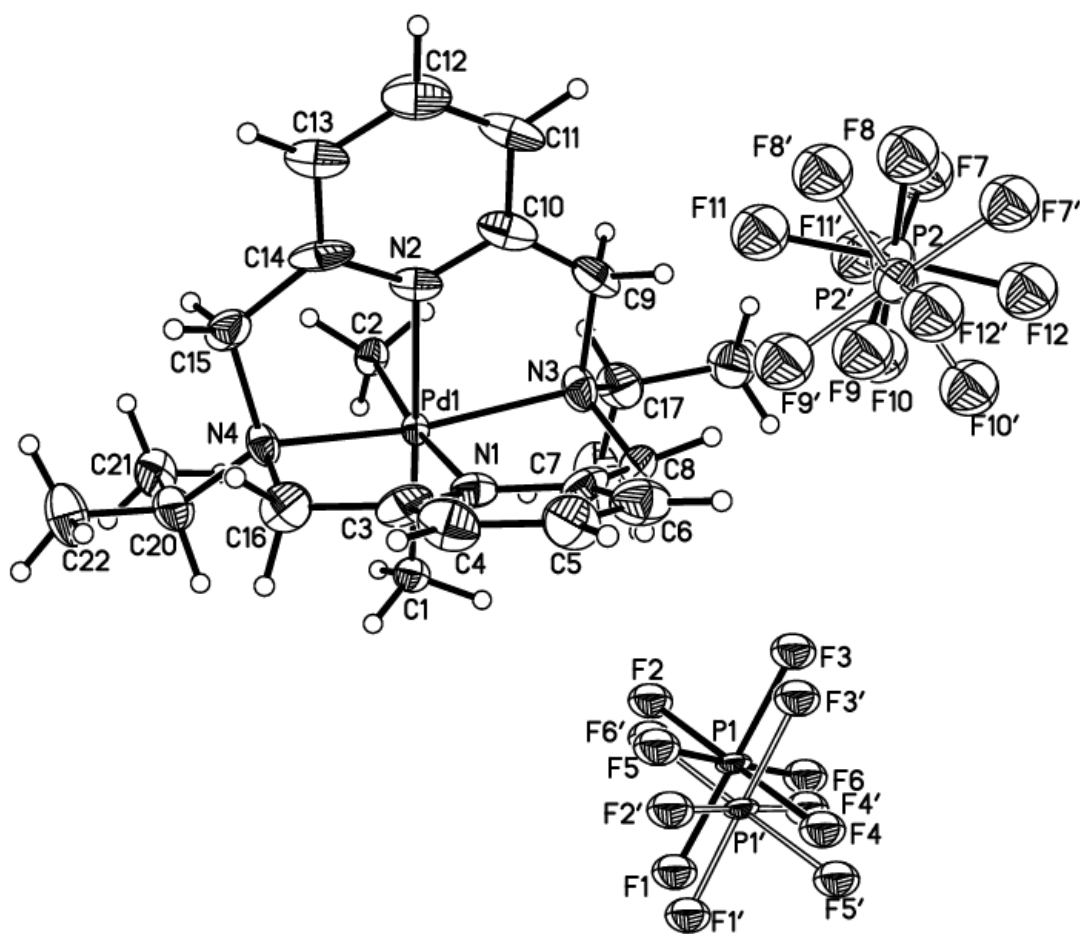


**Figure S66.** Projection view of  $[4^{2+}](PF_6)_2$  with 50% thermal ellipsoids.

## X. References

- (1) Bottino, F.; Di Grazia, M.; Finocchiaro, P.; Fronczek, F. R.; Mamo, A.; Pappalardo, S. *J. Org. Chem.* **1988**, *53*, 3521.
- (2) Gordon, K. A.; Minren, L. *Inorg. Synth.* **1990**, *28*, 60.
- (3) Drew, D.; Doyle, J. R. *Inorg. Synth.* **1972**, *13*, 47.
- (4) Rulke, R. E.; Ernsting, J. M.; Spek, A. L.; Elsevier, C. J.; van Leeuwen, P. W. N. M.; Vrieze, K. *Inorg. Chem.* **1993**, *32*, 5769.
- (5) Byers, P. K.; Canty, A. J.; Jin, H.; Kruis, D.; Markies, B. A.; Boersma, J.; Van Koten, G. *Inorg. Synth.* **1998**, *32*, 162.
- (6) Khusnutdinova, J. R.; Rath, N. P.; Mirica, L. M. *J. Am. Chem. Soc.* **2010**, *132*, 7303.
- (7) Gottlieb, H. E.; Kotlyar, V.; Nudelman, A. *J. Org. Chem.* **1997**, *62*, 7512.
- (8) Evans, D. F. *J. Chem. Soc.* **1959**, 2003.
- (9) Bain, G. A.; Berry, J. F. *J. Chem. Educ.* **2008**, *85*, 532.
- (10) Khusnutdinova, J. R.; Rath, N. P.; Mirica, L. M. *J. Am. Chem. Soc.* **2012**, *134*, 2414.
- (11) Meneghetti, S. P.; Lutz, P. J.; Kress, J. *Organometallics* **2001**, *20*, 5050.